IMPORTANCE OF DIMERIZATION IN THE ADENOSINE 5' MONOPHOSPHATE ACTIVATION OF BIODEGRADATIVE L-THREONINE DEHYDRASE FROM ESCHERICIA COLI

and

DETERMINATION OF ENZYME KINETIC PARAMETERS BY CONTINUOUS ADDITION OF SUBSTRATE TO A SINGLE REACTION MIXTURE AND ANALYSIS BY A TANGENT-SLOPE PROCEDURE

By

David Joseph LeBlond

A DISSERTATION

Submitted to
Michigan State University
in partial fulfillment of the requirements
for the degree of

DOCTOR OF PHILOSOPHY

Department of Biochemistry

1980

A simple

biodegradativ

ted by using

order of the

a rate-limitin

gress curves

sec^{-7} at 28°C.

TDH was

ine. This rad

bound to CNBr-

of matrix-boun

soluble enzyme

AMP (matrix-bo

fer resulted i

matrix-bound,

characteristic

ABSTRACT

IMPORTANCE OF DIMERIZATION IN THE
ADENOSINE 5' MONOPHOSPHATE ACTIVATION OF
BIODEGRADATIVE L-THREONINE DEHYDRASE
FROM ESCHERICIA COLI

and

DETERMINATION OF ENZYME KINETIC PARAMETERS
BY CONTINUOUS ADDITION OF SUBSTRATE TO A SINGLE
REACTION MIXTURE AND ANALYSIS BY
A TANGENT-SLOPE PROCEDURE

By

David Joseph LeBlond

A simple affinity purification procedure has been developed for the biodegradative threonine dehydrase (TDH) of Eschericia coli. TDH isolated by using this procedure is estimated to be 87-96% pure. The protein order of the AMP activation of TDH was found to be 2.01, consistent with a rate-limiting subunit dimerization step. Analysis of activation progress curves yielded a dimerization rate constant of 8.8×10^5 M^{-1} sec^{-7} at 28°C.

TDH was radioactively labelled by growing E. coli on ^{3}[H]pyridoxine. This radioactively-labelled enzyme has been used to quantitate TDH bound to CNBr-activated Sepharose. The specific activity and $S_{0.5}$ of matrix-bound TDH, in the presence of AMP, were similar to those of the soluble enzyme. When TDH was attached to CL-Sepharose in the presence of AMP (matrix-bound, associated TDH), washing the matrix with AMP-free buffer resulted in removal of 50% of the matrix-bound TDH. The resulting matrix-bound, dissociated TDH possesses an activity in the absence of AMP characteristic of soluble unactivated TDH. It is capable of binding

nearly
of AMP a
bound de
These ob
quaterna
bound, d
however,
failure o
strongly
of the en

In su
provides r
tion progr
substrate
puter gener
were fit to
(ii) a tang
ferentiated
analyzed as
estimates of
at least ten
tial guesses
The tangent-s
of 1.5 to 10;
during the as
concentration
serious errors

nearly an equal amount of soluble TDH when placed again in the presence of AMP and this treatment raises the specific enzyme activity of the bound dehydrase to 83% of that of the matrix-bound, associated TDH. These observations correlate with the effects of AMP on the activity and quaternary structure of soluble TDH. When AMP is added to the matrix-bound, dissociated TDH, a fraction (38%) of the TDH is activated; however, the remaining dehydrase is not significantly affected. The failure of AMP to activate the major fraction of immobilized TDH monomer strongly suggest that dimerization of TDH is required in the activation of the enzyme by AMP.

In support of these studies, a new method has been developed which provides reliable estimates of enzyme kinetic constants from single reaction progress curves recorded under conditions of continuously increasing substrate concentration. The approach was first investigated using computer generated data containing known amounts of random noise. Such data were fit to the Hill equation by (i) direct nonlinear curvefitting, and (ii) a tangent-slope technique in which the raw data are numerically differentiated, transformed into substrate versus velocity data, and then analyzed as linear plots. Both procedures provided accurate and precise estimates of the Hill parameters. However, the tangent-slope method was at least tenfold faster to compute and was not dependent on accurate initial guesses of the Hill parameters or integration of the rate equation. The tangent-slope method was reliable over a range of $S_{max}/S_{0.5}$ of 1.5 to 10; the optimal value was 3. Slow enzyme inactivation (4% loss during the assay), or product competitive inhibition (maximum product concentration 30% of the inhibitor dissociation constant) do not produce serious errors in the Hill parameters.

eters

a Gilf

to a s

on pape

from th

agreemer

rabbit m

Sepharos

enzymes a

This approach for semi-automated evaluation of enzyme kinetic parameters was tested in a newly devised instrumental system. It consists of a Gilford spectrophotometer modified for continuous addition of substrate to a stirred enzyme mixture, and for recording of absorbance data coded on paper tape. The Hill parameters for a number of enzymes, obtained from these data by tangent-slope or curve-fitting procedures, are in good agreement with published or manually determined values. Experiments with rabbit muscle lactate dehydrogenase covalently linked to Sephadex G-50 or Sepharose 4-B examine the feasibility of this approach when applied to enzymes attached to solid supports.

I am more
than the atoms
tho I am
of atoms made.

For no atom
ever fell in love
nor on his
guitar played.

Neither has
a symmetry
of only space
and time

heard the yearnings
of his soul
and answered back
in rhyme.

- D.J.L.

To my wife, Cr

waited through

. . . and foun

DEDICATION

To my wife, Christine, and my little children, Scott and Cherie, who waited through their lonely nights so I could live out a boyhood daydream . . . and found me with their smiles.

I would like
encouragemer

he help an
remembered.

I would l
Ashencel
careful
to my ow

The sup
Univers
acknowl

ACKNOWLEDGMENTS

I would like to thank my advisor Dr. W.A. Wood for his confidence and encouragement.

The help and warm friendships of John Reibow and Doris Bauer will be long remembered.

I would like to acknowledge the substantial contributions of Curt Ashendel who wrote the original version of the TANKIN program and whose careful initial studies of substrate addition methodology gave direction to my own.

The support of NIH Training Grant number GM1091 from Michigan State University, and of NSF Research Grant number PCM08586 is gratefully acknowledged.

[illegible] . . . .

DEDICATION .

[illegible]

LIST OF TABLE

LIST OF FIG

[illegible]S AND A

[illegible]RODUCTION

1. IMPORTA
MORPHOS
L-THREON

4. LITE

1.

2.

3.

TABLE OF CONTENTS

	Page
POEM	ii
DEDICATION	iii
ACKNOWLEDGMENTS	iv
LIST OF TABLES	xii
LIST OF FIGURES	xiii
SYMBOLS AND ABBREVIATIONS	xvi
INTRODUCTION	1
I. IMPORTANCE OF DIMERIZATION IN THE ADENOSINE 5' MONOPHOSPHATE (AMP) ACTIVATION OF BIODEGRADATIVE L-THREONINE DEHYDRASE (TDH) FROM ESCHERICIA COLI	5
A. LITERATURE REVIEW	5
1. Regulation of Activity Through Subunit Interaction	5
a. Models of Allostery Involving Subunit Interaction	5
b. Ligand-Regulated Oligomerization	6
2. Assessing the Importance of Subunit Association	7
a. Equilibrium or Steady State Methods	7
b. Association Kinetics	8
c. Immobilized Subunits	12
d. Stabilized Subunits	13
3. Regulation of the Biodegradative TDH of Eschericia coli	14

a

b.

c

4. A

d.

6. MATER

1. B

2.

3.

4.

5.

Page

a. Role in Energy Metabolism 14

b. Activation of TDH by AMP 14

c. Inhibition of TDH by α-Ketobutyrate and Pyruvate 15

4. Allosteric Models Applicable to TDH 16

a. Ligand Induced Oligomerization-Deoligomerization 16

b. Changes in Quaternary Structure During Catalysis 20

B. MATERIALS AND METHODS 22

1. Bacteriological 22

2. Determination of TDH Activity 25

a. Standard Catalytic Assay 25

b. Assays Employing Rapid Mixing 25

3. Determination of Protein 26

a. Soluble Proteins 26

b. Immobilized TDH 26

4. Determination of Radioactivity 27

a. Aqueous Solutions 27

b. Sepharose Suspensions 28

c. Polyacrylamide Gel Slices 28

5. Purification of TDH by Affinity Chromatography 28

a. Preparation of Crude Extract 28

b. Chromatography on N6-linked AMP-Sepharose 29

c. Concentration and Final Centrifugation 30

d. Production of ^{3}H-labelled TDH 30

6. Production of AMP-Free Dehydrase 30

Page

7. Polyacrylamide Gel Electrophoresis of TDH 31

a. Native Gels 31

b. Electrophoresis in the Presence of SDS 31

8. Reduction of TDH by $NaBH_4$ 32

9. Immobilization of TDH 32

a. Quantitation and Handling of CL-Sepharose Suspensions 32

b. Immobilization of TDH to CL-Sepharose 33

10. Collection and Analysis of Reaction Progress Curves 34

a. Instrumental System 34

b. Absorbance Calibration 34

c. Determination of Hill Parameters by Substrate Addition 35

d. Data Collection and Differentiation 35

e. Analysis of Activation Curves by First or Second Order Kinetic Plots 36

11. Least Squares Treatment of Data 37

12. Analytical Ultracentrifugation 38

C. RESULTS 39

1. Improved Purification Procedure for TDH 39

a. Chromatography of TDH on AMP-Sepharose 39

b. Gel Filtration of AMP Sepharose Purified TDH on Sephadex G-200 40

c. Electrophoresis of TDH on SDS Polyacrylamide Gels 40

d. Polyacrylamide Gel Electrophoresis of Native TDH 44

2. Preparation of ^{3}H-PLP-Labelled TDH 45

Page

a. Affinity Chromatography of TDH Labelled In Vivo with ^{3}H-Pyridoxine 45

b. Association of ^{3}H-TDH Radioactivity with the PLP Cofactor 46

3. Activation of Soluble TDH by AMP 54

a. Kinetic Properties with Respect to L-Threonine 54

b. Protein Order Dependence of the Activation Process 57

c. Nature of the Process of AMP Activation 66

i. Analysis of Progress Curves of AMP Activation 66

ii. Pre-established Polymerization as an Alternative Hypothesis 74

iii. Rate constant for the Activation Process 77

d. Effect of Sucrose on the Rate of Reactivation 87

e. Effect of Temperature on the Rate of Activation 91

4. Activation of Immobilized TDH by AMP 94

a. Properties of TDH Immobilized on CL-Sepharose 94

b. Removal of AMP from Matrix-Bound, Associated TDH 97

c. Treatment of Sepharose Bound TDH with Urea and $NaBH_4$ 103

i. Measurement of Radioactivity 103

ii. Measurement of Enzyme Activity 103

d. Uptake of Soluble TDH Monomers by Matrix-Bound, Dissociated TDH in the Presence of TDH . . . 107

e. Kinetic Behavior of Immobilized TDH 110

1.

2. I

3. A

II. DETERMI
TIN
MIXTURE

A. LITE

1.

2.

3.

4.

1.

2.

3.

1.

Page

i. Hysteresis in the AMP Activation of Matrix-Bound, Dissociated TDH 110

ii. Effect of L-Threonine on the Activity of Matrix-Bound TDH 113

B. DISCUSSION 119

1. Improved Purification Procedure 119

2. *In Vivo* Labelling of TDH Using ^{3}H-Pyridoxine 119

3. Activation of Soluble TDH by AMP 120

II. DETERMINATION OF ENZYME KINETIC PARAMETERS BY CONTINUOUS ADDITION OF SUBSTRATE TO A SINGLE REACTION MIXTURE AND ANALYSIS BY A TANGENT-SLOPE PROCEDURE 123

A. LITERATURE REVIEW 123

1. The Hill Equation 123

2. Kinetic Analysis of Single Reaction Progress Curves 124

3. Independent Control of Substrate Concentration 125

4. Automation in Enzyme Kinetic Analysis 126

B. MATHEMATICAL ANALYSIS OF THE METHOD 128

1. Control of Substrate Concentration by Continuous Addition 128

2. Analysis of Raw, Undifferentiated Data (Curve-Fit Method) 128

3. Analysis of Differentiated Data (Tangent-Slope Method) 132

C. MATERIALS AND METHODS 136

1. Computer Programs 136

a. Optimizing Experimental Variables (SSOP) 136

b. Generation of Simulated Data (SIMUL) 137

c. Integral Analysis of Data (MARQ) 138

d. Differential Analysis of Data (TANKIN) 139

Page

e. Weighting in the Analysis of Differentiated Data 143

2. Experimental 147

a Biochemicals 147

b. Immobilization of LDH 147

c. Enzyme Assays 148

d. Instrumental System 152

e. Operation of the System 155

f. Absorbance Correction and Data Storage 156

D. RESULTS 161

1. Analysis of Simulated Data 161

a. Determination of Optimal Window Size for the Tangent-Slope Method 161

b. Determination of Optimal Substrate Concentration Range 164

c. Comparison of the Tangent-Slope and Curve-Fit Methods 165

d. Time or Product-Dependent Effects 170

2. System Performance and Analysis of Real Data 178

a. Preliminary Evaluation of the System 178

b. Kinetic Constants Estimated for Soluble Enzymes 181

c. Kinetic Constants for Immobilized LDH 191

E. DISCUSSION 196

1. Analysis of Simulated Data 196

2. Analysis of Real Data 198

SYNOPSIS AND CONCLUSIONS 204

APPENDIX 205

FOOTNOTES 212

Page

REFERENCES 216

Table	
1	Impu… Cata…
2	Impu… Allos…
3	Disso… state…
4	Comb… Proce… with … Preli…
5	Labe… E. c…
6	Kine…
7	Opti… Curv… Proc…
8	Effe… Unir… ciat…
9	Spec…
10	Mic… of …
11	Proj…
12	Nois… Cuve…
13	Kine…
14	Kine… ized…

LIST OF TABLES

Table		Page
1	Importance of Subunit Association in the Catalytic Activity of Enzymes	9
2	Importance of Subunit Association in the Allosteric Functions of Enzymes	10-11
3	Dissociation Constants for Subunit, Substate, and Activator Equilibria for TDH	19
4	Comparison of the Affinity Purification Procedure of TDH used in these Studies with a Non-Affinity Procedure used in Preliminary Studies	43
5	Labelling of TDH with ^{3}H-PLP by Growth of *E. coli* on ^{3}H-Pyridoxine	51
6	Kinetic Constants for Soluble TDH	55
7	Optimized Linear Fits of Activation Progress Curves to Either a First or Second Order Processes	71
8	Effect of Urea or AMP-Free Buffer Wash on Untreated or Reduced Matrix-Bound, Associated ^{3}H-PLP-Labelled TDH	104
9	Specific Uptake of Soluble TDH	108
10	Michaelis-Menten Parameters of Various Forms of Matrix Bound TDH	117
11	Protocols for Enzyme Assays	149-151
12	Noise of Spectrophotometric System and Cuvet Contents	179
13	Kinetic Constants for Soluble Enzymes	188-189
14	Kinetic Constants for Soluble and Immobilized LDH	192-193

Fig.

1 Link-
vator

2 TSH

3 Sepha
Puri

4 Chro
Line

5 Natu
of 3,

6 Seph
of 3,
NaBH

7 Hyste

8 Acti
Time

9 Dete
of T
Conc

10 Inve
plet

11 Exte
the
to u

12 Boun
Abse
trat

13 Seco
Prog

LIST OF FIGURES

Fig.		Page
1	Linked TDH Subunit, Substrate and Activator Equilibria	17
2	TDH Induction Kinetics	23
3	Sephadex G-200 Gel Filtration of TDH Purified by N^6-Linked AMP Sepharose	41
4	Chromatography of ^3H-Labelled TDH on N^6-Linked AMP Sepharose	47
5	Native Polyacrylamide Gel Electrophoresis of ^3H-PLP-Labelled TDH	49
6	Sephadex G-25 Gel Filtration in 8 M Urea of ^3H-PLP Labelled TDH with and Without $NaBH_4$ Pretreatment	52
7	Hysteresis in the Activation of TDH by AMP	58
8	Activation of TDH by AMP as a Function of Time with Variation in Enzyme Concentration	61
9	Determination of the Order of the Initial Rate of TDH AMP-Activation with Respect to Protein Concentration by the Differential Method	64
10	Inverse Time Plot Showing Approach to Completion of Activation of TDH by AMP	67
11	Extent of Reactivation by AMP as a Function of the TDH Concentration and of the Procedure used to Determine Maximum Reactivation	72
12	Boundary Sedimentation Velocity of TDH in the Absence of AMP as a Function of Enzyme Concentration	75
13	Second Order Kinetic Plot of TDH AMP-Activation Progress Curves	78

Fig.

14

15

16

17

18

19

20

21

22

23

24

25

26

27

28

29

30

31

Fig.		Page
14	Determination of the Apparent Order Rate Constant for Activation of TDH by AMP	81
15	First Order Kinetic Plot of TDH AMP-Activation Progress Curves	83
16	Determination of the Apparent First Order Rate Constant for Activation of TDH by AMP	85
17	Dependence of Second Order Reactivation Rate Constant on Viscosity	88
18	Determination of the Apparent Arrhenius Activation Energy for the AMP-Activation of TDH	92
19	Effect of CNBr Concentration on the Specific Activity of Matrix Bound, Associated TDH	95
20	Release of TDH Activity from Matrix Bound, Associated TDH Upon Removal of AMP from Wash Buffer	98
21	TDH Remaining Matrix Bound After Washing the Matrix with AMP-Free Buffer	101
22	Renaturation of TDH from 9 M Urea	105
23	Reduced Total Activation and Hysteresis in the AMP Activation of Matrix Bound, Dissociated TDH	111
24	Substrate Saturation Steady State Kinetics of Various Forms of Matrix-Bound TDH	114
25	A Hypothetical Substrate Addition Experiment	129
26	Graphic Illustration of Tangent-Slope Estimation of Reaction Velocity	133
27	General Flow Chart for the Computer Program TANKIN	140
28	A Semi-Automated System for Kinetic Analysis of Enzyme Reactions used in the Present Studies	153
29	Correction of Raw Absorbance Data	157
30	Determination of Optimal Window Sizes for use in Tangent-Slope Estimation of Velocities at Three Data Noise Levels	162
31	Determination of Optimal Substrate Concentration Range for TANKIN Tangent-Slope Estimation of Hill Parameters	166

Fig.		Page
32	Comparison of the Accuracy and Precision of the MARQ and the TANKIN Methods	168
33	Effect of End Point Deletion on the Final Correlation Coefficient (A) and Apparent Hill n (B) at Various Levels of Simulated First Order Enzyme Inactivation	172
34	Effect of Varying t_f (A and C) or P_f (B and D) During a Simulated Substrate Addition	176
35	Typical Results of Single Cuvet Assays of Hill Parameters for LDH (A and B) and β-Galactosidase (C and D)	183
36	Proposed, Fully Automated System for Kinetic Analysis of Enzyme Reactions	202
37	CD Observed During the Exchange of Denterium into α-Ketobutyrate from D_2O Catalyzed by KDPG-Aldolase	207
38	CD Observed During the TDH Reaction in D_2O as a Function of Buffer Conditions and the Presence or Absence of AMP	210

SYMBOLS AND ABBREVIATIONS

A	absorbance
AMP,ADP,ATP	adenosine mono-, di-, tri-phosphate
c	concentration of substrate solution being added (M)
C	cosubstrate concentration (M)
Ci	curie
C1,C2,C3,CC	apparent linear correlation coefficients
DTT	dithiothreitol
EDTA	ethylenediaminetetraacetate
E	molar extinction coefficient for 1 cm light path ($M^{-1}cm^{-1}$)
f (subscript)	final value
F	convergence criterion for the program TANKIN
FDP	fructose diphosphate
FTHF	formyl tetrahydrofolate
H	concentration of activated TDH subunits (M)
i (subscript)	the ith value
k	first order constant for enzyme inactivation (min^{-1})
k_2	second order rate constant for dimerization ($M^{-1}sec^{-1}$)
K_i	inhibition constant of product (M)
KCPM	thousand counts per minute
KDPG	2-keto-3-deoxy-6-phosphogluconate
l	liter

L	concentration of the unactivated TDH subunits (M)
LDH	lactate dehydrogenase
n	Hill coefficient
N	number of data points per run
NAD,NADP	nicotine-adenine dinucteotide, nicotine-adenine dinucleotide phosphate
o (subscript)	initial value
O	observed absorbance
ONPG	ortho-nitrophenyl-β-D-galactoside
P	product (moles)
PEP	phospho-enol pyruvate
PLP	pyridoxal phosphate
PMSF	pheyl methyl sulfonyl fluoride
q	order of dependence of activation rate on subunit concentration
r	rate of substrate addition (1/min)
RMS	root mean squared deviation of noise
s	seconds
S	substrate concentration (M)
$S_{0.5}$	S at Vmax/2
SDS	sodium dodecyl sulfate
SOPC	S-o-nitrophenyl-L-cysteine
t,Δt	time, time interval between points (min)
TCA	trichloroacetic acid
TDH	biodegradative threonine dehydrase of E. coli
TDH	biodegradative threonine dehydrase of E. coli
V	catalytic reaction velocity (micromoles/min)
V_H	expected V if all subunits activated

V_L	expected V if all subunits inactivated
V_{max}	expected V if all active sites are saturated
VV	variance of V
w	number of data points in window (odd number)

INTRODUCTION

The tenuous rhythm of the living state is maintained by a complex system of information processing. The transducers of this system are proteins that sense their environments and adjust their activities in symphony. As the spectrum of protein activity is wide, so the patterns of regulation of that activity are diverse. Some generalizations, however, seem possible.

Regulation appears where and when it is needed: at key points in metabolism that irreversibly commit biological resources, or whenever homeostatis requires modulation of certain processes. These control mechanisms may act at the level of protein synthesis, degradation, compartmentalization or structure-function.

Structural alterations are often the result of binding of small molecules in the environment. Such regulatory ligands act via the tertiary or quaternary structure to communicate information in the form of conformational adjustments. Subunit interfaces are evidently quite vulnerable to this kind of disturbance and often the attachment of ligands will change the strength of association between subunits.

The importance of this subunit structure in regulation of protein function has been recognized since x-ray analysis failed to confirm the concept of direct heme-heme interaction in hemoglobin (1). Indeed, regulatory proteins are often found to possess complex quaternary structures. In some instances ligand binding may thus lead to a change in oligomeric

state of a regulatory protein which can offer some unique opportunities for metabolic control.

The biodegradative threonine dehydrase from Eschericia coli catalyzes the first step in the utilization of L-threonine for ATP generation. The synthesis of this enzyme is mediated by cyclic AMP with glucose and oxygen as repressors and amino acids as inducers (2). Its activity is further regulated by AMP activation (3), product (α-ketobutyrate) inhibition (4), and pyruvate (5) and serine (6) inactivation.

This enzyme is a prime example of regulation by ligand-induced oligomerization-deoligomerization. Inhibition of the enzyme by α-ketobutyrate pyruvate, or sulfhydryl oxidation is accompanied by subunit deoligomerization (4,5,7), while activation by AMP correlates with an increase in molecular weight (3). It is clear that both activity and oligomeric state are related to ligand binding (8,9,10), but it is less certain whether quaternary structure alterations act in concert with ligand binding to alter enzyme activity or whether oligomerization is merely a by-product of ligand binding, possibly with some other metabolic function.

The research to be described was undertaken to further clarify the role of oligomerization in the AMP-induced activation of biodegradative L-threonine dehydrase of E. coli.

At low enzyme concentration, AMP induces a dimerization of the enzyme. Previous studies of pre-steady state kinetics of AMP activation have suggested that dimerization was necessary for activation (11). These studies were re-examined over a much wider range of enzyme concentration using an improved analytical instrument. The present results are

in substantial agreement with earlier findings (11) and prompted further characterization of the hysteretic[1] activation process.

The progress of activation was examined and found to be consistent with either a first or second order process. However, a first order fit to the activation time course required restrictive assumptions about the quaternary structure and activity of the inactivated dehydrase. A second order fit did not require such assumptions and was consistent with a rate limiting dimerization process in AMP activation.

From these data, a second order rate constant for dimerization was calculated. From the value of this rate constant and its dependence on viscosity it was felt that the dimerization process may itself be diffusion controlled. However, it was not possible to obtain strong support for this possibility from temperature dependence studies.

To obtain more direct information about the importance of oligomerization, the enzyme was immobilized on Sepharose 4B under conditions which produced minimal alterations in kinetic properties. Evidence is presented that the AMP-activated dimer becomes attached to the matrix via only one subunit. This product is referred to as the "matrix-bound <u>associated</u> enzyme" since its properties appear to resemble those of the soluble TDH <u>dimer</u>. When AMP is removed from wash solutions, non-covalently linked monomer can be eluted from the matrix in a process resembling the de-oligomerization[2] which takes place in solution. The remaining "matrix-bound, <u>dissociated</u> enzyme" will also reassociate with soluble monomers in the presence of AMP to form a "matrix-bound <u>reassociated</u> enzyme".

The matrix-bound, dissociated enzyme shows a reduced AMP activation and no significant hysteresis in the activation process. The steady state kinetics of this enzyme form show that this reduced activation is

due to a fraction of enzyme which can be fully reactivated while the majority of the enzyme appear unaffected by AMP. It is argued that this smaller fraction represents subunits attached to the matrix in adjacent positions allowing rapid dimerization and activation while the remainder of the protomers cannot be activated because they are unable to dimerize. The matrix-bound reassociated, enzyme is fully activatable, lending weight to the concept that dimerization is necessary for AMP activation.

In support of this main theme, a new enzyme preparation was developed based on affinity chromotography which is simpler and more reproducible than a previous protocol. In addition, in order to quantitate immobilized threonine hydrase a method was developed to radioactively label the PLP requiring enzyme in vivo with ^{3}H-pyridoxine. These techniques simplified isolation of the large quantities of labelled enzyme needed for these studies and are described, along with the examination of AMP activation, in Chapter I of this dissertation.

To aid in the kinetic analysis of threonine dehydrase, a new method was developed for obtaining kinetic constants from a single reaction mixture. The method was validated statistically using artificial data and further tested with a variety of enzymes both soluble and immobilized. As this project developed, it became largely removed from studies of TDH and consequently it is treated independently in Chapter II.

The Appendix of this dissertation presents the results of a preliminary investigation of the effect of AMP on the stereospecificity and mechanism of TDH.

CHAPTER I

IMPORTANCE OF DIMERIZATION IN THE ADENOSINE-5'-MONOPHOSPHATE ACTIVATION OF BIODEGRADATIVE L-THREONINE DEHYDRASE FROM ESCHERICIA COLI

A. LITERATURE REVIEW

1. Regulation of Enzyme Activity Through Subunit Interaction

a. Models of Allostery Involving Subunit Interaction

The complex tertiary and quaternary structure of some proteins allows them to govern the interaction of a set of dissimilar molecules or ligands. The indirect nature of these interactions is best illustrated in proteins such as hemoglobin (13) or aspartate transcarbamylase (14) where communication must occur between ligand binding sites on different peptide chains. Conformational alterations wrought at one site must, in these cases, be translated to distant sites through subunit interfaces. The discourse of structurally related (homotropic) or unrelated (heterotropic) ligands through the language of protein conformational change has come to be called allostery.

An early model of allostery (15) considered proteins to be bistable elements with the relative populations of the two tautomeric states perturbed by the energetics of ligand binding. All subunits of a given protein molecle were postulated to occupy the same state. Allostery was thus the result of functional differences in the two tautomers. This model satisfactorily described the coooperative homotropic binding of oxygen to hemoglobin and the allostery exhibited by phosphofructokinase. The symmetrical nature of the equilibrium between states, however, was admittedly (15) unrealistic.

A more flexible formulation (16) postulated that tautomeric changes were not necessarily pre-extant, but were induced by ligand-protein

interaction. In addition, allowance was made for intermediate tautomeric states depending upon the subunit arrangement and the sequence by which subunit binding sites take up ligand. This sequential model could account for the anti-cooperative binding of NAD to glyceraldehyde-3-phosphate dehydrogenase (17).

Both the symmetrical and sequential models are themselves limiting cases of even more general models (18). However, the utility of such general models is restricted by the multitude of tautomeric equilibria that must be analyzed.

Simplified models have contributed conceptual viewpoints from which to consider allosteric phenomena. However as the diversity of enzyme regulation has become clearer, it seems much less probable that any one mechanism can ever unify our concept of allosteric behavior.

b. Ligand Regulated Oligomerization

It has recently been argued (19,20), that mechanistic interpretations are misleading and that allostery is better characterized in terms of energetics. In this view, cooperativity results from the need to balance the free energy changes that define variously liganded states of oligomeric proteins. Further, ligand binding site interactions should be described by changes in subunit-subunit dissociation constants which may be more readily detectable than changes in tautomeric states. Subunit equilibria have been used to probe the allostery of hemoglobin (21) and CTP-synthetase (22). A consideration of subunit association-dissociations is particularly appropriate since such equilibria may be important regulatory features of many enzymes (8).

The kinetic consequences of ligand regulated enzyme-oligomerization have been extensively examined from a theoretical point of view (23). The kinetic properties of such systems appear to have the potential for great regulatory flexibility with a minimum expenditure of energy.

Lists of enzyme which exhibit ligand regulated oligomerization have been given by Frieden (12), Lavitsky and Koshland (17), Klotz (24), Kurgonov (25) and more recently by Dunne and Wood (8). Although the phenomenon is apparently widespread in nature, few detailed characterizations have been made.

In particular, it is rarely clear whether allostery is dependent upon -- or merely coincident with -- the observed changes in oligomeric state.

2. Assessing the Importance of Subunit Association

a. Equilibrium or Steady State Methods

The techniques used to examine the importance of quaternary structure on enzyme activity have classicially involved equilibrium methods. Such methods, which probe only isolated states of oligomerization, are poorly suited for probing cause-effect relationships important in mechanistic investigations.

In addition, in order to demonstrate that the functional state at equilibrium reflects the quaternary structure rather than merely the degree of ligand binding, it is necessary to simultaneously monitor (a) enzymatic activity, (b) quaternary structure and (c) stoichiometry of ligand binding. It would be fortuitous if subunit and ligand dissociation constants as well as intrinsic catalytic rate were all of the proper magnitude to allow such simultaneous measurements. While specialized

rapid reaction or active enzyme centrifugation techniques may prove useful, the above constraints probably account for the dearth of studies where such direct correlations have been attempted. An example of such a study concerned the effect of glutamate dehydrogenase concentration on enzyme activity and effector binding (26). These authors, using light scattering, direct equilibrium binding, and rapid steady-state kinetic techniques, provided data consistent with an important role for oligomerization in determining enzymatic response to effectors. These results implied that subunits may themselves behave as effector "ligands". The information from these equilibrium experiments was less than definitive, however, and data from acetylated (non-oligomerizing) enzyme was needed to strengthen this conclusion (27).

This example illustrates the weakness of equilibrium/steady state techniques in elucidating the importance of subunit interaction in allosteric interactions. The most satisfying answers to the question of the importance of subunit association in the catalytic and regulatory functions of enzymes have come from experiments employing one of the following techniques: (1) Association Kinetics, (2) Immobilized Monomer, or (3) Stabilized Monomer (see Tables 1 and 2).

b. Association Kinetics

If subunit associations are required for the catalytic or regulatory functions of an enzyme, then changes in enzyme function should be observed when isolated subunits of an enzyme polymerize into the associated form. If isolated subunits can be obtained under conditions where association proceeds spontaneously, and if the association step is rate-limiting, then the association process can be studied by observing

Table 1

Importance of Subunit Association
in the Catalytic Activity of Enzymes

Enzyme	Subunit Association Required for Activity?		
	Association Kinetics	Immobilized Monomer	Stabilized Monomer
Alcohol Dehydrogenase	yes (28)[a]		
Arginase		no (29)	
Aldolase	no (30)	no (31)	no (32)
Transaldolase		no (33)	
Phosphorylase b		yes (34)	
Triose Phosphate Isomerase	yes (35)		
Alkaline Phosphatase		yes (36)	
Glyceraldehyde 3 Phosphate Dehydrogenase	inact. monomer (37)	no (38)	
β-Galactosidase	yes (39)	yes (39)	
Malate Dehydrogenase	yes (40)		
LDH	prob(41)	yes (42)	
Avidin[b]	no (43)	no (44)	
Creatine Kinase		yes (36)	

[a]References to Literature are enclosed in parentheses.
[b]Measured activit is the ability to bind biotin.

Table 2

Importance of Subunit Association
in the Allosteric Functions of Enzymes

Enzyme	Function	Subunit Association Required for Function*		
		Assoc. Kinetics	Immob. Monomer	Stabil. Monomer
Aspartate Transcarbamolyase	CTP/ATP Regul.	yes (46)	yes (47)	
Aspartokinase-Homoserine Dehydrogenase I	L-threonine activ., polym.			yes (48)
Phosphofructo Kinase	ATP/PEP inact., dissoc.	yes (49)		
Phosphoenol-Pyruvate Carboxylase	PEP activ., polym.	yes (50)		
Isocitrate Dehydrogenase	Isocitrate/Mg activ., polym.	yes (51)		yes (52)
FTHF Synthetase	M+ activ., polym.	yes (53)		
Glycerol Kinase	FDP inact., polym.	yes (54)		yes (54)
Enolase	Substr. activ., polym.	yes (55)		

Table 2 (contd.)

Importance of Subunit Association
in the Allosteric Functions of Enzymes

Enzyme	Function	Subunit Association Required for Function? Assoc. Kinetics	Immob. Monomer	Stabil. Monomer
Glutamate Dehydrogenase	GTP/GDP inact., dissoc.		no (56)	yes (27)
	ATP activ., polym.		no (56)	
Glyceraldehyde-3-Phosphate Dehydrogenase	ATP, inact., dissoc.	maybe (37)		
Creatine Kinase	Acetate activ., polym.		maybe (56)	
Pyruvate Kinae	PEP/Mg activ., polym.	yes (57)		
TDH	AMP activ., polym.	yes (11,a)	yes (a)	

[a]This dissertation.

changes in enzyme catalytic or regulatory function with time. Since associations proceed at a rate which is second order or greater in subunit concentration, a catalytic or regulatory change whose appearance is at least second order in subunit concentration may require subunit association. Thus association kinetics have been used to determine the requirement for association of a large number of catalytic (Table 1) or regulatory (Table 2) functions of enzymes.

For enzymes known to undergo ligand mediated changes in oligomeric state (e.g. glycerol kinase, aspartokinase-homoserine dehydrogenase I, isocitrate dehydrogenase or TDH (Table 2)), association from isolated subunits can be made favorable by rapid changes in ligand concentration. In other cases isolated subunits must be obtained under more drastic conditions such as urea or guanidine·HCl denaturation or by temperature or pH changes (e.g. aspartate transcarbamoylase (Table 2), aldolase, triose phosphate isomerase, or avidin (Table 1)). In these latter instances significant subunit refolding often occurs and detailed kinetic schema must be considered.

c. Immobilized Subunits

A significant problem with equilibrium methods (described above) is that often the equilibrium constant for subunit association is so great that isolated, stable subunits cannot be examined at the concentration required for catalytic enzyme assays. Thus a general method whereby association can be prevented would be very useful. The technique of enzyme immobilization is such a method.

The use of enzyme immobilization to investigate the significance of subunit associations has been pioneered by Chan (58). His work has lead

to methods for handling and assaying Sepharose-bound enzymes, and conditions under which relatively unmodified matrix-bound monomer species may be obtained. He has used enzyme immobilization to examine the properties of aldolase, transaldolase, and lactate dehydrogenase (Table 1) and aspartate transcarbamoylase (Table 2).

In an interesting combination of approaches, the inactive LDH monomer was bound to Sepharose through a reducible disulfide bridge. Kinetics of reappearance of LDH activity upon reduction suggested that reassociation was required for appearance of catalytic activity (42).

d. Stabilized Subunits

An alternative to immobilization would be to stabilize the monomeric form of the enzyme in some way. Occasionally this can be done by mere dilution (e.g. glycerol kinase, Table 2). However more often, a very specific chemical modification is required.

Glutamate dehydrogenase subunits can be stabilized by acetylation, and become insensitive to the effects of guanine nucleotide (Table 2). On the other hand, aldolase subunits acetylated during renaturation are unable to tetramerize, yet still retain catalytic activity.

The more drastic the dissociation procedure, the more uncertain is the meaning of the observed results on catalytic or regulatory activity. Thus the implications of observed inactive subunits of acid dissociated LDH (42) is best judged only in the light of other studies of reassociation kinetics or of the immobilized monomer.

3. Regulation of the Biodegradative TDH of Escherichia coli

a. Role in Energy Metabolism

TDH[3] catalyzes the production of α-ketobutyrate and ammonia from L-threonine. E. coli synthesizes two TDH forms: a biosynthetic TDH, active in the biosynthesis of isoleucine and a biodegradative TDH which seems to represent the first step in catabolism of L-threonine for the generation of ATP (59). The latter dehydrase is synthesized only during anaerobic growth on a complex amino acid containing medium devoid of glucose or similar energy source (60,61). Conditions which result in a temporary energy deficit in the E. coli cell accentuate TDH synthesis apparently through an elevation in the level of cyclic AMP (2).

An analogous enzyme from Clostridium tetanomorphum appears linked to ATP generation via the intermediates α-ketobutyrate and propionylphosphate (62). It appears possible that the TDH of E. coli may be similarly linked to ATP formation since propionate is produced by anaerobically grown E. coli cells on a medium devoid of glucose but high in L-threonine (63).

b. Activation of TDH by AMP

Further evidence implicating TDH in an energy generating role is its activation by AMP. AMP lowers the $S_{0.5}$ value of the enzyme for threonine 20-50 fold (64). AMP may also increase the V_{max} of the enzyme (7) although this latter effect remains uncertain due to the reported instability of the enzyme in the absence of AMP (64).

The process of activation has been shown to involve both changes in quaternary structure of the enzyme and facilitation of substrate binding in the reaction mechanism (11,65).

At TDH concentrations above 1 mg/ml, the enzyme appears to be a tetramer (66). At lower concentrations (i.e., those found under catalytic assay conditions) and in the absence of AMP, TDH dissociates ultimately to a monomer (11). However the smallest structure observed in the presence of AMP is a dimer (8). A study of the kinetics of AMP association of TDH indicates that a dimerization of the monomer species in some way facilitates the AMP activation (11), however an absolute requirement for dimerization in the AMP activation of TDH has not been established. Whether or not AMP affects the terminal steps in the reaction mechanism is also not known.

c. Inhibition of TDH by α-ketobutyrate and pyruvate

In the absence of AMP, TDH is inhibited by both α-ketobutyrate (4) and pyruvate (5). The inhibition of both of these α-ketoacids is similar in some respects and highlights the importance of AMP and oligomerization in the regulation of TDH.

The inhibition by α-ketobutyrate is competitive with respect to the binding of AMP, and the degree of inhibition is more marked at low concentrations at which the tetrameric enzyme dissociates to a dimeric or monomeric form (4). Furthermore α-ketobutyrate itself can cause the enzyme to dissociate to its subunits, and conversely AMP counteracts this product-induced dissociation.

The mechanism of TDH inactivation by pyruvate involves covalent attachment to the active oligomeric form of the enzyme followed by dissociation of the oligomer to yield inactive enzyme (5). Increasing dehydrase and/or AMP reduces the rate of pyruvate inactivation.

Thus these inhibitors alter the enzymes association-dissociation equilibrium in favor of dissociation, whereas the AMP activator alters it in favor of association. This observation suggests that the oligomeric state may well be a determining factor in the activity of the enzyme and that activators and inhibitors may act in part by influencing the quaternary structure. Thus the quaternary structure may play more than merely a passive role in the allosteric regulation of TDH.

4. Allosteric Models Applicable to TDH

a. Ligand Induced Oligomerization - Deoligomerization

The interdependance of activity, quaternary structure and AMP concentration as described above have led Dunne and Wood to propose a ligand induced oligomerization model for TDH regulation (8). They have analyzed this model in terms of substrate, activator, and subunit binding equilibria which are linked thermodynamically (67). This analysis correctly predicts (a) that the affinity for AMP should increase with increasing TDH and/or threonine concentrations (b) that subunit binding should be enhanced by AMP and reduced by L-threonine (c) that the enzymes affinity for L-threonine should be increased by AMP but lowered at elevated protein concentrations.

There are 12 equilibria that describe subunit, substrate, and activator associations (see Figure 1). Thus a rigorous test for consistency of this model requires accurate measurement of a large number of equilibrium constants. Table 3 lists the values of those equilibrium constants for which information is presently available. Only two tests for consistency of the model can presently be made. These involve comparison of calculated values for K_1 and K_5 with the probable ranges for these

Figure 1. Linked TDH Subunit Substrate and Activator Equilibria. M, TDH monomer; D, TDLH dimer; T, L-threonine; A, AMP.

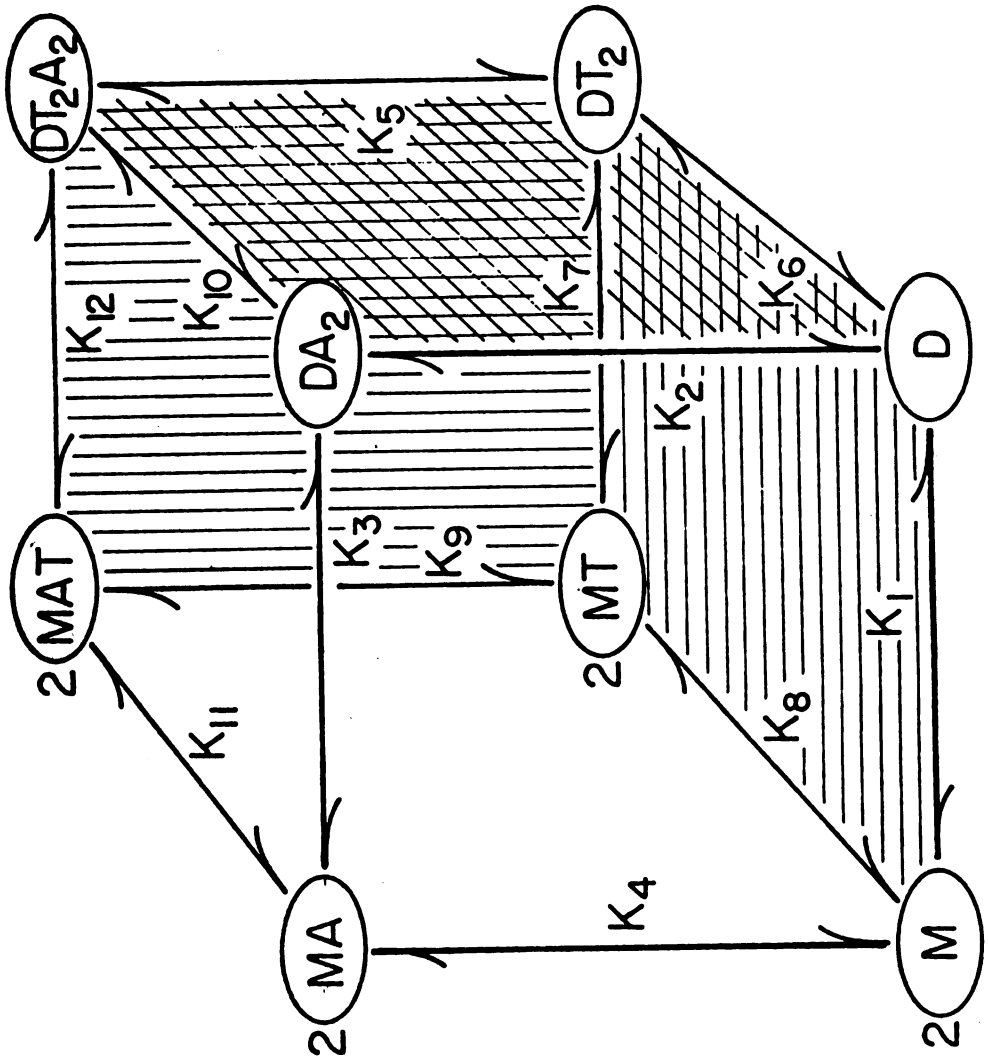
DT2A2
DT2
DA2
D
2MAT
2MT
2MA
2M
K1
K2
K3
K4
K5
K6
K7
K8
K9
K10
K11
K12

Table 3

Dissociation Constants for Subunit, Substrate and Activator Equilibria for TDH

Constant	Binding Equilibrium[a]		Dissociation Constant (M)	Method of Determination	Ref.
K_1	2M	D	$5 - 50 \times 10^{-7}$ (1.1×10^{-7})	Ultracentrifug. Calculation	b c
K_2	2A+D	DA_2	5×10^{-5}	Equilibrium Dialysis	69
K_3	2MA	DA_2			
K_4	A+M	MA			
K_5	$2A+DT_2$	DT_2A_2	2×10^{-6} (0.7×10^{-6})	Steady State Kinet. Calculation	d e
K_6	2T+D	DT_2	2.2×10^{-1}	Stopped Flow	11
K_7	2MT	DT_2	6.7×10^{-6}	Active Enzyme Centrifug.	f
K_8	T+M	MT	6.0×10^{-2}	Steady State Kinet.	11
K_9	A+MT	MAT			
K_{10}	$2T+DA_2$	DT_2A_2	3.0×10^{-3}	Steady State Kinet.	64
K_{11}	T+MA	MAT			
K_{12}	2MAT	DT_2A_2	$<10^{-8}$	Active Enzyme Centr.	63

[a]M, D, A and T represent the dehydrase Monomer, dehydrase dimer, AMP and L-threonine respectively.

[b]This dissertation: see Discussion associated with Fig. 11.

[c]Calculated from thermodynamics: $K_1 = K_7 \cdot K_8^2/K_6$

[d]Based on steady state kinetic measurements made at elevated TDH concentration of 1.6×10^{-6}M where the dehydrase may have been highly dimerized (4).

[e]Calculated from thermodynamics: $K_5 = K_2 \cdot K_{10}/K_6$

[f]Approximate value obtained by extrapolation (68).

constants based on experimental work. As seen in Table 3, calculated values are within an order of magnitude of measured values.

Information is not presently available for equilibria in which the species MA or MAT are involved (see Table 3) because the monomeric species has not yet been observed in the presence of AMP. Using active enzyme centrifugation, Menson has shown that in the presence of AMP, TDH exists as a dimer at concentrations as low as 10^{-8}M (0.4 μg/ml) (68) and thus K_{12} must be less than 10^{-8}M. One of the purposes of this dissertation was to establish some of the properties of monomeric dehydrase in the presence of AMP.

b. Changes in Quaternary Structure During Catalysis

A very different view of the significance of TDH quaternary structure is presented by Hayaishi (10). Based upon spectral measurements and steady state kinetic determinations at high TDH concentrations (71), he has proposed that the oligomer formed at high protein concentration or in the presence of AMP is catalytically inactive although it possesses a high affinity for L-threonine. The monomer on the other hand is catalytically active but has a poor affinity for substrate.

While only the steady-state/equilibrium aspects of this model have been tested with any rigor (71), the model is discussed at length in terms of kinetic predictions (10). The overall TDH reaction supposedly requires substrate binding by the oligomer followed by dissociation and catalysis. Reassociation then completes the reaction cycle (10). In order for this model to be viable the reassociation rate must be at least as great as the observed catalytic rate. At TDH concentrations of 0.1 I.U./ml and in the presence of AMP, where this reaction scheme is

supposed to occur (71), a reassociation rate constant (monomer to dimer) of $10^{11} M^{-1} sec^{-1}$ would be required[4]. Such a rate constant approaches the diffusion limit for second order reactions (72). It is shown in the Results that the association constant of TDH monomers is about $8.8 \times 10^{6} M^{-1} sec^{-1}$, raising doubts about the applicability of this model.

B. MATERIALS AND METHODS

1. Bacteriological

TDH was obtained from an isoleucine-requiring mutant of Eschericia coli (ATCC9739) which lacks the biosynthetic dehydrase. The mutant was re-isolated from stab cultures by combining individual colonies from Levine EMB agar plates. The isoleucine requirement was verified by observing growth on Davis and Mingioli agar plates with and without isoleucine.

The organism was best maintained at 37°C on slant cultures of nutrient broth in 2% agar. Bimonthly transfers on this medium ensured viability.

Liquid cultures were grown at 37°C in 2% N-Z amine NAK (Humko-Sheffield Chemical Co.), 1% yeast extract (Gibco Diagnostics) and 0.5% dibasic potassium phosphate and distilled water. Starting cultures were prepared by loop-transfer from slants into 10 or 100 ml of this medium. Successive transfers were made using 1% innocula. Starting and intermediate cultures were incubated without agitation for 8-12 h. Final cultures were grown under argon with minimal strirring. Large scale cultures (120L) were grown in a New Brunswick Scientific Co. fermentor.

The profile of growth and TDH induction in final culture is shown in Figure 2. Absorbance of the culture at 660nm was taken as a measure of E. coli growth. Prior to assay for TDH activity, a culture suspension was vigorously agitated with a 1% volume of toluene: ethanol (1:9:v/v), then incubated on ice for 15 min. An aliquot of the cell suspension was then added to the standard catalytic assay (see below).

Figure 2. TDH Induction Kinetics. Twelve liters of medium were innoculated with 120 ml of a stationary culture of E. coli. The culture was incubated under argon at 37°C and 50 to 100 ml aliquots were taken at intervals and placed on ice. The assay procedures for TDH activity (□) and cell growth (○) are given in Materials and Methods.

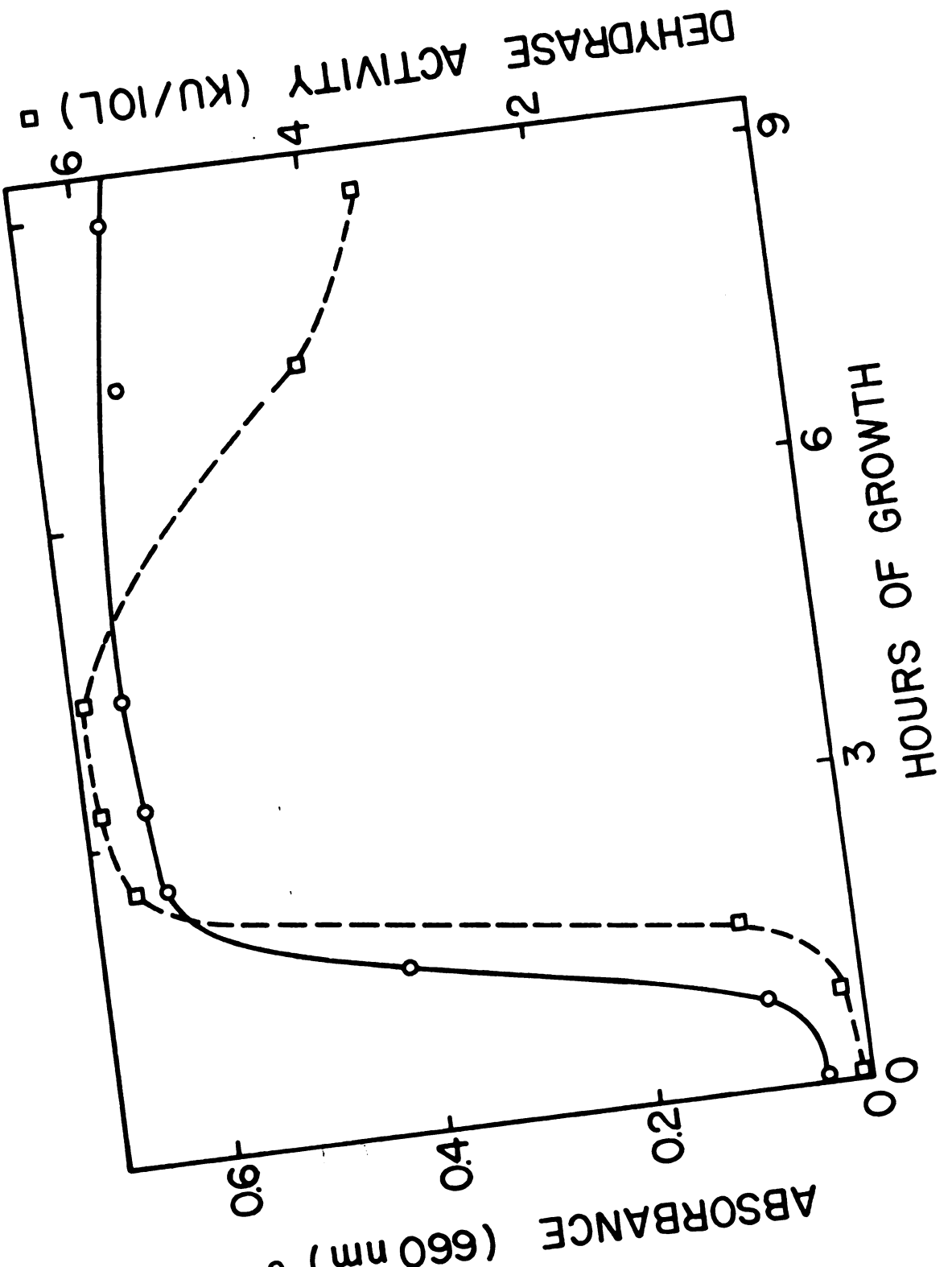
DEHYDRASE ACTIVITY (KU/IOL) □
ABSORBANCE (660 nm) ○
HOURS OF GROWTH
0
2
4
6
0.2
0.4
0.6
3
6
9

2. Determination of TDH Activity

a. Standard Catalytic Assay

The coupled spectrophotometric assay described by Dunne et al. (64) was used to measure TDH catalytic activity. The standard 0.2 ml catalytic assay contained 5 mM DTT, 5 mM AMP, 0.3 mM Na_2NADH, 20 mM L-threonine, 50 µg/ml beef heart LDH and 75 mM potassium phosphate pH 8.0. This concentration of LDH insured that a steady state reaction rate was attained within 1.5 min (73). The assay was performed in a Gilford 2000 recording spectrophotometer at 28°C. The reaction was initiated by addition of TDH to the reaction mixture.

The TDH activity of Sepharose beads was determined using the method of Chan (74). The standard catalytic assay was modified by increasing the assay volume to 2.0 ml and by employing a continuous stirring mechanism (Gilford Model 2445 Spectrostir). Stirring was at the maximum rate of 1000 rpm.

b. Assays Employing Rapid Mixing

When the time course of AMP activation of TDH was studied, the concentration of LDH used in the catalytic assay was increased to 1 mg/ml. This insured attainment of steady state reaction rate within 2 sec (73). AMP was initially absent but was added from a Hamilton syringe by injecting 0.05 ml of a 200 mM potassium AMP, solution pH 8.0 into the 1.95 ml stirred reaction mixture.

Usually, absorbance measurements were made at 340 nm employing an extinction coefficient of 6220 $M^{-1}cm^{-1}$. When elevated concentrations of NADH were required, absorbance measurements were made at higher wavelengths. Relative extinction coefficients at 372.5 nm (2080

M^{-1}), 382.5 nm (1150 M^{-1}) and 384 nm (988 M^{-1}) were determined by comparison of the absorbance of NADH solutions at these wavelengths to that at 340 nm.

Other variations of the standard catalytic assay for rapid mixing experiments were made as described in Results.

3. Determination of Protein

a. Soluble Proteins

For the most part, protein determinations were made by a small scale modification of the Lowry procedure using crystalline bovine serum albumin as a standard (75). However, this procedure ws unreliable when the DTT concentration in the final Lowry mixture exceeded 10 uM. In these cases a method based on fluorescamine was used (76). Unfortunately, this procedure was also found unsuitable if the sample contained excess ammonium ion.

In later work, a Coomassie blue-G procedure (77) proved very convenient. It was not affected by elevated levels of either DTT or ammonium ion. Both the fluorescamine and Coomassie blue procedures were calibrated using a solution of TDH standardized by the Lowry procedure (75).

b. Immobilized TDH

Determinations of the protein content of matrix bound TDH were made by Ms. Doris Bauer of the Department of Biochemistry, Michigan State University on a Beckman 120 C amino acid analyzer according to published methods (78).

A 0.5 ml sample of sepharose suspension (1:1(v/v), determined as described below) was placed in a thick glass walled hydrolysis vial and

lyophilized. To the vial was then added 0.5 ml of 6N HCl. The vial was evaculated, sealed and incubated for 24 h at 110°C. The solutions were centrifuged for 15 min. at 2000xg to remove charred debris, and the supernatant was evaporated to dryness. The solid material was resuspended in 0.7 ml of sample application buffer containing norleucine as an internal standard and 0.5 ml of this solution was submitted to quantitative partial amino acid analysis. The isoleucine content of suspensions of matrix-bound TDH was corrected for that of Sepharose blanks (activated with CNBr and blocked with ethanolamine as described below but not exposed to TDH). The blank content was 50-100%. The protein content of the matrix was then calculated from this isoleucine content, and the known amino acid composition of TDH (69).

4. Determination of Radioactivity

a. Aqueous Solutions

The tritium content of aqueous solutions was determined by liquid scintillation counting at -5°C in a Packard instrument with a gain setting of 75% and a counting window of 50 to 1000. The scintillation cocktail was prepared by mixing 500 ml of toluene, 500 ml of triton X-100, 4 g POP and 0.1 g dimethyl POPOP. Ten milliliters of this cocktail was mixed with 1.0-2.0 ml of aqueous sample. This level of H_2O produced a stable clear solution at room temperature and at -5°C. In some cases the salt content of the sample was lowered by dilution in H_2O to avoid precipitation in the cocktail. Basic samples were acidified with 0.05 ml of 20% TCA in order to avoid phosphorescence background during counting.

All samples were counted until the statistical error in the count (2 S.D.) was less than 5%. Quench corrections were made by addition of an

inte

Count

ume

Seph

ml o

ing

descr

in m

30%

scin

5.

cult

ing

panc

Bran

watt

Main

internal standard consisting of 0.02 ml of ^{3}H-toluene to each sample. Counting efficiencies ranged from 5 to 13% depending upon the sample volume and salt content.

b. Sepharose Suspensions

To determine the tritium content of matrix-bound TDH, 0.4 ml of a Sepharose suspension (1:1 (v/v), as determined below) was mixed with 0.4 ml of concentrated HCl and incubated at 70°C for 10 min. To the resulting clear solution was added 0.8 ml of H_2O. This sample was counted as described above for aqueous samples.

c. Polyacrylamide Gel Slices

Polyacrylamide gel slices (6 mm diameter, 2.5 cm length) were placed in marble capped test tubes and incubated for 3 h at 70°C with 0.2 ml of 30% H_2O_2. The resulting clear solution was then transferred to a scintillation vial and counted as described above for aqueous samples.

5. Purification of TDH by Affinity Chromatography

a. Preparation of Crude Extract

The frozen cell paste (about 144 g wet weight) from a 120 l liquid culture was brought to 2-6°C by suspension in 170 ml of a buffer consisting of 1 mM Na_2 EDTA, 2 mM DTT, 0.05 mg/ml PMSF[5], 0.01 mg/ml bovine pancrease deoxyribonuclease I, and 0.1 M potassium phosphate, pH 6.8.

The cold suspension was placed on ice and sonicated for 3 min using a Branson sonicator fitted with a half-inch tip, and a power setting of 80 watts. This process was repeated 10 times with intermittent cooling to maintain a temperature of less than 10°C.

The sonicate was immediately centrifuged at 2-6°C for 3 h at 31,000 x g in a Beckman J-21C Centrifuge using a J-21 rotor. The resulting clear yellow supernatant was further purified by affinity chromotography.

b. Chromatography on N^6-Linked AMP-Sepharose

A column (9 cm height, 2.5 cm width) of N^6-linked AMP-Sepharose (P and L Biochemical Col, 5.2 μmoles of phosphate per ml of bed) was precycled by first washing with 35 ml of 8 M urea solution, then by resuspension, repacking and equilibration with 2 mM DTT, 1 mM Na_2 EDTA 0.1 M potassium phosphate, pH 6.8 (Wash buffer). The column was equilibrated, used and stored at 2-6°C. The same bed was reused 7 times over a period of 6 months with no apparent changes in binding or flow properties or in the final dehydrase specific activity.

The crude E. coli extract was carefully applied to this column (at 2-6°C) followed by 10 l of wash buffer at a flow rate of 300 ml/h. The column was then washed successively with the following buffers and volumes at about 100 ml/h: (1) wash buffer contaiing 1 M KCl, 100 ml, (2) wash buffer, 20 ml, (3) wash buffer containing 20 mM Na_2ATP, 20 mM Na_2 ADP, 2 mM NADP, and 4 mM NAD, pH 6.8, 40 ml, (4) wash buffer 40 ml and (5) wash buffer containing 5 mM AMP, pH 6.8, 1 l.

During the last wash the effluent was monitored for the first sign of yellow color or fluorescence (using a long-wave UV lamp). As soon as color or fluorescence was visible, the effluent was collected into a separate container. A total of 450 ml of effluent was collected.

c. Concentration and Final Centrifugation

The eluted dehydrase was concentrated for 5 h under 50 psi argon using an Amicon concentrator fitted with a PM-30 membrane. The solution was concentrated to a final volume of 7 ml and centrifuged at 30,000 xg at 2-6°C for 1 h to remove denatured protein. The solution was stored frozen at -20°C in 0.5 ml aliquots until needed. When stored this way no loss in enzyme activity was observed over periods up to 1 year.

d. Production of ^{3}H-Labelled TDH

For production of ^{3}H-labelled TDH, the cell paste from a large scale E. coli culture was combined with that from a smaller (1/10th scale or 12L) culture. The two cultures were grown and harvested simultaneously under identical conditions, with the exception that upon innoculation of the smaller culture, 0.5 to 1.5 ml of G-^{3}H pyridoxine hydrochloride (Amersham Co., 0.6 - 2.1 Curies/mmole) was also added. ^{3}H-TDH was isolated from this combined cell mass exactly as outlined above for unlabelled dehydrase.

6. Production of AMP-Free Dehydrase

AMP was removed from TDH solutons by Sephadex G-25 gel filtration exactly as described by Rabinowitz et al. (65) with the exception that the column length was increased from 4.8 cm to 20 cm. This column provided excellent resolution of TDH from AMP and no significant levels of AMP could be detected in gel-filtered solutions of TDH by either absorbance at 260 nm or by adding ^{14}C-AMP as done by Rabinowitz et al. (65) (data not presented).

TDH solutions lacking AMP were prepared for catalytic assay by first adding a 2.5% volume of 200 mM AMP, pH 8 to an aliquot, incubating at room temperature for 30 min prior to addition to the standard catalytic assay. Such assays showed that recovery from the G-25 procedure was greater than 90%.

7. Polyacrylamide Gel Electrophoresis of TDH

a. Native Gels

Native polyacrylamide gel electrophoresis was conducted at 4°C according to the method of Ornstein (79) and Davis (80). Minor modifications of this method are described in detail by Menson (68) and will not be repeated here. These gels were stained for protein exactly as described by Blakesly and Boezi (81) and for activity exactly as given by Menson (68). Color development in this latter stain was found to be highly non-linear with time (data not shown) possibly due to TDH inactivation during the staining reaction (82). The stain was therefore not used to quantitate TDH activity on gels.

Enzyme activity was quantiated on native gels by cutting the gels into 2 mm sections. The sections were gently crushed and suspended in an equal volume of buffer containing 2 mM AMP, 2 mM DTT, 1 mM EDTA, and 0.1 M potassium phosphate, pH 8.0. The suspension was incubated at 4°C for 24 h and the eluted activity determined using the standard catalytic assay.

b. Electrophoresis in the Presence of SDS.

SDS polyacrylamide gel electrophoresis was performed employing the discontinuous buffer system of Ornstein (79) and Davis (80) according to

the method of Steck (83). The sample was prepared for electrophoresis by TCA precipitation and incubation in excess SDS, and then applied to the gel exactly as prescribed (83). The gels were then stained with Coomassie blue for 3 h and destained over a 3 day period as recommended by Osborn et al. (84).

8. Reduction of TDH by $NaBH_4$.

The Shiff's base linkage of the PLP cofactor to a lysine residue on the TDH protein moiety was reduced with $NaBH_4$ following a standard procedure (85). To 0.4 ml samples of TDH (either soluble dehydrase at 1 mg/ml or immobilized dehydrase in a 1:1 CL-Sepharose suspension (v/v) at about 4-10 μg TDH/ml) were added 0.005 ml of 1-octanol and 0.1 ml of an ice cold, freshly prepared aqueous slurry of $NaBH_4$ (0.4 g/ml). The samples were mixed and incubated in the dark for 1 h at room temperature. Measurements of TDH activity showed that soluble samples contained less than 0.25% of the original activity after this period.

$NaBH_4$ reduced forms of TDH were used immediately at room temperature and exposed to a minimum of light.

9. Immobilization of TDH

a. Quantitation and Handling of CL-Sepharose Suspensions.

Bed volumes of CL-Sepharose of CL-Sepharose bound TDH suspensions were measured by either (a) 1 min centrifugation at 2,000 g or (b) by observing the volume of a completely settled bed in a column. Both methods yielded identical measurements. Working suspensions of these matrices were adjusted such that the volume of supernatant buffer was

equal to the volume of the packed bed (referred to as a 1:1 (v/v) suspension).

The CL-Sepharose beads bound tenaciously to glass and polycarbonate but not to polypropylene surfaces. Therefore all handling and washing of these suspensions was done in disposable syringe barrels fitted at the bottom with fine mesh nylon screen. Pipetting of suspensions was performed using Pipetteman automatic pipetter (Rainin Instruments) and disposable polypropylene pipette tips cut at the end to enlarge the opening as suggested by Chan (58).

b. Immobilization of TDH to CL-Sepharose

TDH was immobilized to CL-Sepharose using the procedure of Axen et al. (86). The activation process was carried out for 15 min at 0-5°C and pH 10.05-11.5. Unless otherwise indicated, 5 mg CNBr were used per ml packed bed volume of CL-Sepharose.

After activation the gel was immediately washed in a Buchner funnel with 100 fold volume of an ice cold buffer consisting of 5 mM AMP, 1 mM DTT, 1 mM EDTA, 0.1 M potassium phosphate, pH 8.0. Supernatant buffer (coupling buffer) was removed by filtration and 2.5 ml of the packed bed was added to 0.5 ml of TDH (2 mg/ml) isolated as described above. The CL-Sepharose was gently re-suspended with a spatula and the slurry allowed to incubate at room temperature for 5 h without further mixing.

The slurry was transferred to a column (2 cm x 10 cm) and washed with 60 ml of coupling buffer followed by 25 ml of coupling buffer containing 0.1 M ethanolamine hydrochloride, pH 8.0. The gel was allowed to incubate 12 h at 2-6°C under this buffer following which it was reequilibrated to room temperature and washed with the following solutions: 40 ml

coupling buffer, 40 ml coupling buffer containnig 1 M KCl, 60 ml coupling buffer. CL-Sepharose linked TDH, prepared in this way is referred to as "matrix bound associated TDH".

In order to produce "matrix bound dissociated THD" (see Results) the matrix bound asociated TDH was further washed with 240 ml of coupling buffer, pH 8.0, which did not contain AMP. This was followed by a wash with 20 ml of AMP-containing coupling buffer.

10. Collection and Analysis of Reaction Progress Curves

a. Instrumental System

The spectrophotometer used in these studies consisted of a Gilford 250 spectrophotometer fitted with a water cooled Peltier effect temperature controlled cuvet housing (Gilford Instrument Laboratories, prototype), which contained an alternating field device for rotating a magnetic stir pellet in the 3 ml cuvet. The sample compartment cover contained a small opening which was used for injection of solutions into the stirred cuvet. The digital output from the spectrophotometer was interfaced to a Hewlett-Packard calculator (model HP9815A). Programs were written for data collection, storage, and analysis by the calculator.

b. Absorbance Calibration

The diode correction network in the Gilford spectrophotometer (87) was bypassed and absorbance correction was done digitally. A table of true (A) and observed (O) absorbance values (obtained as described in Chapter II) was fit to a third degree polynomial,

$$A = a_0 + a_1 O + a_2 O^2 + a_3 O^3,$$

where a_0 to a_3 are adjustable parameters optimized using the computer program POLFIT (88). The standard deviation of the data about the fitted line was 0.7 mA when Amax = 1.7 A but rose to 14 mA when Amax = 2.1. For this reason data were only collected between A = 0.0 and A = 1.7.

c. Determination of Hill Parameters by Substrate Addition

Determinations of Hill parameters for soluble TDH by the method of substrate addition were made exactly as described in Chapter II except that the above instrumental system was used. The Hewlett-Packard programmable calculator model HP9815A was programmed to perform the TANKIN (see Chapter II) analysis with the exception that homogeneous velocity variances were assumed. Performance of the new software was verified by analysis of both artificial data and real data. Data were obtained with the spectrophotometric system described in Chapter II and were analyzed using the Fortran version of TANKIN.

d. Data Collection and Differentiation

Absorbance values were collected at a rate of 7.7 sec^{-1}. From 4 to 32 of these values were averaged by the HP9815A to provide a single smoothed absorbance value. The mean collection time of averages was taken as the time data. Activation progress curves of 220 points and substrate addition curves consisted of 110 points. When differentiated data were analyzed further by least squares treatments, only every eleventh rate point was used because of the correlation between adjacent rate values.

Absorbance - time data were differentiated using standard algorithms (89) to obtain catalytic rate - time data. An 11 point sliding window was used as described in Chapter II.

e. Analysis of Activation Curves by First or Second Order Kinetic Plots

Consider the irreversible conversion of TDH from a less active form of concentration L to a highly active form of concentration H by the action of AMP. If this process is first order in L, then the following relationship may be shown (90):

$$\ln \frac{L_o}{L} = k_1 t \qquad [1]$$

were L_o is the initial concentration of the less active form, k_1 is the first order rate constant of conversion, and t is time.

If, however, the process is second order in L (i.e., a rate limiting dimerization) (90) then

$$\frac{L_o}{L} - 1 = L_o k_2 t \qquad [2]$$

where k_2 is the second order rate constant of conversion.

If TDH is active during this conversion process and the catalytic rate V at any time is related linearly to the changes in L and H, then by conservation of active sites:

$$\frac{L_o}{L} = \frac{V_H - V_L}{V_H - V} \qquad [3]$$

where V_H and V_L represent the limiting catalytic rates expected if all of the active sites were of the H or L form respectively.

Combination of equation 3 with equations 1 and 2 yields

$$\ln \frac{V_H}{V_H - V} = k_1 t + \ln \frac{V_H}{V_H - V_L} \qquad [4]$$

and

$$\frac{V_H}{V_H - V} = \frac{(L_o k_2 t + 1)\, V_H}{V_H - V_L} \qquad [5]$$

for first and second processes respectively. These equations provided linear transformations of catalytic rate - time data and form the basis for Figures 13 and 15. All of the calculations for these analyses were made using the HP9815A calculator. V_H was obtained from independent measurement of the catalytic activity of TDH preincubated and assayed in the presence of AMP. V_L was taken from data collected prior to the addition of AMP. Apparent k_2 values were obtained by unweighted least squares fits of data to equation 5. The variances of the slope and intercept were used to provide a measure of variance in k_2 by the method of error propagation (88).

11. Least-Squares Treatment of Data

Conventional substrate saturation curves were fit to the Michaelis-Menten equation (equation 14 with n = 1) by the linear method of Wilkinson (91). Fits to the Hill equation were made using the program TANKIN (see Chapter II). Saturation curves for matrix-dissociated TDH in the presence of AMP were fit to the following equation:

$$V = \frac{V_H \cdot S}{S + K_H} + \frac{V_L\, S}{S + K_L} \qquad [6]$$

where V_H, K_H, V_L and K_L refer to the Vmax and $S_{0.5}$ values of the high and low activity of forms of TDH. These four parameters were optimized by non-linear regression using the FORTRAN program KINFIT (92).

12.

wit

44,

pho

ate

8.0.

acti

the c

infle

S

20℃

ml/g

12. Analytical Ultracentrifugation

Boundary sedimentation velocity measurements of TDH were performed with the assistance of Dr. Arnold Revzin. Experiments were performed at 44,000 rpm in A Sinco Model E analytical ultracentrifuge equipped with a photometric scanner system. The temperature was maintained at 20°C.

TDH was freed from AMP as described above and diluted to an appropriate concentration in 1 mM DTT, 1 mM EDTA, 0.1 M potassium phosphate pH 8.0. The dilutions were incubated on ice for 5 h and the dehydrase activity determined immediately prior to centrifugation. Distances from the center of rotation, r, were calculated from the position of the inflection point of the scanner tracings.

Sedimentation coefficients were calculated and corrected to water at 20°C by published methods (93). The partial specific volume of 0.738 ml/g was used for TDH as reported (66).

C. RESULTS

1. Improved Purification Scheme for TDH

a. Chromatography of TDH on AMP-Sepharose.

Previous work in this laboratory showed that the semi-purified enzyme could bind tightly to C8-linked AMP Sepharose and slightly to N6-linked AMP Sepharose. (C. Unkefer and W.A. Wood, 1975 unpublished work.) In an effort to improve the purification scheme using affinity techniques, crude E. coli extract (prepared in the absence of AMP) was applied directly to a variety of affinity media. The enzyme would not bind to AMP linked to Sepharose through the ribose group, and was only slightly retarded by blue dextran Sepharose. The enzyme did bind, however, to C8 Sepharose and could be eluted after lengthy buffer pre-washing with a gradient of 0 to 100 mM AMP. The enzyme eluted between 2 other components (data not shown).

While this work was in progress, a very similar affinity purification procedure was published for Salmonella typhimurium (94) TDH and subsequently used for the purification of E. coli TDH (95). This procedure utilized an N6-linked-AMP Sepharose column and a nucleotide pre-wash (containing 0.01 mM ADP, 1 mM ATP, 0.2 mM NAD and 0.1 mM NADP), elution with 5 mM AMP, and subsequent gel filtration on Sephadex G-200. This procedure was re-examined in the present investigation.

The elution profile from the N6-matrix resolved only one component which contained TDH activity: The specific activity of this pooled eluted enzyme was 325 I.U./mg. Further studies were then made using the N6-linked AMP Sepharose.

b. Gel Filtration of AMP Sepharose Purified TDH on Sephadex G-200

The TDH eluted from the N6-linked AMP Sepharose was not pure and could be separated from a higher molecular weight contaminant by chromatograhy on G-200 (Figure 3A). However when the concentration of nucleotides in the N6-AMP Sepharose Chromatography pre-wash was increased, the specific activity of the N6 AMP eluant rose to 450 iu/mg and these contaminants were largely eliminated (Figure 3B). This G-200 chromatography did not further improve the specific activity of enzyme eluted from N6-AMP Sepharose after prewash at elevated nucleotide concentration. Because it resulted in a 15% loss in activity, the G-200 step was not used in subsequent preparations. The full details of the enzyme purification used in these studies is given in Materials and Methods. Table 4 gives a comparison of this procedure with the previous non-affinity procedure (68). The affinity procedure results in a greatly reproducible specific activity. Based on the estimated specific activity for the pure enzyme of 480 I.U./mg (68), this enzyme is about 87-96% pure.

c. Electrophoresis of TDH on SDS Polyacrylamide Gels

The purity of the enzyme preparation was further examined by gel electrophoresis under denaturing conditions. The non-affinity procedure usually produced a profile containing a major band, accounting for about 48% of the optical density in the stained gel, and at least two minor bands. With non-affinity preparations of higher specific activity, only one contaminant was observed corresponding to a previously identified TDH II (68). The affinity-purified enzyme contained only a single stained band coinciding with the major band obseved in non-affinity purified TDH (data not shown).

Figure 3. Sephadex G-200 Gel Filtration of TDH Purified by N^6-Linked AMP Sepharose Chromatography. TDH was purified by AMP affinity chromatography as described in Materials and Methods except that the concentration of nucleotides in the wash buffer was either 1 mM ATP, 0.01 mM ADP, 0.1 mM NADP, and 0.2 mM NAD, (A) or 20 mM ATP, 20 mM ADP, 2 mM NADP and 4 mM NAD (B). This enzyme solution (7 ml) was applied to a Sephadex G-200 column (90 x 2.5 cm) equilibrated with 1 mM DTT, 5 mM AMP, 0.1 M potassium phosphate pH 6.8. The activity was eluted by ascending chromatography with the same buffer. Five ml fractions were collected at a flow rate of 4.0 ml/h. TDH activity and protein were determined as described in Materials and Methods.

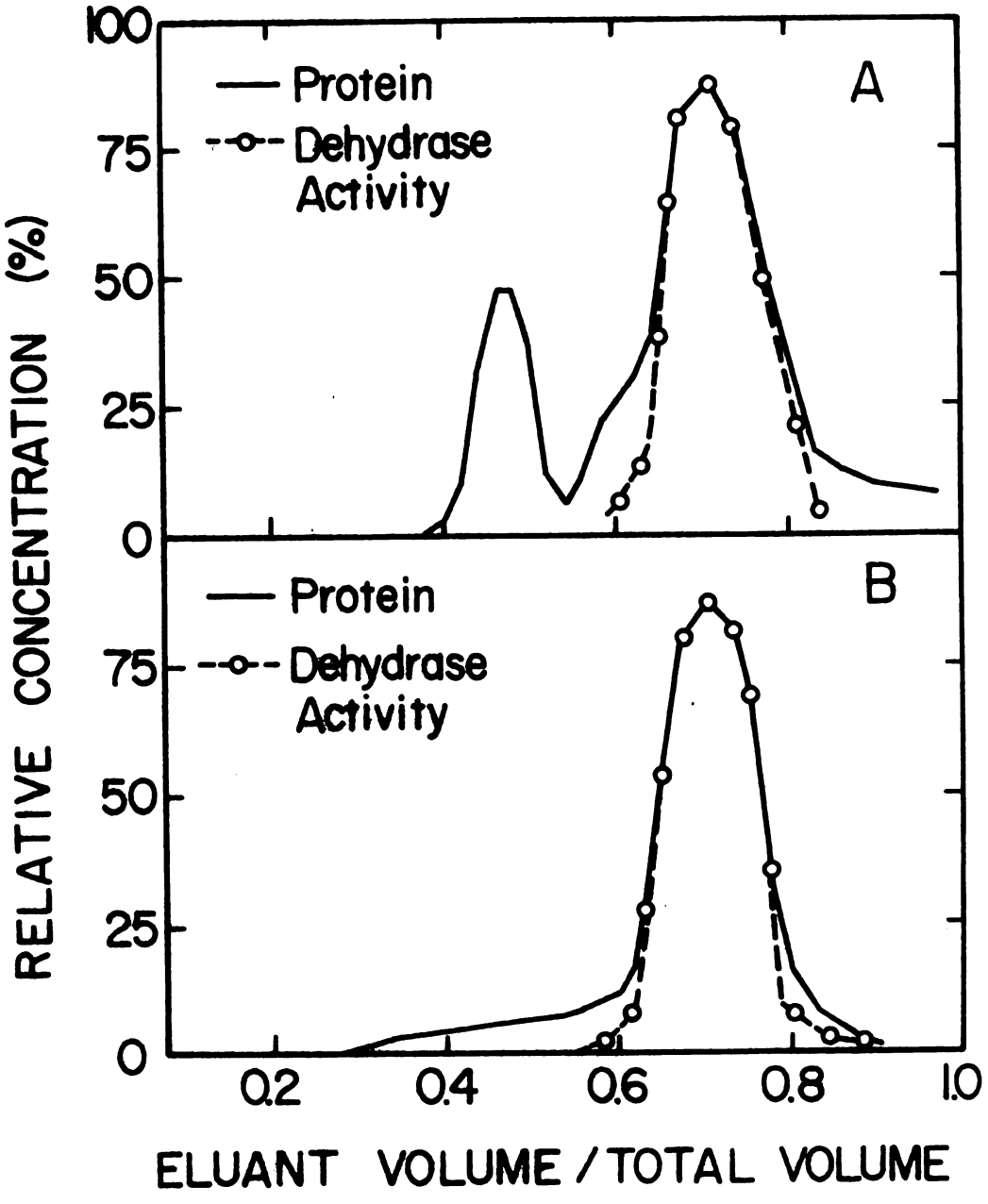
100
75
50
25
0
Protein
Dehydrase Activity
A
Protein
Dehydrase Activity
B
RELATIVE CONCENTRATION (%)
0.2
0.4
0.6
0.8
1.0
ELUANT VOLUME / TOTAL VOLUME

Table 4

Comparison of the Affinity Purification Procedure of TDH Used in These Studies with a Non-Affinity Procedure Used in Preliminary Experiments

Procedure[a]	Yield ± s.d. (I.U. TDH/g cell paste)	Final Specific Activity ± s.d. (I.U./mg)
Non Affinity (n = 5)	33.3 ± 32	246 ± 135
Affinity (n = 4)	131.0 ± 34	441 ± 20

[1]The non-affinity procedure used was that of Menson (68). The affinity procedure is given in detail in Materials and Methods. The n value represents the number of times the procedure was repeated.

d. Polyacrylamide Gel Electrophoresis of Native TDH and the Nature of TDH II.

A previous study of TDH II revealed that it was distinct kinetically and structurally from the major TDH component but large scale separation of these two components was not obtained (68). The apparent ability of the affinity procedure to separate the two forms was therefore further investigated.

When native TDH, purified by the non-affinity method submited to gel electrophoresis the minor component appears as a band of protein and activity migrating slightly behind the major TDH band (68). When the non-affinity purified TDH was further purified on N6-linked AMP Sepharose, the contaminating enzyme activity (visualized with TDH activity strain: see Methods) was still present although the protein band had nearly disappeared (data not given). It is possible that the contaminating activity was not associated with the protein removed from this gel position, but actually represented an altered form of the main TDH component resulting from, for instance, sulfydryl cross linking. Since the activity stain response in these experiments was not linear with time (LeBlond and Wood, 1976 unpublished), the contaminating activity may have been a small percentage of the total.

When the TDH activities were eluted from native gels and assayed (see Materials and Methods), the TDH II component accounted for less than 2% of the total activity recovered from the gels. No significant change in recovered TDH II activity was observed upon chromatography on AMP Sepharose. When enzyme activity eluted from the main TDH band was re-electrophoresed, the minor TDH II activity band reappeared. It was thus apparent that the minor component was in fact derived from the major

TDH band, in contrast to the Conclusions of Menson (68), who regarded TDH II as having a distinct nature.

When the primary TDH activity band was sliced from native gels and immediately re-electrophoresed, no minor contaminant was apparent. Incubation of the gel slice at 4°C for 45 min or 11 hours did not result in an observable TDH II band. However, if the gel slice was incubated before re-electrophoresis for 37 h at 4°C in phosphate buffer not containing DTT or AMP, the TDH II activity reappeared.

From these results it was concluded that the TDH II activity represents a minor aggregated form of the major TDH component. Because it probably accounted for less than 2% of the enzyme activity, it was not investigated further. Possible reasons for the differences between these conclusions and those of Menson are presented in Discussion.

2. Preparation of ^{3}H PLP-Labelled TDH

a. Affinity Chromatography of TDH-Labelled In Vivo with ^{3}H-pyridoxine.

During experiments with immobilized TDH, the need for a convenient routine method for quantitating matrix-bound TDH became apparent. PLP is tightly bound at the active site of this enzyme (96), and the possibility of obtaining TDH with a highly radioactive cofactor was attractive. Small scale (12 liter) *E. coli* cultures grown in the presence of ^{3}H pyridoxine (1.4 μM, 359 mCi/mmol) as described in Materials and Methods, incorporated 32% of the radioactivity into the wet cell paste. When this wet cell paste (14 g) was combined with that obtained from a large scale culture (139 g) and submitted to TDH purification (see Materials and Methods) the resulting TDH was highly radioactive.

The N6-AMP Sepharose elution profile of this material is shown in Figure 4. The profile of radioactivity was coincident with that of both protein and enzyme activity. Native gel electrophoresis of this preparation showed that only the major TDH band contained significant radioactivity (Figure 5). These results established that the radioactivity is indeed associated with TDH.

b. Association of ^{3}H-TDH Radioactivity with the PLP Cofactor

The specific radioactivity of labelled enzyme subunits (experiment of Figure 5) was calculated assuming a subunit molecular weight of 40,000 (66) and a specific enzyme activity of purified TDH of 480 I.U./mg (68). This value was calculated to be 395 mCi/mmol subunit which approximated the specific radioactivity of the starting ^{3}H pyridoxine (359 mCi/mmol, taking into account the pyridoxine content of yeast extract of 11 mg/100 g (data obtained from technical bulletin supplied with product)).

The specific radioactivity of the enzyme subunits was found to be close to the specific activity of the original ^{3}H-pyridoxine regardless of the pyridoxine concentration in the E. coli growth medium (Table 5), indicating that significant catabolism of ^{3}H-pyridoxine was not occuring prior to incorporation of radioactivity into TDH, but that the ^{3}H-pyridoxine is phosphorylated and incorporated directly into TDH subunits as ^{3}H-PLP with little loss of radioactivity.

To provide more direct evidence of ^{3}H PLP in TDH, the ^{3}H-labelled TDH was denatured by exposure to 9 M urea and chromatographed on Sephadex G-25 in 9 M urea (Figure 6, open circles). The elution profile showed two peaks of radioactivity corresponding to small and large molecular weight fractions. Quantitation of these peaks showed that 97.1% of the

Figure 4. Chromatography of ^{3}H-Labelled TDH on N6-Linked AMP Sepharose. *In vivo* ^{3}H-labelling of TDH, affinity chromatography, and dehydrase, protein and radioactivity assays were performed as described in Materials and Methods. Fifteen ml fractions were collected from the first appearance of yellow fluorescence in the eluant.

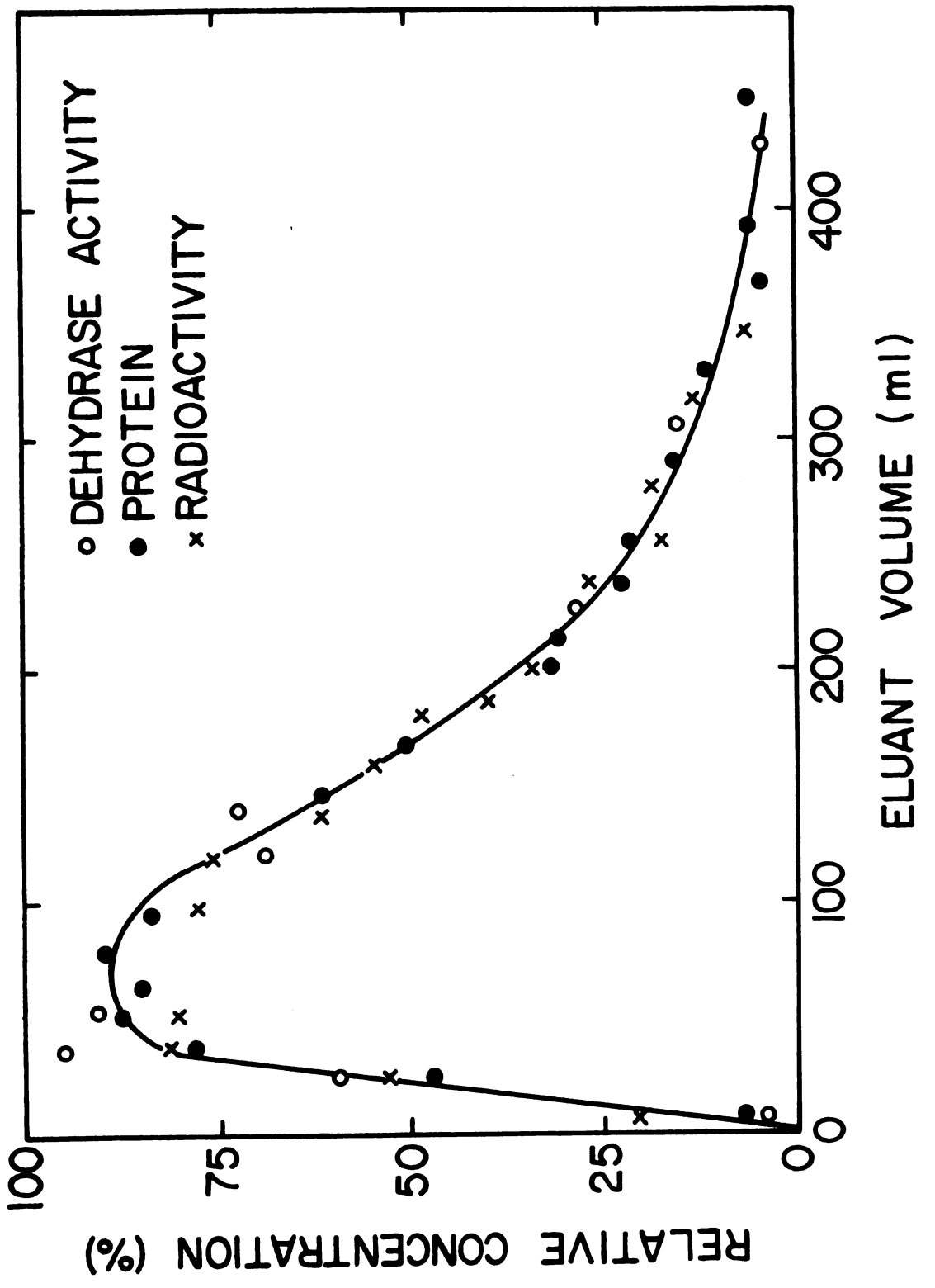
DEHYDRASE ACTIVITY
PROTEIN
RADIOACTIVITY
RELATIVE CONCENTRATION (%)
100
75
50
25
0
0
100
200
300
400
ELUANT VOLUME (ml)

Figure 5. Native Polyacrylamide Gel Electrophoresis of ^{3}H-PLP-labelled TDH. ^{3}H-PLP labelled TDH (407 I.U./mg, 1.5 x 10^{-3} I.U./dpm) was electrophoresed, as described in Materials and Methods. The volume applied to 2 identical gels was 0.025 ml containing 0.1 mg of protein. One gel (solid line) was stained as described in Materials and Methods and scanned at 600 nm in a Gilford spectophotometer fitted with a linear transport. The other (●) was sliced in 0.2-0.25 cm sections and counted as described in Materials and Methods.

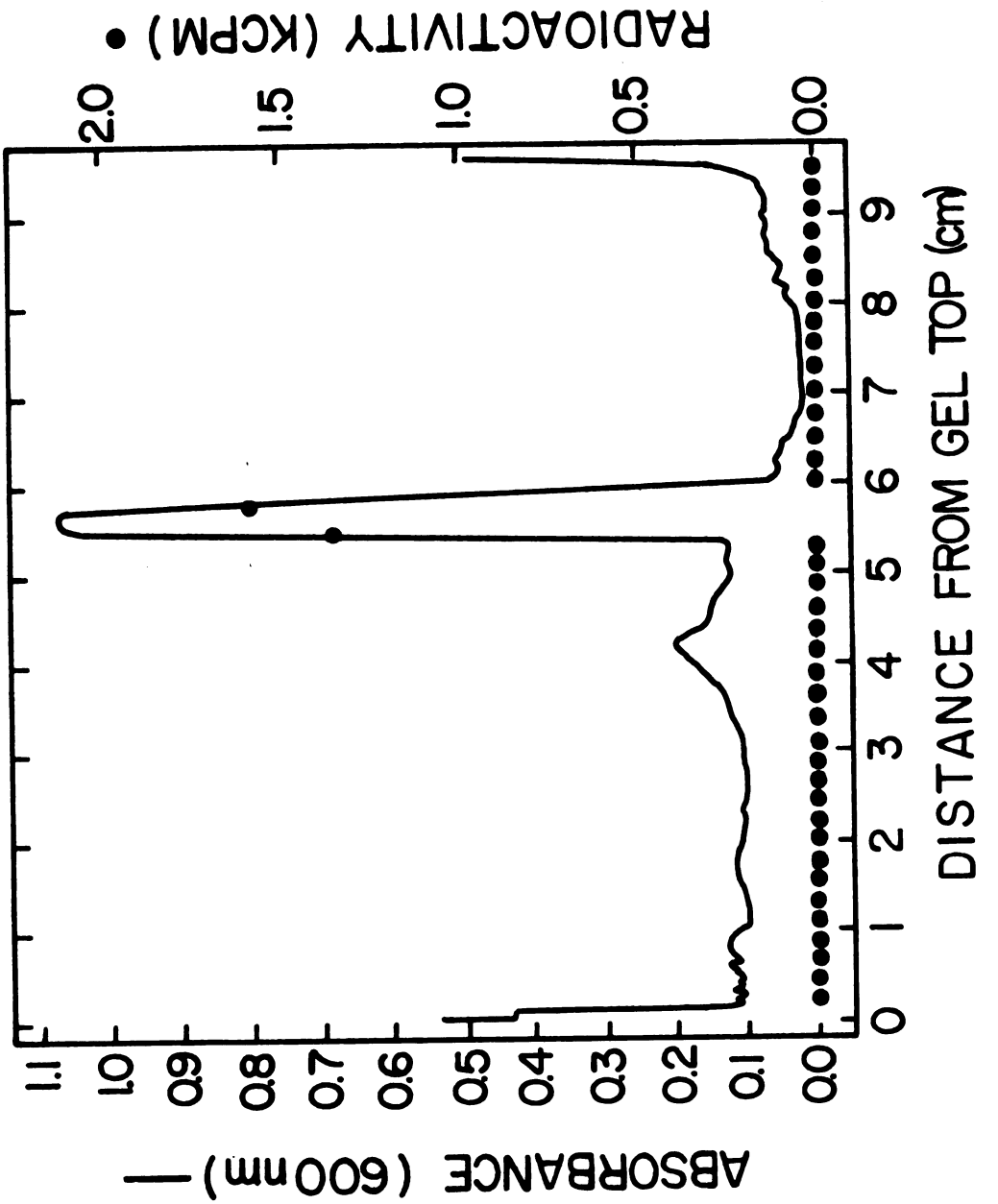
RADIOACTIVITY (KCPM) •
2.0
1.5
1.0
0.5
0.0
ABSORBANCE (600nm) —
1.1
1.0
0.9
0.8
0.7
0.6
0.5
0.4
0.3
0.2
0.1
0.0
0 1 2 3 4 5 6 7 8 9
DISTANCE FROM GEL TOP (cm)

Table 5

Labelling of TDH with ^{3}H-PLP by Growth of *E. Coli* on ^{3}H-Pyridoxine

Experiment	Pyridoxine Concentration[a] (Micromolar)	Specific Radioactivity		
		Pyridoxine (Ci/mole)	TDH[b] (Ci/mole)	TDH (% of Pyridoxine)
1	1.39	358.7	395.0	110.0
2	1.39	358.7	322.9	90.0
3	0.92	538.0	645.0	119.9
4	0.64	208.4	249.0	119.5
5	0.59	249.3	237.5	95.3

[a]Calculated from the amount of labelled pyridoxine added plus the amount present in yeast extract (1.1 mg/100 g, given by supplier).

[b]Specific radioactivity of the labelled subunit calculated assuming 1 PLP per subunit of molecular weight 40,000 and specific dehydrase activity of 480 I.U./mg.

Figure 6. Sephadex G-25 Gel Filtration in 8 M Urea of ^{3}H-PLP-labelled TDH with and without $NaBH_4$ as described in Materials and Methods. To the reduced dehydrase was added solid penicillamine to a final concentration of 50 mM and solid urea to a final concentration of 8 M. After incubation at room temperature for 30 min, the solution was gel filtered through a column (0.7 x 20 cm) of Sephadex G-25, equilibrated with 8 M urea, 1 mM DTT, 1 mM EDTA, 50 mM penicillamine, 0.1 M potassium phosphate pH 7 (●). Another sample of ^{3}H-PLP-labelled TDH was treated identically but was not exposed to $NaBH_4$ (○). Chromatography was at room temperature in the dark. Material was eluted using the above buffer at a flow rate of about 0.1 ml/min. Five min fractions were collected into gradient tubes. A 0.05 ml aliquot from each tube was counted as described in Materials and Methods.

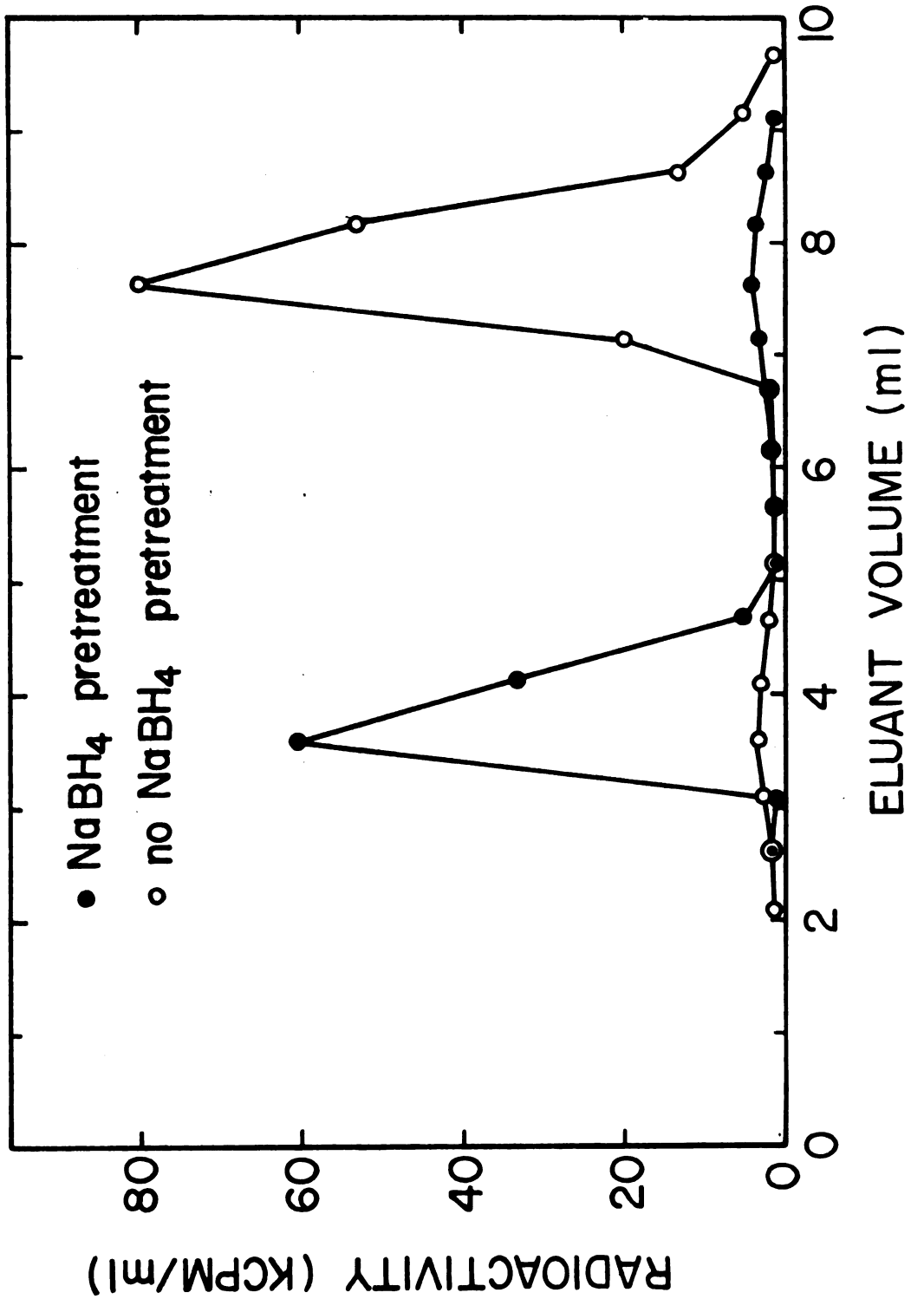
• $NaBH_4$ pretreatment
○ no $NaBH_4$ pretreatment
RADIOACTIVITY (KCPM/ml)
ELUANT VOLUME (ml)
0
20
40
60
80
0
2
4
6
8
10

radioactivity was contained in the low molecular weight fraction. This result would be expected if the great majority of radioactivity was associated with PLP.

The PLP on TDH may be covalently attached to the enzyme by borohydride reduction (97). When ^{3}H-labelled TDH was treated with $NaBH_4$ prior to gel filtration in urea, 92.3% of the radioactivity remained associated with the large molecular weight fraction. This behavior suggests that 92-97% of the radioactivity is in a form which can be both resolved by denaturation in urea and covalently attached to the enzyme by $NaBH_4$ reduction. These properties are to be expected for the PLP cofactor of TDH. Because urea denaturation and borohydride reduction may not be complete, it is likely that nearly 100% of the radioactivity is in the form of ^{3}H-PLP.

3. Activation of Soluble TDH by AMP.

a. Kinetic Properties with Respect to L-threonine.

To learn more about the role of oligomerization in the AMP activation of TDH, the hysteresis of the activation process was studied. To ensure 90% of steady state reaction rate within 2 s, 0.5 mg/ml of lactate dehydrogenase was required (see Methods). Because the coupling enzyme is stored in concentrated ammonium sulfate, the final ammonium sulfate concentration in the experimental solution was 0.11 M. Attempts to remove this salt by dialysis or gel filtration resulted in large losses in lactate dehydrogenase activity and instability of the desalted enzyme.

Because the $S_{0.5}$ of TDH is affected by ionic strength (64), these values were re-determined under conditions to be used in studies of the activation process. Table 6 presents the parameters of the Hill

Table 6

Kinetic Constants for Soluble TDH[a]

AMP	V_{max} (± s.d.) (I.U. x 10^{-4}/dpm)	$S_{0.5}$ (± s.d.) (mM)	Hill n (± s.d.)	Correlation Coefficient
+	3.51 ± 0.03	6.75 ± 0.5	1.17 ± 0.03	0.9955
+b	3.20 ± 0.2	7.63 ± 0.2	1.08 ± 0.007	0.9960
-	1.88 ± 0.04	264. ± 17.	1.1 ± 0.02	0.9924

[a]Initial rate data were processed using the TANKIN program described in Chapter II.

[b]Values were averaged from 4 determinations made by the method of substrate addition as described in Chapter II. Correlation coefficient represents an average value.

equation which describe saturation of TDH by its substrate, L-threonine at elevated ammonium sulfate. The Hill coefficient is very near unity whether determined in the presence or absence of the activator as previously reported (64). If significant homotropic interaction, substrate protection or inactivation of TDH were present, this value might be expected to deviate markedly from 1.0

In the presence of AMP, the $S_{0.5}$ value was 6.7 mM (see Table 6). This value is approximately 2-3 fold greater than that determined by others at reduced concentrations of ammonium sulfate and coupling enzyme, and is consistent with expected effect of ionic strength on TDH kinetic parameters (64). In the absence of AMP, $S_{0.5}$ was about 264 mM which is 2-4 fold greater than that determined previously in the absence of elevated salt.

The V_{max} value in the absence of AMP was nearly half that obtained in the presence of the activator. Dunne et al. have explained this phenomenon on the basis of enzyme instability in the absence of AMP and have shown, using an internal correction procedure, that V_{max} is independent of activator concentration (64). As shown below in the Results Section, under the assay conditions employed in the present work, it seemed unnecessary to make such corrections.

The kinetic constants in the presence of AMP were also determined using a rapid, single cuvet assay technique described extensively in Chapter II of this dissertation. This "reaction progress" method is more sensitive than the usual multi-cuvet technique to anomalous effects such as coupling enzyme inadequacy, product inhibition, enzyme inactivation, hysteresis, etc. However, as shown in Table 6, single suvet derived values agree reasonably well with those obtained by the standard method. No

hysteresis was observed in the multi-cuvet reaction progress curves, suggesting that this effect is probably absent under similar conditions employed in the single cuvet assay.

The kinetic constants for AMP were not determined. Throughout these studies AMP, where present in diluents and assays, was 5 mM. Reaction rates of activated TDH were not significantly affected by halving or doubling the AMP concentration.

b. Protein Order Dependence of the Activation Process

Gerlt et al. (11) were the first to study the transient-presteady state period observed upon addition of AMP to otherwise complete reaction mixtures. These authors measured initial rates of TDH activation and found these to have a second order dependency on enzyme concentration. This indicated that a subunit dimerization was rate limiting in the activation reaction.

These studies were limited by the available instrumentation which required manual mixing upon addition of AMP. Although absorbance data were collected automatically at 1s data intervals, the information which could be gathered during the initial phases of activation was limited. Because of these limitations, only reduced enzyme concentrations in the range of 0.005-0.02 I.U./ml could be examined[6] (11,98). Therefore, it was not determined whether different processes (i.e. first order conformational change) became rate limiting at elevated enzyme concentrations.

The improved spectrophotometric system described in Materials and Methods was capable of relatively rapid mixing and data collection rates ($7.7s^{-1}$). The initial activation time course, measured with this improved system at two enzyme concentrations is shown in Figure 7. The

Figure 7. Hysteresis in the Activation of TDH by AMP. Changes in the absorbance of a stirring cuvette containing 1 mM DTT, 0.275 mM NADH, 1 mg/ml bovine heart LDH, 0.1 M potassium phosphate pH 8.0 and either 0.035 or 0.35 I.U. of TDH (designated by 1 or 10 in the figure) were measured before and after the addition of 0.05 ml of 200 mM KAMP, pH 8.0 (at the spike). Data were collected and stored as described in Materials and Methods. The solid lines represent tracings of data plotted using an HP 7200 flat bed plotter interfaced to the HP9815A.

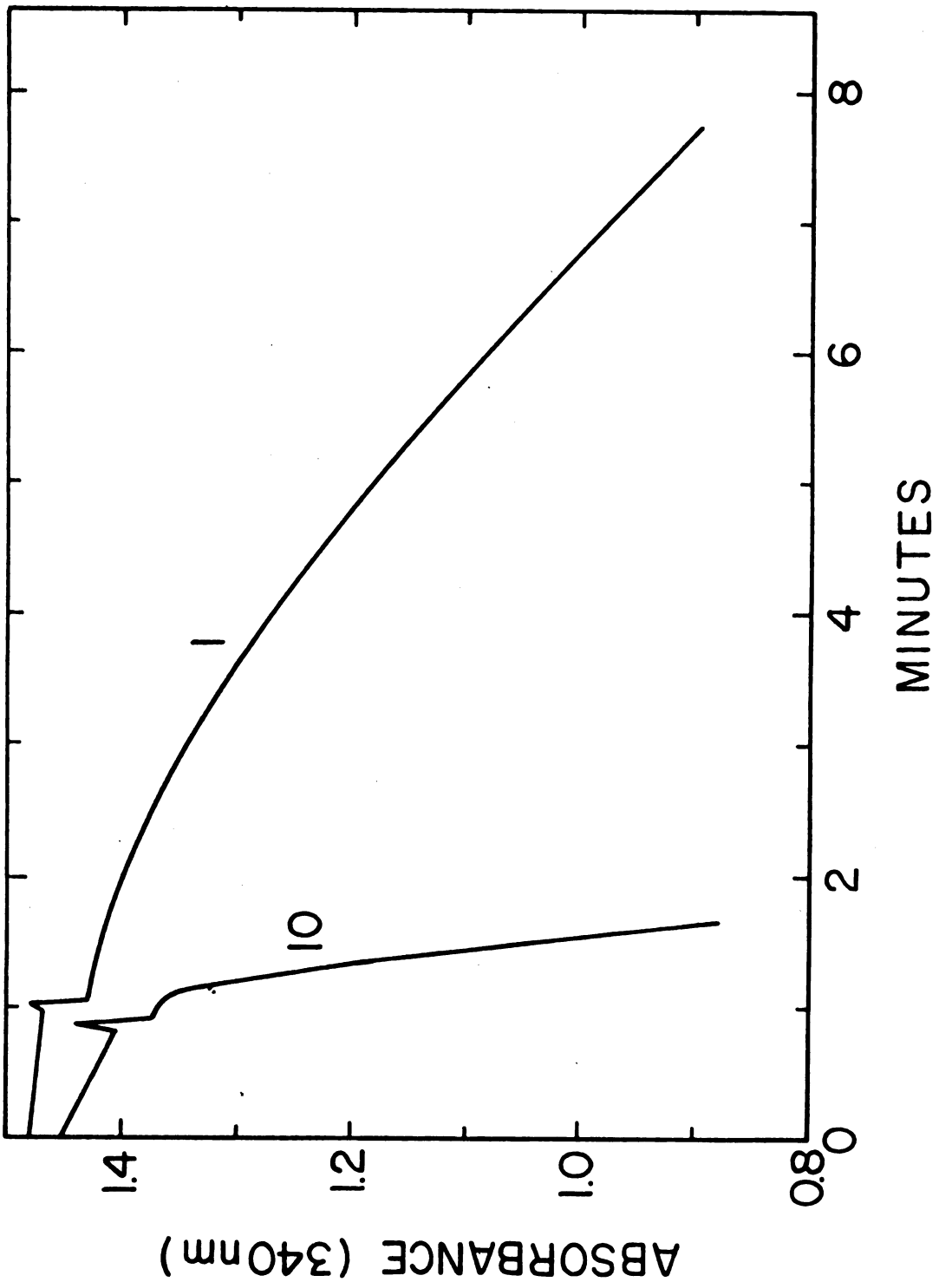
ABSORBANCE (340nm)
1.4
1.2
1.0
0.8
0
2
4
6
8
MINUTES
1
10

initial linear portion of the curves represents the reaction rate in the absence of AMP. AMP was added to the stirring cuvet solution at the spike and activation was observed subsequently. With this system it was possible to add as much as 1.1 I.U. of dehydrase per ml in the kinetic assay or about 50-fold above that used in previous studies (11). The data for the lower curve in Figure 12 were collected at a TDH concentration of 0.26 I.U./ml. At such elevated enzyme levels, the activation process appeared more rapid relative to the catalytic rate than at lower enzyme concentrations (upper curve, Figure 12, collected at 0.026 I.U./ml) and measurments of the maximum extent of activation in a single reaction mixture seemed feasible at elevated dehydrase levels.[7]

The data from a number of curves such as those shown in Figure 7 were differentiated numerically as described in Materials and Methods and the activation rate at any given time was divided by the rate observed prior to the addition of AMP. These normalized rates representing the fold activation obtained at enzyme concentrations of 0.007-1.1 I.U./ml are plotted vs. time after addition of AMP in Figure 8.

The kinetic constants given in Table 6 predict a maximum activation of about 20 fold.[8] Only at the highest enzyme concentration (1.1 I.U./ml) was it possible to achieve activation approaching the maximum. At this enzyme level this value appeared to be at least 20-fold. However, even at enzyme concentrations of 0.026-0.052 I.U./ml this value reached 13-14 fold and was still increasing steadily. The face that the fold activation approaches the expected value suggests that irreversible enzyme inactivation is not occuring under these conditions as suggested by the dilution experiments of Dunne et al. (64).

Figure 8. Activation of TDH by AMP as a Function of Time with Varying Enzyme Concentration. To a stirred cuvet containing 1 mM DTT, 0.275 mM NADH, 1 mg/ml bovine heart LDH, 0.1 M potassium phosphate, pH 8 and various amounts of TDH in a volume of 2 ml, was added 0.05 ml of a solution of 200 mM potassium AMP, pH 8.0. The absorbance was measured at 340 nm and differentiated as described in Materials and Methods. Catalytic reaction rates are expressed as a fraction of that observed prior to the addition of AMP (Fold Activation). TDH was separated from AMP as described in Materials and Methods. The quantity of TDH added to the cuvet was determined by assaying the stock of TDH (1 mg/ml) by spiking it with a 2.5% volume of 200 mM AMP, pH 8 and incubating at room temperature for 1 h before assaying with the standard catalytic assay. The TDH levels present in the cuvets were: 2.2 (▽), 1.1 (△), 0.05 (□), 0.025 (○), (A) and 0.01 (▽), 0.005 (△), 0.0025 (□) and 0.0012 (○) (B) I.U. The smooth lines through the points were drawn with the aid of a French curve.

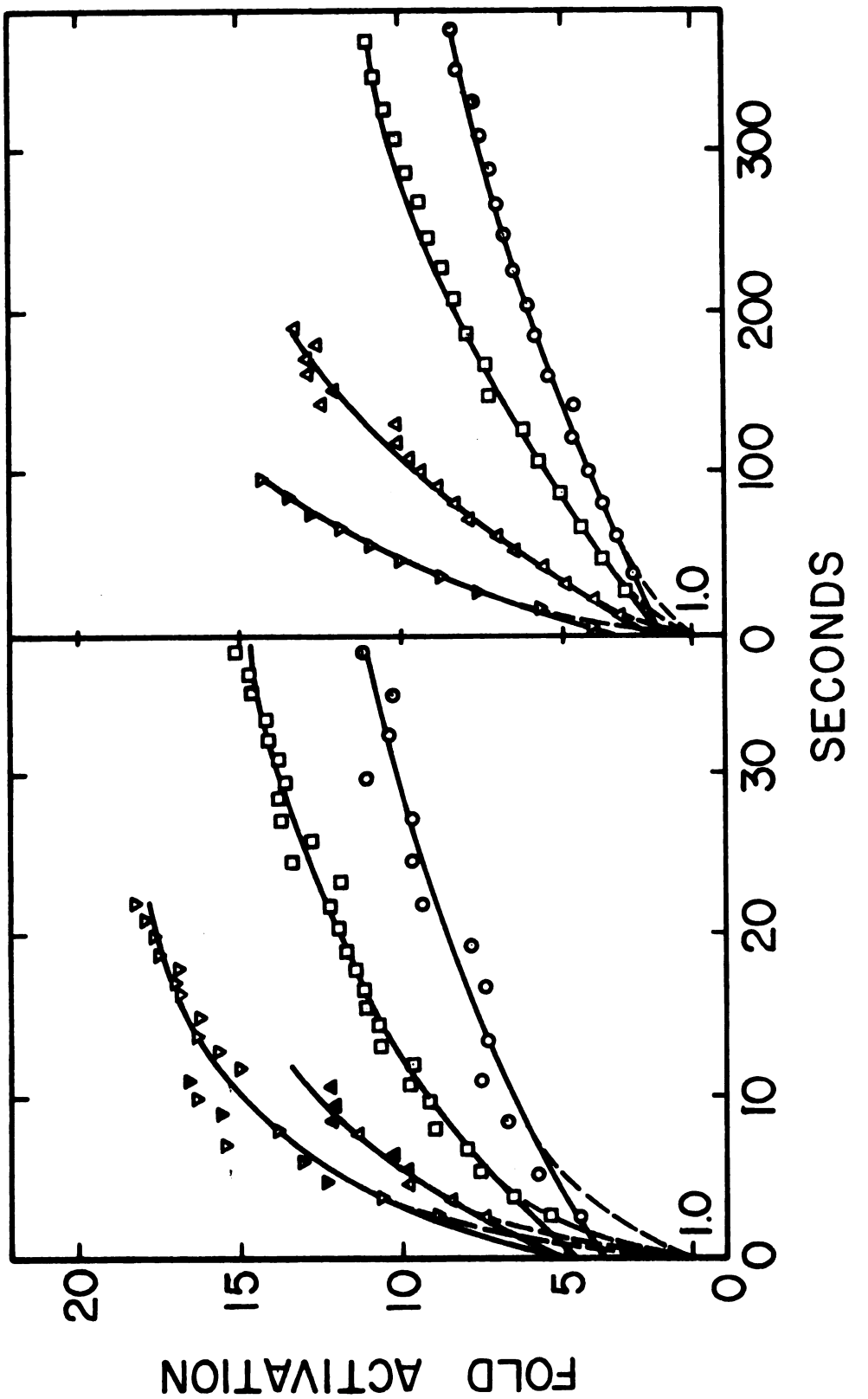
FOLD ACTIVATION
0
5
10
15
20
1.0
0
10
20
30
1.0
0
100
200
300
SECONDS

Smooth lines were drawn through the data points with the aid of a French curve[9]. Back extrapolation of these lines to zero time was made assuming an initial fold activation value of 1.0 (dashed lines of Figure 7). Despite the scatter in the data, it also appeared possible that the initial fold activation was greater than 1.0 (solid lines) suggesting an immediate activation of the enzyme upon addition of AMP. At very low enzyme concentrations these lines back extrapolated to about two, however at elevated enzyme concentrations this value was as high as five. Thus activation by AMP might actually be divided into fast and slow phases, both of which are affected by enzyme concentration. The possibility of a fast phase is examined in the Discussion.

The nature of the slow or transient phase was further investigated with the aid of a differential plot as follows. Initial rates of activation were obtained from the initial slopes of the smooth solid lines in Figure 8. These slopes were plotted against TDH concentration on a double log scale (Figure 9).[10] The least squares line through the data has a slope of 2.02 ± 0.06 (s.d.). This slope is consistent with a rate-limiting subunit dimerization in the activation process and corroborates the conclusions of others (11). The ordinate intercept of this line is 14.49 ± 0.5 (s.d.). With this value and with the assumption of a rate-limitng protomer dimerization step in the activation, it is possible to calculate a second order rate constant for protomer association of 2.7×10^5 M^{-1}.[11] This value is highly approximate and is the standard deviation of the intercept (± 0.5) suggests, may be in error by an order of magnitude.

Figure 9. Determination of the Order (q) of the Initial Rate of TDH AMP-Activation with Respect to Protein concentration by the Differential Method. Initial rates of activation were determined from the data in Figure 8 by estimating the initial slopes of the smooth lines through the points. These data were replotted according to equations given in footnote 11. The dehydrase monomer concentration was calculated from the I.U. added to the cuvet (from Figure 8), a monomer molecular weight of 40,000 (66) and a maximum specific activity of 480 I.U./mg. The slope of the least squares line through the points in the figure gives a q value and its standard deviation of 2.02 ± 0.06.

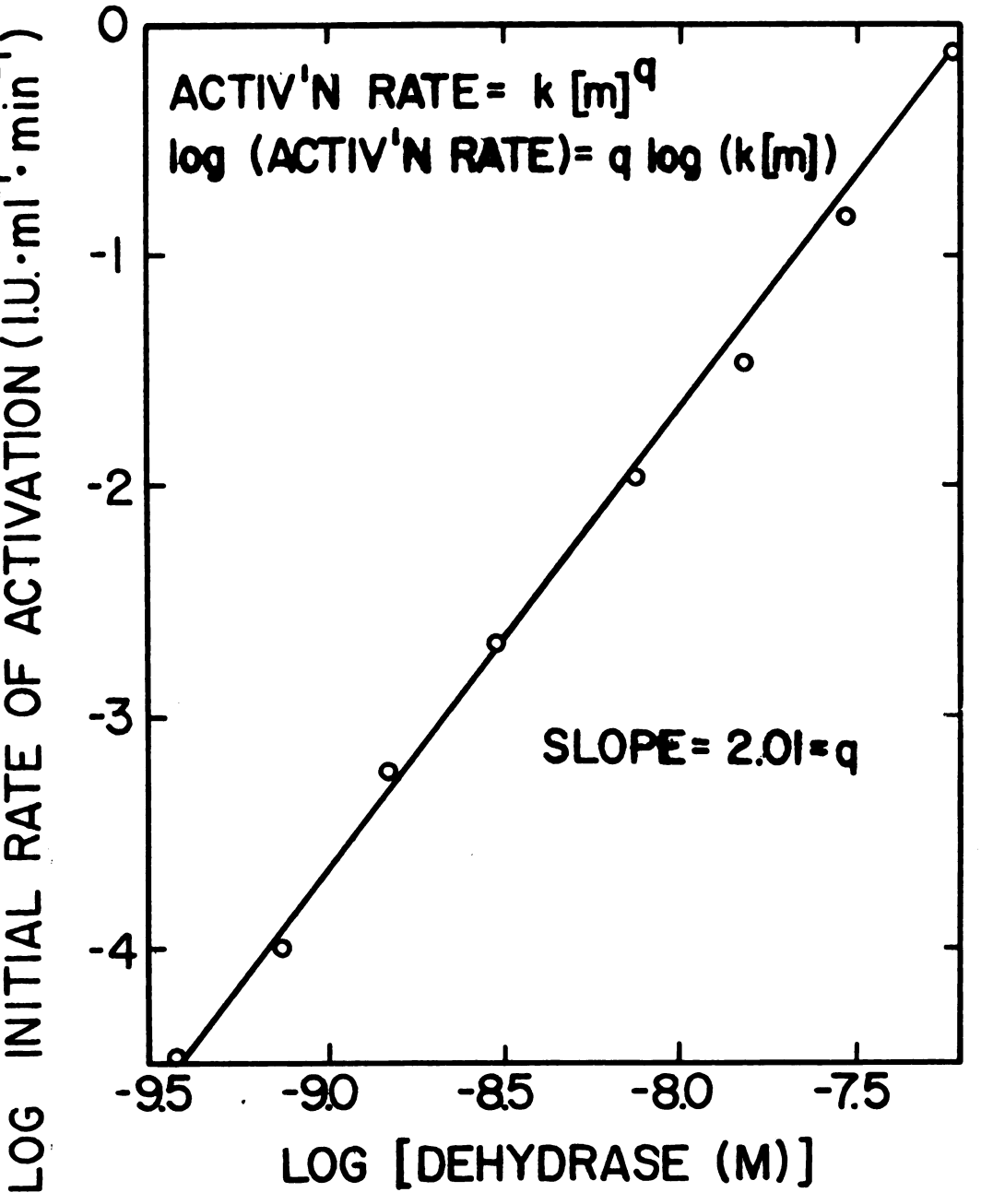
ACTIV'N RATE = k [m]^q
log (ACTIV'N RATE) = q log (k[m])
SLOPE = 2.01 = q
LOG INITIAL RATE OF ACTIVATION (I.U.·ml⁻¹·min⁻¹)
LOG [DEHYDRASE (M)]
0
-1
-2
-3
-4
-9.5
-9.0
-8.5
-8.0
-7.5

c. Nature of the Process of AMP Activation

i. Analysis of the Progress of AMP Activation

As discussed in the Literature Review, the activation process should consist of some combination of (a) pseudo first order binding reactions of AMP or threonine to the enzyme (b) first order conformational changes (c) second order dimerization reactions. The previous results suggest that it is a second order dimerization reaction which is rate limiting for activation. From the data so far presented, however, it is difficult to rule out a process in which the enzyme undergoes a concentration dependent dimerization in the assay system prior to addition of AMP, while the subsequent AMP activation reaction proceeds by first order to pseudo first order steps. An apparent increase in activation rate would be observed when enzyme concentration was increased if dimers activated more rapidly than monomers. To distinguish between a rate limiting and a "pre-established" dimerization, the process of activation was analyzed to determine whether it proceeded by first or second order rate limiting steps. When these reaction progress data were differentiated as described in Materials and Methods and plotted on an inverse time axis, plots such as that shown in Figure 10 were obtained. The reaction velocities extrapolate to a final activated velocity (V_H) at infinite time. However this final velocity is ill-determined because the activation process is terminated before completion.[12]

In an attempt to determine the order of the activation process, the velocity-time data in Figure 10 were fit to linear transformations of either first or second order integrated equations as described in Materials and Methods. In this fitting method, the V_H value was adjusted to maximize the strength of the linear fit. Although the fit to the second

Figure 10. Inverse Time Plot Showing Approach to Completion of the Activation of TDH by AMP. To a stirred cuvette containing 1 mM DTT, 0.275 mM NADH, 1 mg/ml bovine heart LDH, 0.1 M potassium phosphate, pH 8.0, and 0.12 8 I.U. of TDH activity 2 ml volume, was added 0.05 ml of a solution fo 200 mM KAMP, pH 8.0. The catalytic reaction was followed at 340 nm and reaction rates calculated as described in Materials and Methods. V_H values expected for first and second order processes were estimated by a parabolic search which maximized the strength of linear fits to either equation 4 or 5. The V_L value for these fits were obtained from the reaction rates observed prior to the addition of AMP. Dehydrase monomer concentration (L_O) was obtained assuming a molecular weight of 40,000 and a specific activity of 480 I.U./mg. Points represent a tracing of differentiated data plotted using a HP7200 plotter interfaced to the HP9815A. Theoretical lines for a second order (dashed line) or first order (dashed-dotted line) were calculated from the optimized fits of equation 5 or 4 to the data.

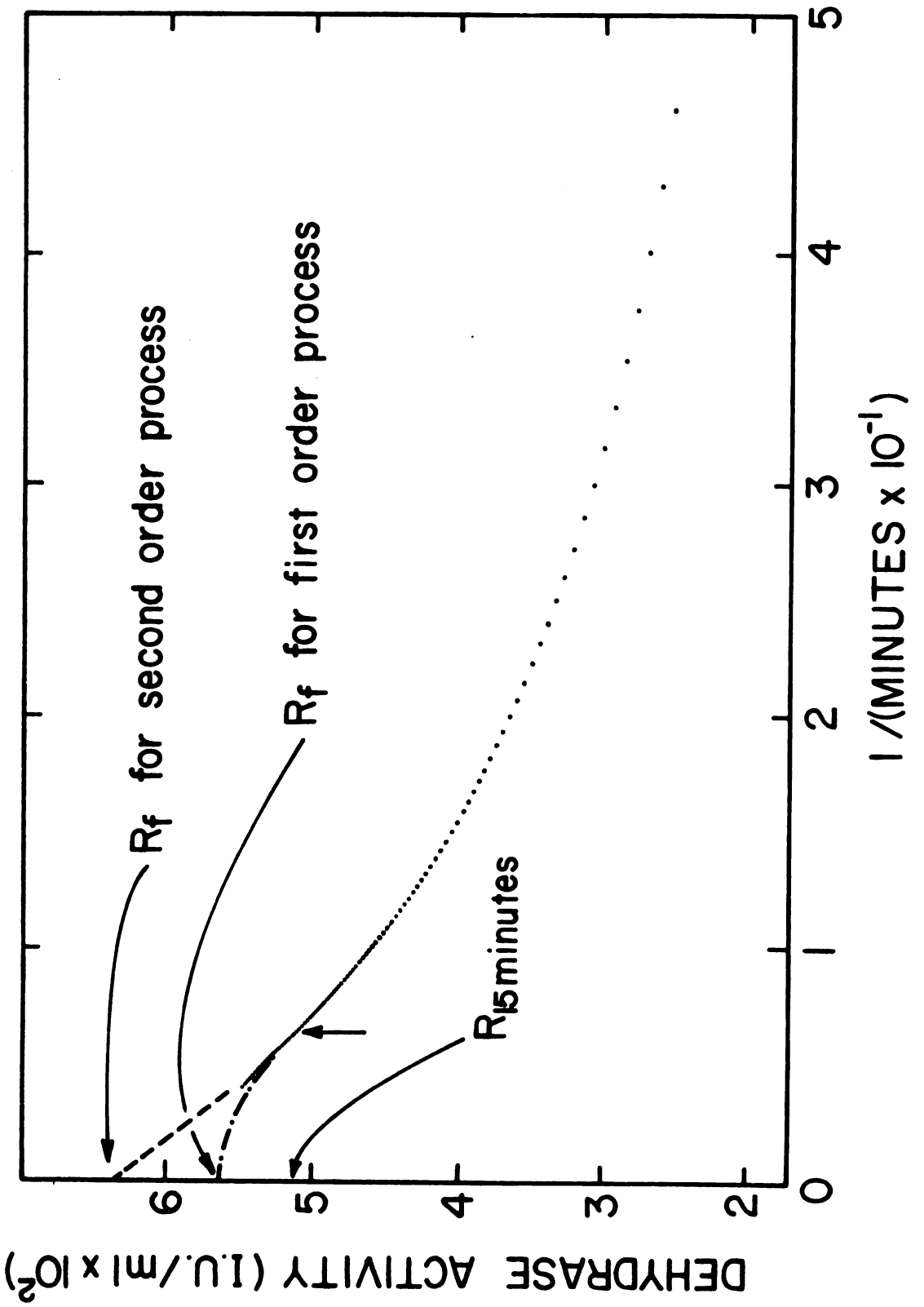
DEHYDRASE ACTIVITY (I.U./ml x 10^2)
1/(MINUTES x 10^{-1})
R_f for second order process
R_f for first order process
$R_{15 minutes}$
0
1
2
3
4
5
2
3
4
5
6

order equation was slightly better, the data were found to correlate well with either first or second order models, and neither could be rejected on this basis alone. Figure 10 shows that a second order process predicts a continuous rise in the absolute value of the slope of this plot, however a first order process predicts an inflection point at the position of the arrow, and a leveling off of the velocity to a lower V_H value. In the region where data are available the curves are smaller. Although a slight inflection appears in the data near the position of the arrow, it is difficult to rule out enzyme inactivation as a cause for the fall off in rate. Evidence that a second order fit is more appropriate comes from the fact that the optimal V_H (0.064 I.U.) for a second order fit is very close to the number of units added to the cuvet as measured by the standard assay (0.0638 I.U.), whereas the optimal V_H for the second order fit (0.057 I.U.) would require extensive enzyme inactivation to have occured during dilution procedures and/or assay. Such inactivation has been postulated to account for apparent losses in enzyme activity upon dilution into buffers not containing AMP (64), however these studies (64) took the 15-min reaction rate ($V_{15\ min}$) as a measure of the final extent of reactivation. However, as shown in Figure 10 this measurement underestimates the true V_H significantly. This underestimation could be more extensive if assay conditions were not optimized to maximize the extent of reactivation during the assay.[11]

In this connection, although activation appears very nearly complete toward the end of the period in curve 1, Figure 7, an analysis of this curve similar to that in Figure 10 shows that the activation may only be 60% complete if a second order process is involved. This example demonstrates the error of using an apparently linear portion of the activation

progress curve as a measure of V_H as was done previously (64). This error may be aggravated by slight systematic errors in absorbance measurement as discussed in the Methods section of Chapters I and II.

Table 7 compares the linear correlation coefficients obtained for first or second order fits to a number of data sets similar to that in Figure 10. As the concentration of enzyme in the reaction is increased, a small increase occurs in the % completion attained by the end of the activation curve (see footnote 7). The linear correlation coefficients of the optimal first or second order fits do not differ at low enzyme concentrations. However, when the final extent of reactivation enters the region where these curves tend to diverge (about 81% in Figure 10) the first order fit becomes slightly poorer.

When the optimal first or second order V_H values are plotted as a percentage of enzyme concentration (in V units) added in the reaction (Figure 11) it can be seen that a first order fit (open circles) requires an anomalous loss of 10-30% of the TDH activity during dilution and/or assay in the absence of AMP. Assumption of a second order process, on the other hand, requires no loss at elevated enzyme concentrations and only a 12% loss at the lowest enzyme level. The lower curve shows the percentage of completion after a 15 minute activation period as a percent of added TDH. This curve is similar to one presented by others, as evidence for an anomalous loss in enzyme activity upon TDH dilution into AMP deficient buffers (64).

The data presented in Figures 10 and 11 and in Table 7 indicate that the activation process occurs via a second order process. Figure 11 shows that assumption of an anomalous loss is not necessary at higher

Table 7

Optimized Linear Fits of Activation Progress Curves to Either a First or Second Order Processes[a]

TDH Concentration (I.U./ml)	Duration of Activation (min.)	Linear Correlation Coefficient		Difference (Second - First)
		Second Order	First Order	
0.0076	34	0.9979	0.99989	-0.00010
0.0152	35	0.99985	0.99970	0.00015
0.0305	32	0.99972	0.99927	0.00045
0.0636	25	0.99960	0.99948	0.00012
0.0636	15	0.99987	0.99912	0.00075
0.0708	26	0.99967	0.99839	0.00128
0.1220	13	0.99983	0.99857	0.00126

[a]Activation Progress Curves were identical to those described in Figure 11.

Figure 11. Extent of Reactivation by AMP as a Function of TDH concentration and of the Procedure Used to Determine Maximum Reactivation. Reactivation experiments identical to that described in Figure 10 were performed but with varying concentrations of TDH in the cuvet. The data were analyzed by either equation 5 (●) or 4 (○) using a parabolic search routine which varied V_H to maximize the strength of the linear fit. Alternatively the V_H was taken to be the observed catalytic activity after 15 minutes of reactivation as done by Dunne *et al.* (64) (△). The determined V_H (I.U./ml) value was expressed as a percent of the concentration (I.U./ml) of TDH in the cuvet (determined by separate experiments as described in Materials and Methods).

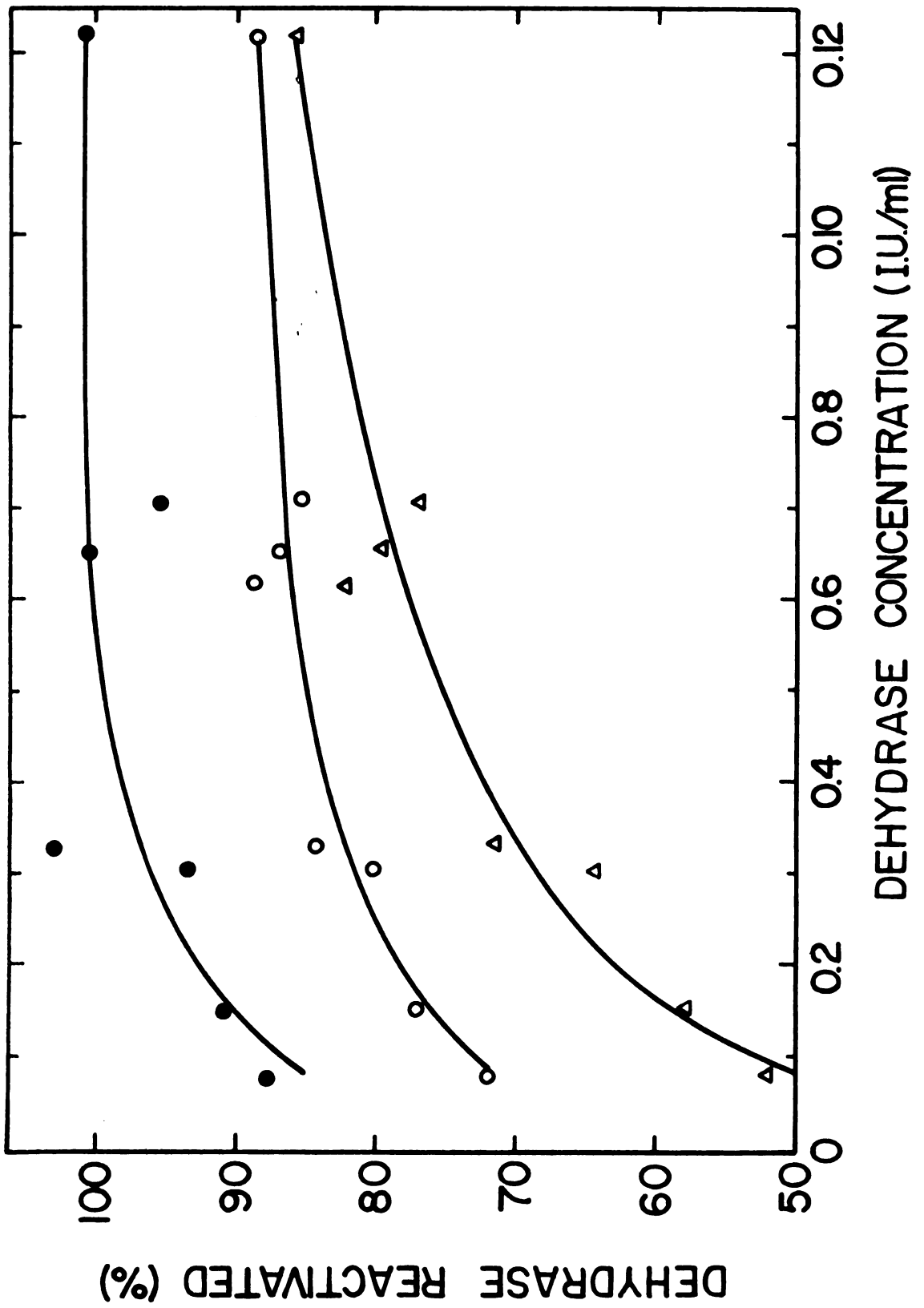
DEHYDRASE REACTIVATED (%)
100
90
80
70
60
50
0
0.2
0.4
0.6
0.8
0.10
0.12
DEHYDRASE CONCENTRATION (I.U./ml)

enzyme levels if the prolonged nature of this second order process is taken into account.

ii. Pre-established Polymerization as an Alternative Hypothesis

The possibility that a concentration dependent, pre-established polymerization contributes to the protein order dependence of activation rate was tested by examining the structure of TDH in the absence of AMP.

Dependence of molecular weight on protein concentration in the absence of AMP has already been demonstrated by sucrose denisty centrifugation (7). Boundary sedimentation velocity experiments were performed in the absence of AMP at two concentrations of TDH (Figure 12). The raw sedimentation coefficients were corrected for viscosity and density of the buffer solution using literature data (93). From the S_{20w} values of Figure 12 and from available nomograms (99), approximate molecular weights of 40,000 and 100,000 may be estimated at TDH concentrations of 8.4 and 107 I.U./ml respectively. Since the molecular weight of the TDH protomer is known to be about 40,000 (66), it may be concluded that dimerization was very low at the lower of these enzyme concentrations but that it was complete at the higher enzyme level. From these data, a range for the enzyme dissociation constant can be set between 10 and 100 I.U./ml[13] (5-50 x 10^{-7} M in conventional units, assuming a specific enzyme activity of 480 I.U./mg).

The highest enzyme concentraion used in the present studies of the activation process was 1.1 I.U./ml (see Figure 8). It may be shown that at this enzyme concentraion less than 16% of enzyme monomers would have been dimerized in the absence of AMP. It is difficult to imagine how the change in structure of only 16 percent of the enzyme protomers present

Figure 12. Boundary Sedimentation Velocity of TDH in the Absence of AMP as a Function of Enzyme Concentration. Ultracentrifugation of TDH in the absence of AMP was carried out as described in Materials and Methods. The enzyme concentration of the centrifuged solutions are given in the figure. The photometer was set to either 280 nm (○) or to 230 nm (△). Best fit lines through the points were determined by least squares regression.

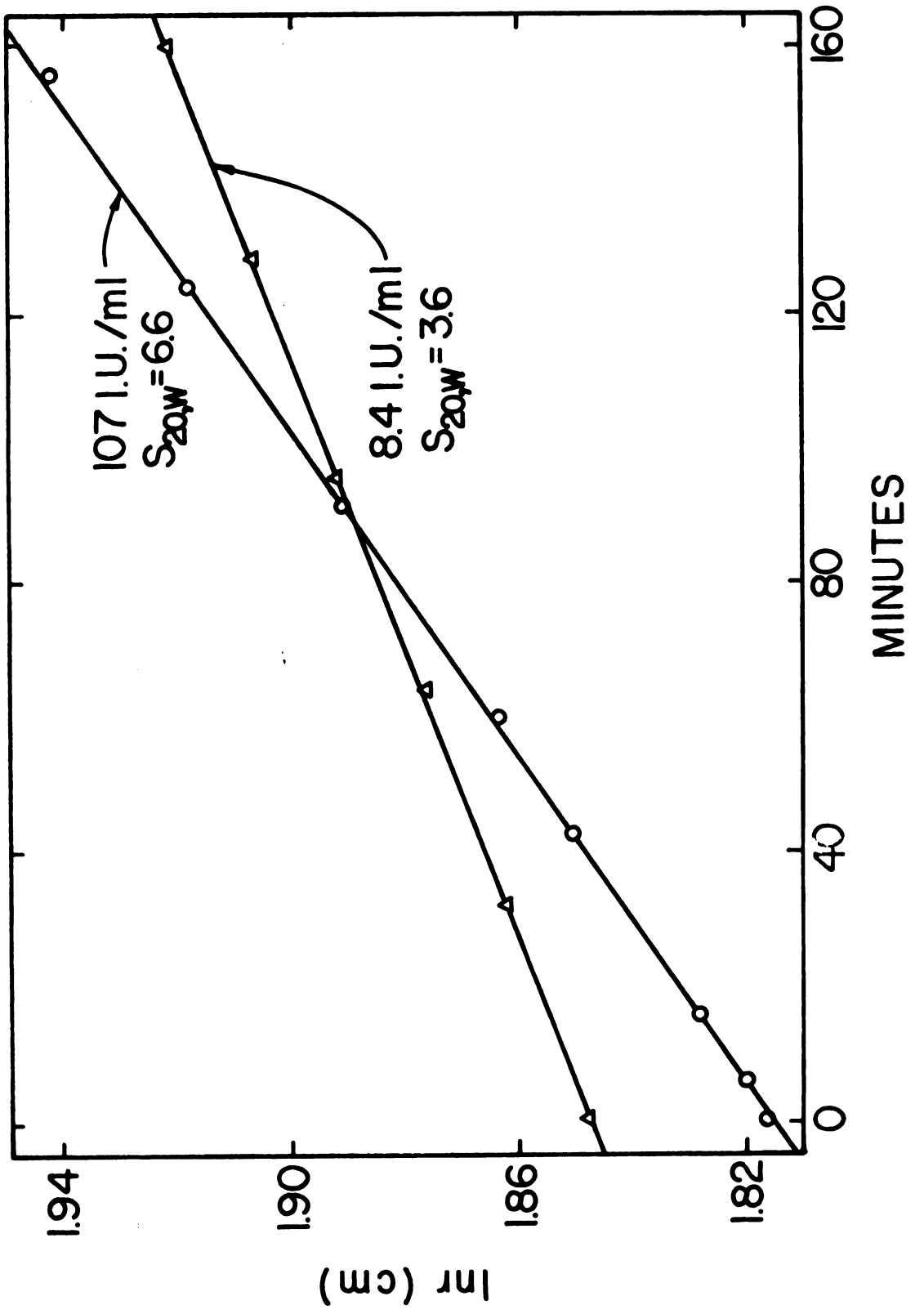
1.94
1.90
1.86
1.82
lnr (cm)
0
40
80
120
160
MINUTES
107 I.U./ml
$S_{20,w}$=6.6
8.4 I.U./ml
$S_{20,w}$=3.6

could account for the large changes in activation rate illustrated in Figure 9. However, the presence of 5-15% protomers already associated might be expected to be rapidly activated by AMP and to produce a rapid increase in reaction velocity if this small percentage was not required to dissociate and redimerize upon binding of AMP. Such a burst in the activation process was observed in Figure 8 and this hypotheiss is further considered in later sections of this thesis.

It should be pointed out that the above sedimentation experiments yield only an approximate dissociation constant because these measurements were not made at elevated concentrations of ammonium sulfate and coupling enzyme nor in the presence of 20 mM substrate as prevailed in the AMP activation experiments. Active enzyme centrifugation in the presence of L-threonine has been performed by others (68). This work suggests that the apparent dissociation constant for the monomer-dimer equilibrium in the absence of AMP increases with increasing L-threonine concentration. At 100 mM L-threonine the value is about 45 I.U./ml[14] and is consistent with the results presented here.

iii. Rate Constant for the Activation Process

When activation time course data, such as those obtained in Figure 10, were transformed and presented as second order plots (see Materials and Methods), using the quantity of enzyme added a a measure of V_H, plots such as those in Figure 13 were obtained. The data appear fairly linear over the ten-fold range of enzyme concentrations examined.

As described in Materials and Methods, it is possible to calculate a second order rate constant for activation from a single experiment.

Figure 13. Second Order Integrated Kinetic Plot of TDH AMP-Activation Progress Curves. Data from activation progress curves similar to that described in Figure 10 were differentiated as described in Materials and Methods and treated according to equation 4. The numbers adjacent to the lines give the enzyme concentration during the activation process in units of I.U./ml x 10^{-2}. The catalytic assay was determined at 382.5 nm (●, ○, □) 372.5 nm (△) and 340 nm (▽) as described in Materials and Methods.

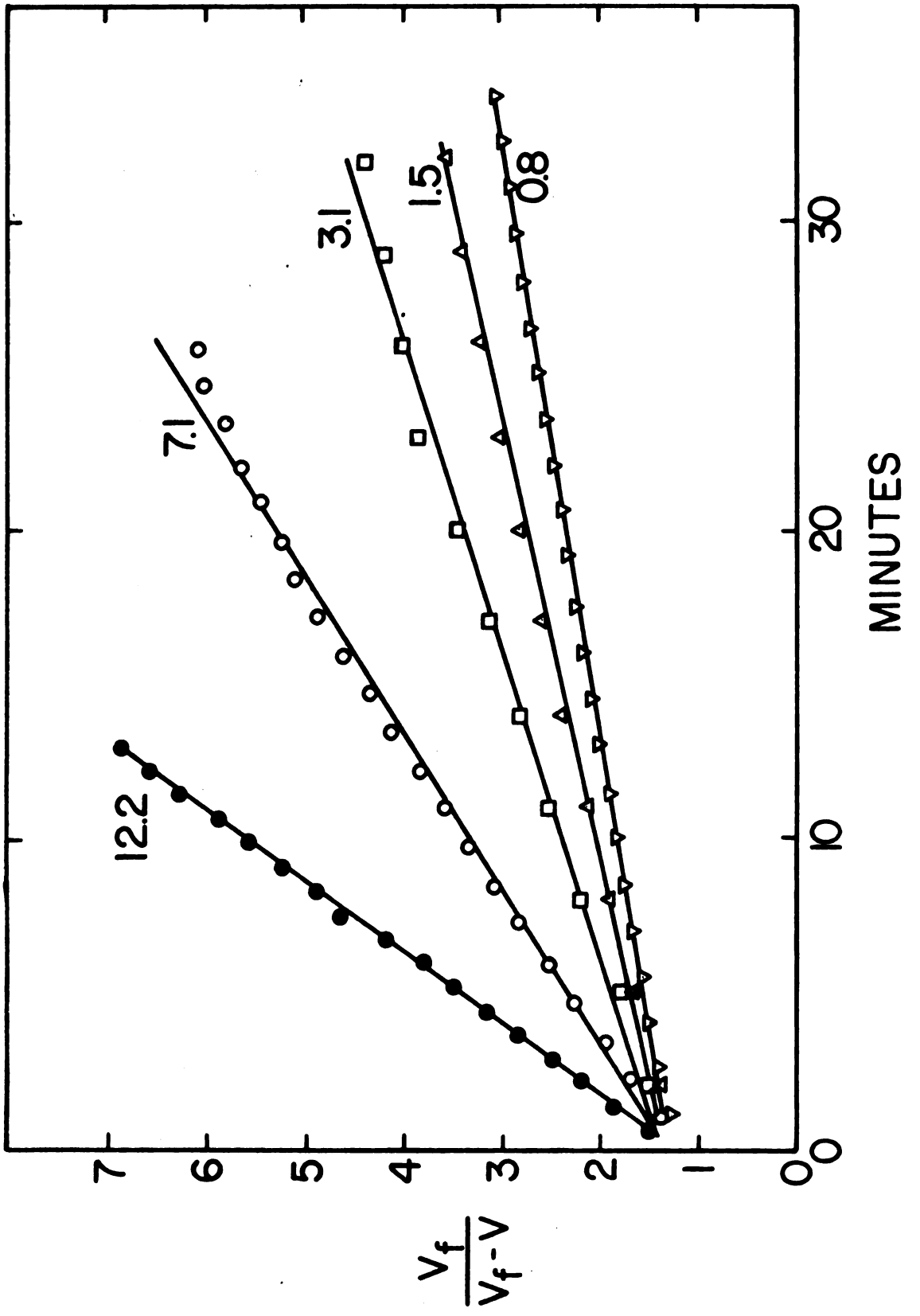
12.2
7.1
3.1
1.5
0.8
0
10
20
30
MINUTES
1
2
3
4
5
6
7
$\frac{V_f}{V_f - V}$

However the information from all of these experiments may be combined by replotting the SLOPE/INTERCEPT ratios vs. enzyme concentration as shown in Figure 14.

As described in Materials and Methods, this plot should yield a straight line passing through the origin, whose slope equals the second order rate constant for activation. The weighted least squares line in Figure 14 fits the data with a linear correlation coefficient of .967 and passes close to the origin. The slope of this line is 8.8 (± 1) x 10^5 $M^{-1}sec^{-1}$ providing a measure of the second order activation rate constant. This value agrees well with the value of 2.7 x 10^5 $M^{-1}sec^{-1}$ determined from Figure 9 considering the large error in the determination of the latter value (see discussion in the RESULTS associated with Figure 9). The lines drawn through the data in Figure 13 are theoretical lines calculated assuming a second order rate constant for activation of 8.8 x 10^5 $M^{-1}sec^{-1}$.

For comparison, the first order plots of these data are shown in Figure 15. Smooth curves through these data illustrate the non-linearity of these plots. As described earlier, it was possible to obtain linear first order plots by adjusting the V_H value used in the calculation. When optimal V_H values were used to transform these data, the slopes of these lines (data not presented) can be replotted as shown in Figure 16. The equations derived in Materials and Methods show that these slopes should equal the hypothetical first order rate constant of activation. Figure 15 shows that this hypothetical rate constant varies with enzyme concentration. This means that the activation process cannot be characterized by a single first order rate constant.

Figure 14. Determination of Second Order Rate Constant for Activation of TDH by AMP. Slopes and intercepts were obtained from Figure 13 (data from 2 additional experiments are included) and the ratio plotted versus TDH concentration as described in Materials and Methods and Results. The catalytic reaction was determined by measuring the absorbance at 340 nm (●), 372.5 nm (○), or 382.5 (□). The Bars represent the approximate standard deviation of the SLOPE/INTERCEPT ratio determined from SLOPE and INTERCEPT variances in the least squares fits of Figure 13. The weighted data were fitted to a least squares line and the k_2 calculated from this slope according to equation 5. The k_2 and its approximate standard deviation determined from this analysis was 8.8 (± 1.0) x 10^5 M^{-1} sec^{-1}.

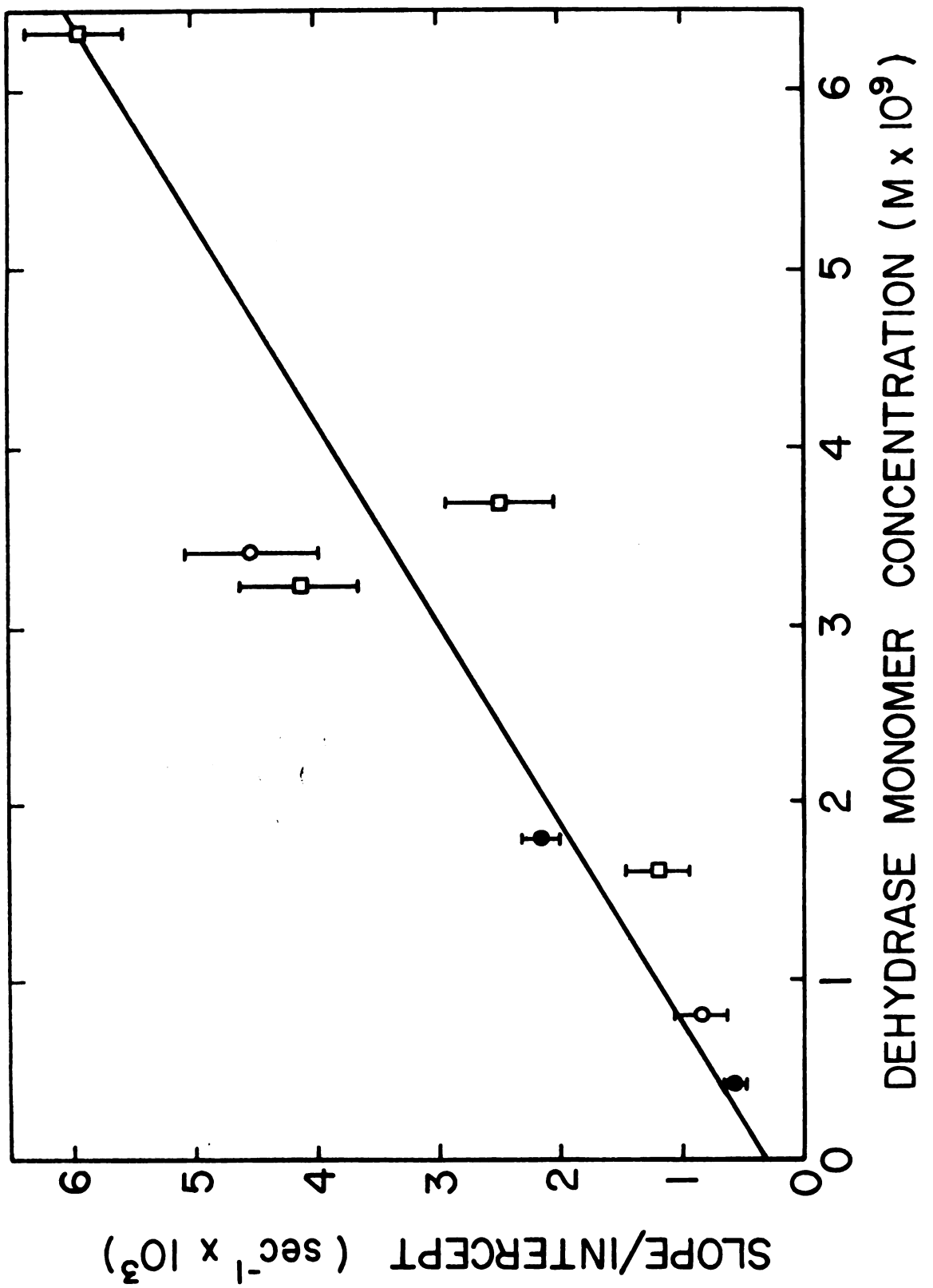
SLOPE/INTERCEPT (sec^{-1} x 10^3)
0
1
2
3
4
5
6
DEHYDRASE MONOMER CONCENTRATION (M x 10^9)
0
1
2
3
4
5
6

Figure 15. First Order Integrated Kinetic Plot of TDH AMP-Activation Progress Curves. Data described in Figure 13 were reanalyzed according to equation 4. The numbers and symbols have the same meaning as given in Figure 13. Hand drawn smooth lines through the data are added for clarity.

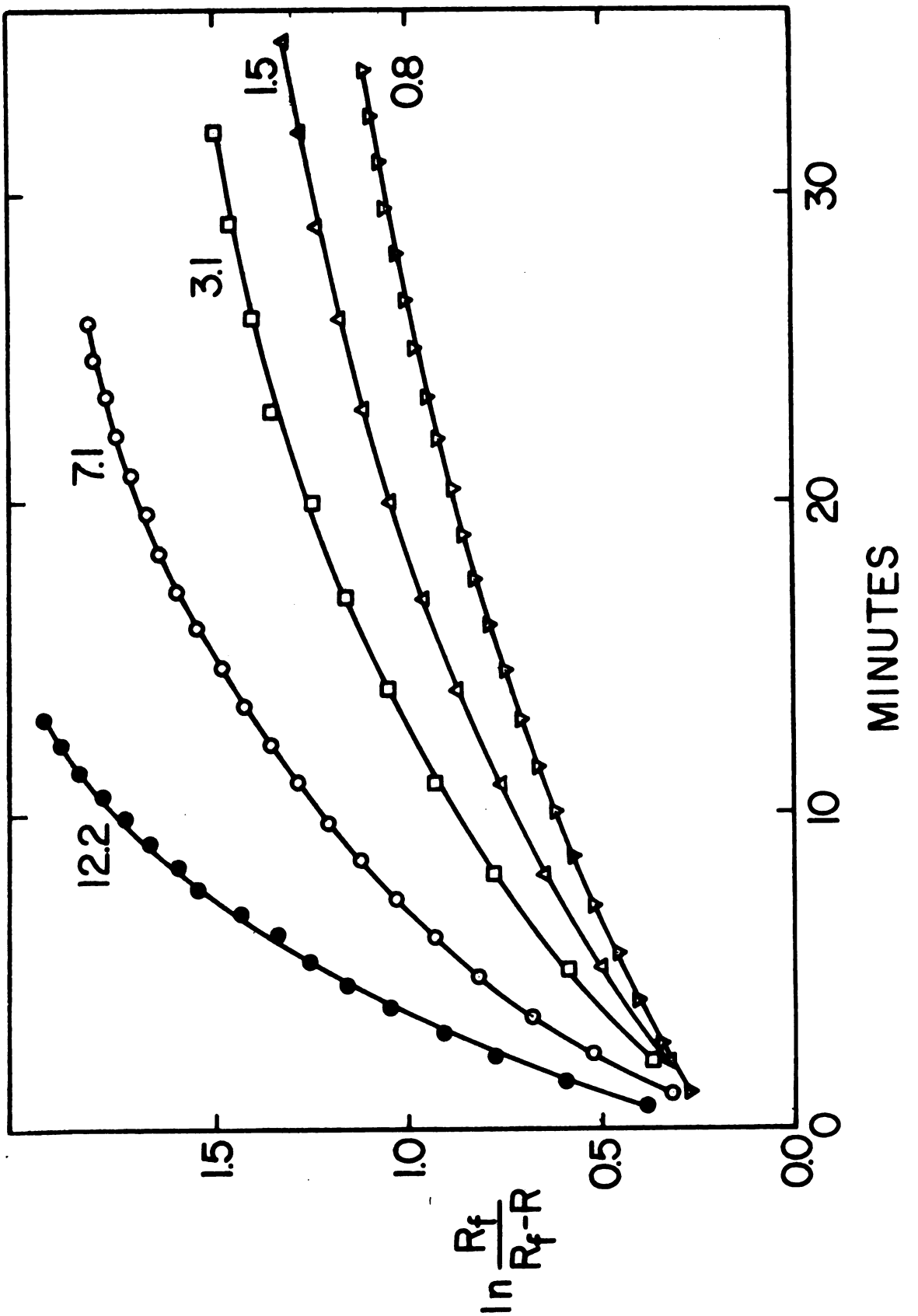
12.2
7.1
3.1
1.5
0.8
0.0
0.5
1.0
1.5
0
10
20
30
MINUTES
ln Rf/Rf-R

Figure 16. Determination of Apparent First Order Rate Constant for Activation of TDH by AMP. The same data as described in Figure 13 were re-analyzed according to equation 4. The V_H value for each experiment was varied as a parameter in a parabolic search to maximize the strength of the linear fit to equation 4. The least squares slopes and their associated standard deviations (bars) are plotted above according to equation 4. The catalytic reaction was determined by measuring the absorbance at 340 nm (●), 372.5 nm (○) or 382.5 nm (□).

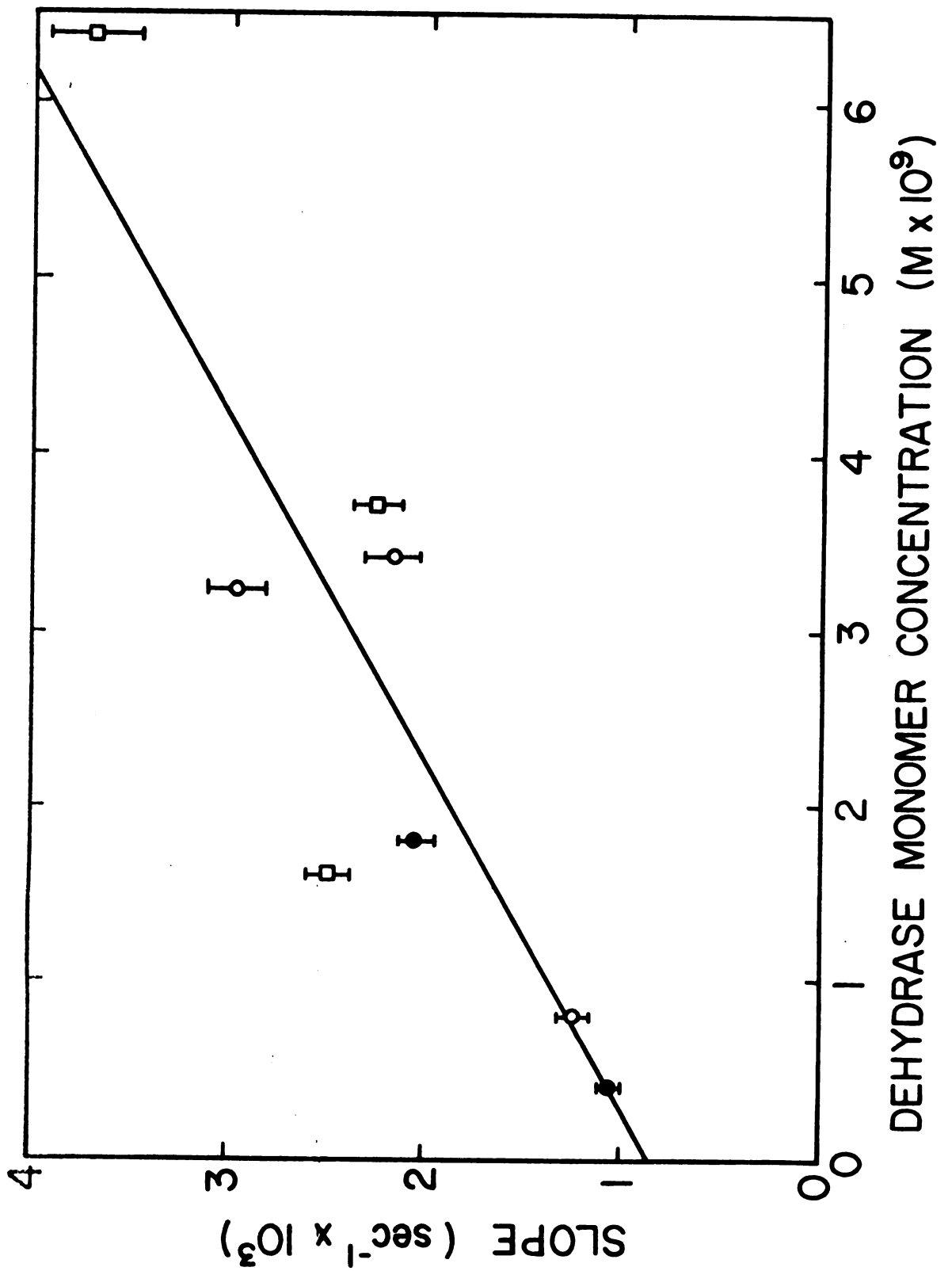
SLOPE (sec^{-1} x 10^3)
DEHYDRASE MONOMER CONCENTRATION (M x 10^9)
0
1
2
3
4
5
6

d. Effect of Sucrose on the Rate of Reactivation

As considered in both Literature Review and Discussion of this chapter, a second order rate constant for association of 8.8×10^5 $M^{-1}sec^{-1}$ is of a magnitude which could be considered diffusion controlled if the dimerization is very highly sterically restricted and if the highly charged nature of TDH is taken into account. The upper limit for a second order rate constant may be obtained from diffusion theory as follows (100):

$$k_2 = \frac{8\pi N}{1000} aDe$$

where N is Avagodro's Number, a is the distance of closest approach of the dimerizing species, D is the diffusion coefficent of the monomer, and e is a factor which takes into account electrostatic interactions between reactants. From Fick's first law of diffusion of spherical particles in ideal solution (100),

$$D = \frac{RT}{fh}$$

where R is the gas constant, T is temperature, f is the frictional coefficient of the diffusing species and h is the viscosity of the medium. Combining these equations gives:

$$k_2 = \frac{8\pi NaRTe}{1000fh} \qquad [7]$$

This predicts that a diffusion controlled bimolecular rate constant should be inversely proportional to the viscosity of the solution at constant temperature.

When the concentration of sucrose was varied in the AMP-activation medium, the second order rate constant, determined from second order plots for activation was affected as shown in Figure 17. As predicted by

Figure 17. Dependence of Second Order Reactivation Rate Constant on Viscosity. The apparent k_2 for reactivation was determined from reactivation progress curve data as described in Figure 10 and in the test. Either 2 (●), 4 (○) or 6 (△) micrograms of TDH (specific activity 463 I.U./ml) were added to the stirred cuvet. Error bars on the data points represent the standard deviations of the determined k_2 value and were used to weight the fit of the data to the least squares line indicated in the figure. The numbers adjacent to each point give the concentration in percent (w/v) of sucrose present in the activation mixture.

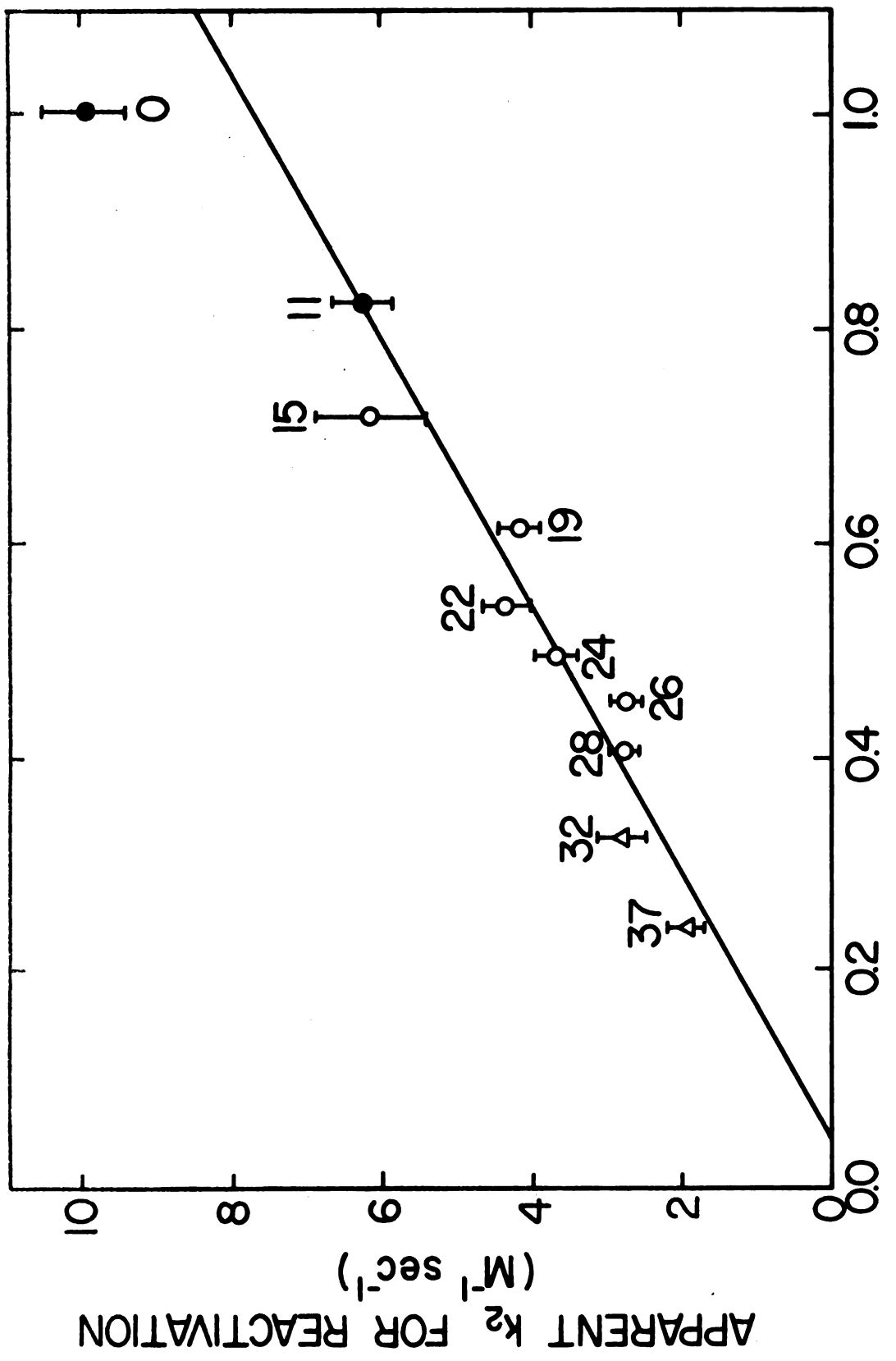
APPARENT k_2 FOR REACTIVATION
(M^{-1} sec^{-1})
I/RELATIVE VISCOSITY
0.0
0.2
0.4
0.6
0.8
1.0
2
4
6
8
10
0
11
15
19
22
24
26
28
32
37

equation 7, the data are reasonable well fit by a straight line (linear correlation coefficient = 0.935) which passes close to the origin.

The assumption was made in calculating the rate constants in Figure 17 that sucrose did not raise the dissociation constant for dimerization. Since the AMP induced oligomerization of TDH is also observed to occur in sucrose density gradients (7), a major effect seems unlikely, at least at the lower sucrose concentrations. The V_H values used in calculating the second order rate constants for Figure 17 were obtained by separate measurements of enzyme activity at the given sucrose concentrations. As the concentration of sucrose was raised, the enzyme activity decreased. At the highest sucrose concentration (37%, w/v) the TDH activity was reduced by 50%. A loss of "activatable" subunits however, is unlikely to be the sole cause for the effect on the activation rate since at this same sucrose concentration, the rate constant for activation was lowered by a factor of about 5. A reduction in activatable subunits by 50% could only introduce a 2-fold error in the calculation of the rate constant as seen from Equation 5 in Materials and Methods. It was assumed that the effect of sucrose was to decrease the specific activity of all the threonine dehydrase active sites rather than specifically alter a fraction of the molecules. Such a general effect should not interfere with the methods used here to determine the rate constant.

To test further whether the effect of sucrose was specific or general, glycerol was used in place of sucrose to increase the solution viscosity during activation. At a concentration of glycerol expected to approximately double the solution viscosity (19.5% v/v, see reference 101), the second order rate constant was reduced from 8.9 (± 0.2) x 10^5 $M^{-1}sec^{-1}$ to 4.7 (± 0.3) x 10^5 $M^{-1}sec^{-1}$. These data

suggest that in the case of glycerol too, the rate constant is approximately proportional to solution viscosity. At this concentration of glycerol, the enzyme activity was also reduced by 50%.

e. Effect of Temperature on the Rate of Activation

If the dimerization process is diffusion controlled as suggested by the above measurements in the presence of sucrose, then dimerization should have a low energy of activation (100). Experiments were conducted to measure the Arrhenius activation energy of the process of AMP activation.

Measurements of k_2 (the apparent second order dimerization constant) were made at a series of temperatures. Calculation of this rate constant was made from second order plots of activation progress curves. V_H values necessary for these plots were determined by separate measurement of enzyme activity at the various temperatures. The results of these experiments are shown in the Arrhenius plot of Figure 18. The slope of this plot yields an activation energy of 6.2 (± 0.4) kcal/mol. This value is slightly higher than 2-4 kcal/mole which would be anticipated for a diffusion controlled reaction (100). From this figure, it can be calculated that the apparent rate constant for activation, k_2, varies by a factor of 2 over the 23° K range where data were available. This value is a much larger change than would be expected based upon Equation 7, and is somewhat at variance with results from the viscosity experiments described above. However, it is important to emphasize the preliminary nature of these experiments, as these temperature studies assume that the quantity of activatable subunits is not affected by temperature. Of course the question of diffusion control concerns the

Figure 18. Determination of the Apparent Arrhenius Activaton Energy for the AMP-Activation of TDH. Activation experiments were performed as described in Figure 10 except that the temperature was varied as shown on the abscissa. The data was treated according to equation 5 to determine the second order rate constant for activation, k_2, and its associated standard deviation (bars). The cuvet contained either 0.038 (□) or 0.076 (○) I.U. of TDH as determined by separate catalytic assays. The solid line represents a weighted least squares fit to the data. The Arrhenius activation energy (and its standard deviation) calculated from this line is 6.2 (± 0.4) K cal/mol.

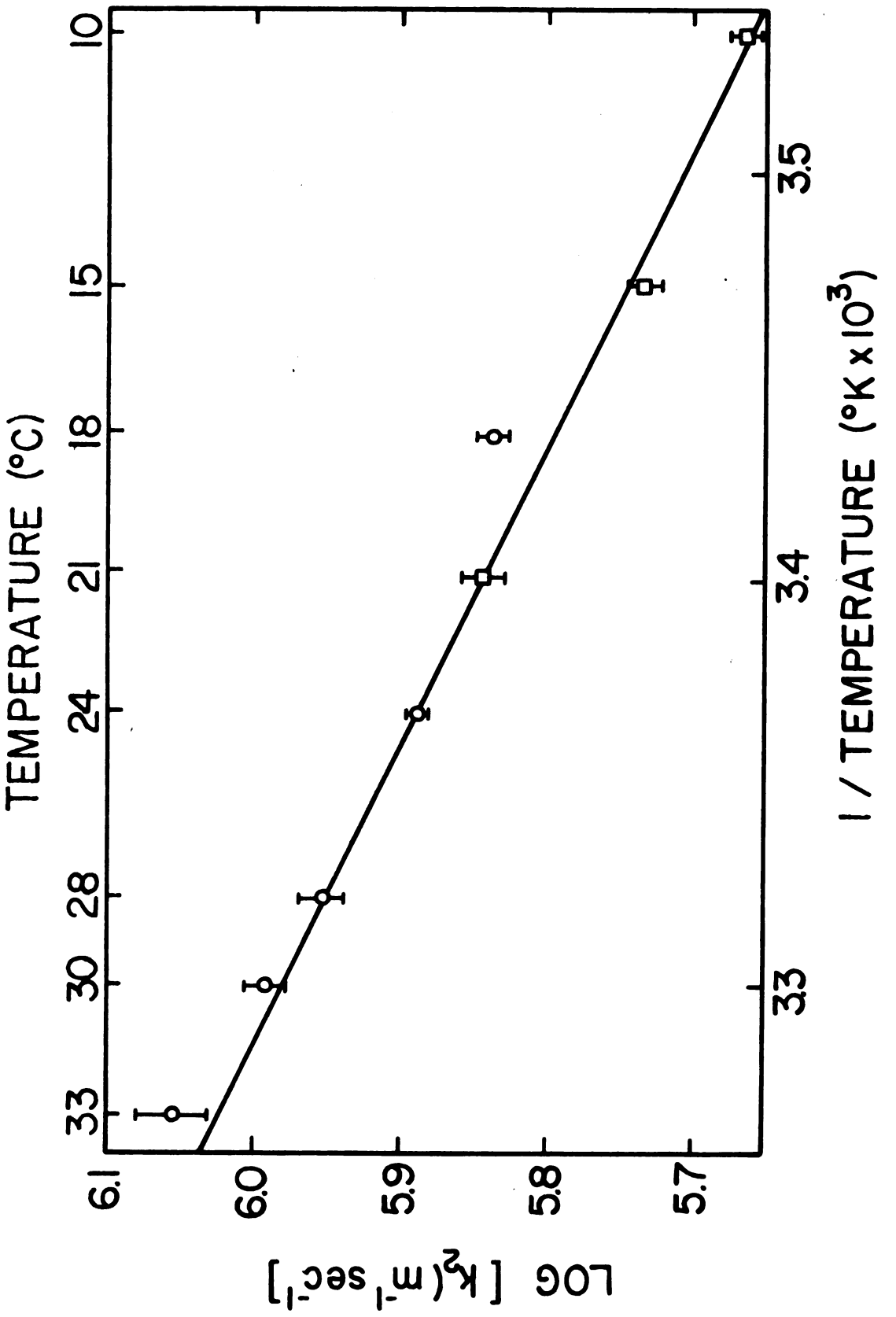
TEMPERATURE (°C)
10
15
18
21
24
28
30
33
1 / TEMPERATURE (°K x 10³)
3.5
3.4
3.3
LOG [k_g(m⁻¹sec⁻¹)]
6.1
6.0
5.9
5.8
5.7

mechanism of the dimerization and does not affect the conclusion that the dimerization is the rate limiting step in the process of activation.

4. Activation of Matrix-Bound TDH by AMP

a. Properties of TDH Immobilized on Sepharose

The experiments so far presented suggest that a dimerization process is the slow step in the activation of TDH by AMP. These results were obtained by measurements of the progress of the activation as it occurs with soluble dehydrase. An alternate approach involves observation of the effect of AMP under conditions where dimerization cannot occur. For this purpose TDH was immobilized on cross-linked Sepharose 4-B activated by cyanogen bromide treatment (86), and the properties of the covalently bound enzyme were examined.

Initially the effect of immobilization upon TDH specific enzyme activity in the presence of AMP was examined. As shown in Figure 19, as the quantity of cyanogen bromide used to activate the matrix was increased, the specific enzyme activity of the resulting immobilized enzyme decreased. In this experiment, activity was measured in the standard catalytic assay, and the quantity of enzyme present on the matrix was determined from the radioactivity of a quantity of matrix containing immobilized ^{3}H-TDH. Figure 19 shows that the specific enzyme activity (expressed as I.U./dpm) of the TDH attached using low cyanogen bromide concentrations (2-5 mg CNBr/ml Sepharose) is about 75% that of soluble enzyme, but drops to 15% at elevated levels (80-160 mg CNBr/ml). This shows that it is possible to prepare a matrix-bound TDH which possesses a high percentage of the specific activity of the soluble enzyme. The decrease in specific activity at elevated levels of CNBr may be due

Figure 19. Effect of CNBr Concentration on the Specific Activity of Matrix-Bound, Associated TDH. Matrix-bound, associated TDH was prepared using ^{3}H-PLP-labelled TDH as described in Materials and Methods. The concentration of CNBr in the CNBr-Activation step was varied as shown on the abscissa. Dehydrase specific activity in I.U./dpm is expressed as a percentage of that of the soluble TDH (3.51×10^{-4} I.U./dpm). Dehydrase catalytic activity and radioactivity attached to CL-Sepharose were determined as described in Materials and Methods.

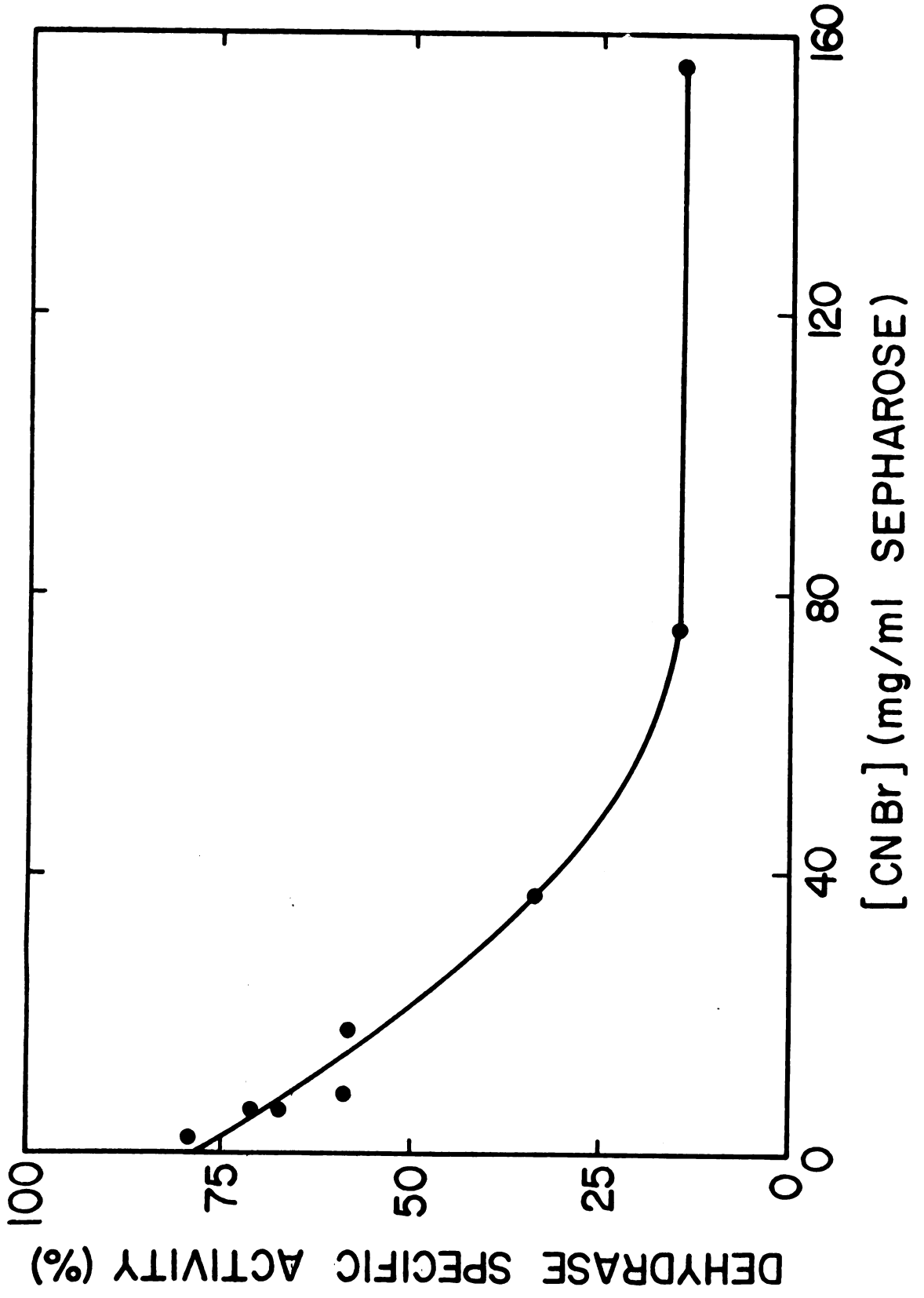
DEHYDRASE SPECIFIC ACTIVITY (%)
100
75
50
25
0
0
40
80
120
160
[CNBr] (mg/ml SEPHAROSE)

either to diffusion effects on substrate and/or product to and from internal TDH, structural distortions of the enzyme active site caused by multiple linkage of subunits to the matrix, or to loss of catalytically important groups from attachment.

The amount of TDH bound to the matrix increased with the concentration of CNBr used for activation and with the concentration of TDH added during the coupling phase. Usually about 300 I.U./ml was present during coupling. At this level and using Sepharose activated at 2.5 mg/ml CNBr, the resulting matrix bound 2-5 I.U. per ml of packed Sepharose. At higher levels of CNBr, up to 74 I.U./ml of TDH were matrix bound.

Soluble dehydrase in the presence of AMP at the concentrations present during coupling and washing has been shown to exist as a dimer (68). It thus seems reasonable to assume that the enzyme is bound to the matrix through one or more bonds as a dimer. For this reason, dehydrase bound to the matrix under these conditions is referred to as "matrix-bound, associated TDH".

b. Removal of AMP from Matrix-Bound, Associated TDH

Washing matrix-bound associated TDH with 1 M KCl solutions containing AMP as described in Materials and Methods, released less than 5% of the bound enzyme or radioactivity. Concentrations of enzyme activity and radioactivity in AMP containing buffer washes were typically 0.5% of that on the matrix. However, if AMP was removed from the wash buffer, a large fraction of enzyme activity was released from the gel (see Figure 20). This activity was released slowly from the matrix. At low degrees of substitution (2-5 mg/ml CNBr), 8 columns volumes of AMP free buffer were required. Three times more was required at high CNBr activation. At the

Figure 20. Release of TDH Activity from Matrix Bound Associated TDH Upon Removal of AMP from Wash Buffer. Matrix bound, associated TDH was prepared as described in Materials and Methods. Four ml of the coupled matrix were washed at room temperature in a 10 ml disposable column supported by a nylon mesh screen. The flow rate was 1-3 ml per min and 1 ml fractions were collected. These fractions were immediately assayed for dehydrase activity. The matrix was initially washed with coupling buffer (see Materials and Methods) containing 5 mM AMP. At the position of the arrow, this was replaced by coupling buffer devoid of AMP.

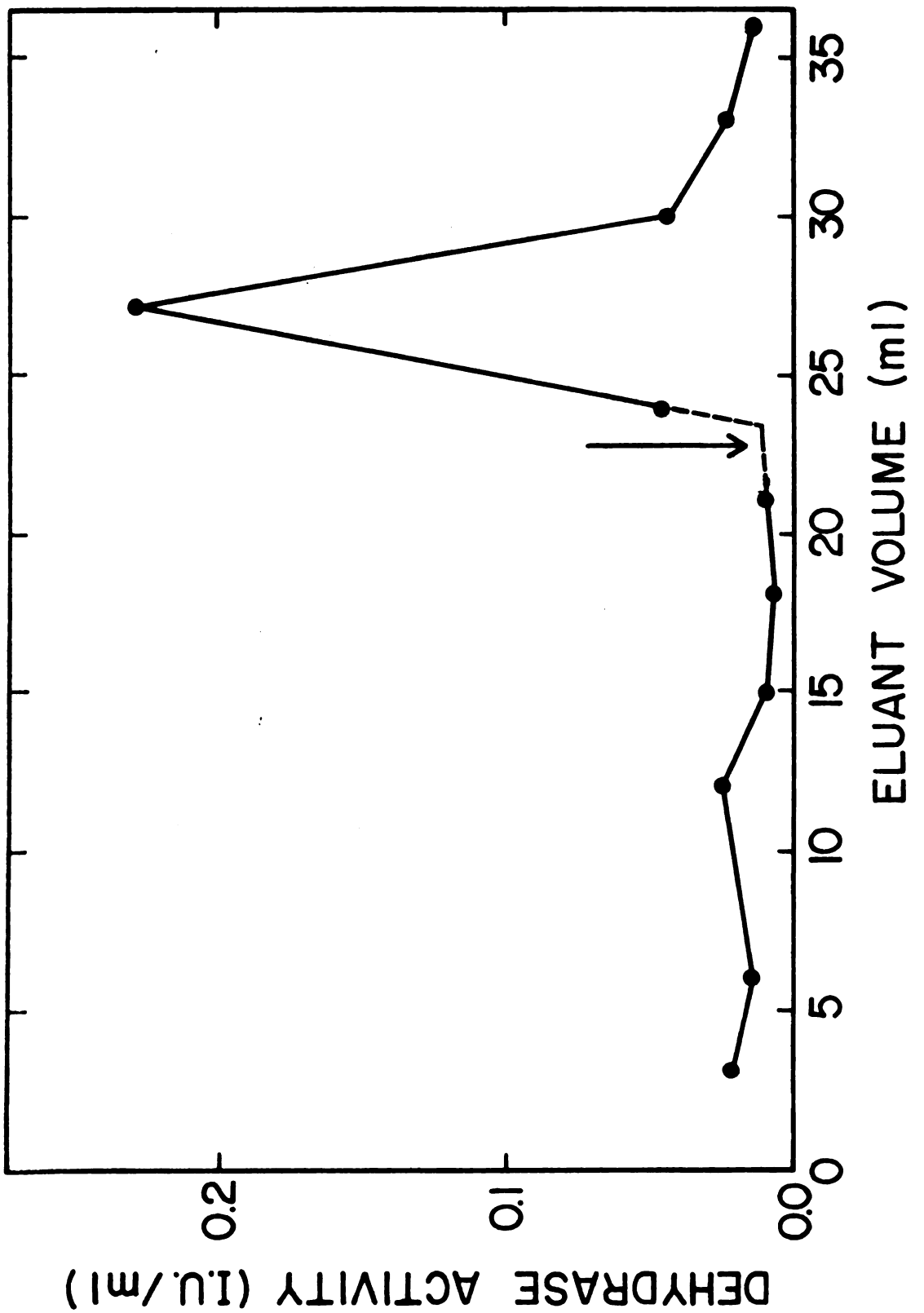
DEHYDRASE ACTIVITY (I.U./ml)
0.0
0.1
0.2
0
5
10
15
20
25
30
35
ELUANT VOLUME (ml)

lower CNBr concentration, the AMP deficient buffer wash contained 30-40% of the originally bound enzyme activity and 40-50% of the original radioactivity. Recycling this same matrix with AMP-containing, and then AMP-free buffer did not release further activity or radioactivity.

The quantity of enzyme activity and radioactivity which remained bound to the marix varied with the CNBr concentration used to activate the matrix (Figure 21). As the concentration of cyanogen bromide was decreased, the amount of radioactivity remaining bound after an AMP-free buffer wash decreased to 50% of that present while the quantity of enzyme activity decreased to about 25%. The protein remaining bound to the matrix was determined by amino acid analysis to be 44% ± 10% (n=3) of that present before the AMP deficient buffer wash.

The dissociation of 50% of the radioactivity from the matrix with a wash buffer devoid of AMP would seem to resemble the de-oligomerization of the dimer into a monomer species which is known to occur upon removing AMP from soluble TDH in several ways, including sedimentation into AMP deficient buffer (68). This suggests that the majority of the remaining bound molecules are monomers. Consequently, matrix-bound, associated TDH treated with AMP-free buffers to remove non-covalently bound subunits is referred to as "matrix-bound, dissociated TDH".

The remainder of studies in this dissertation were made using Sepharose 4 B activated at a CNBr concentration of 2.5 mg/ml. The degree of gel activation at this concentration produced a convenient level of enzyme activity and radioactivity for routine assays, maximized dehydrase specific activity, and reduced the probability of double-linkage.[15]

Figure 21. TDH remaining Matrix-Bound After Washing the Matrix with AMP-Free Buffer. Matrix-bound, dissociated TDH was prepared using ^{3}H-PLP-labelled TDH as described in Materials and Methods, except that the concentration of CNBr was varied as shown on the abscissa. Each matrix preparation was washed with coupling buffer devoid of AMP until the TDH activity concentration in the eluant represented less than 2% of that in the matrix bed. The resulting matrix was assayed for TDH activity and radioactivity as described in Materials and Methods. The results are expressed as a percentage of the among present in the matrix-bound, associated TDH assayed immediately prior to washing.

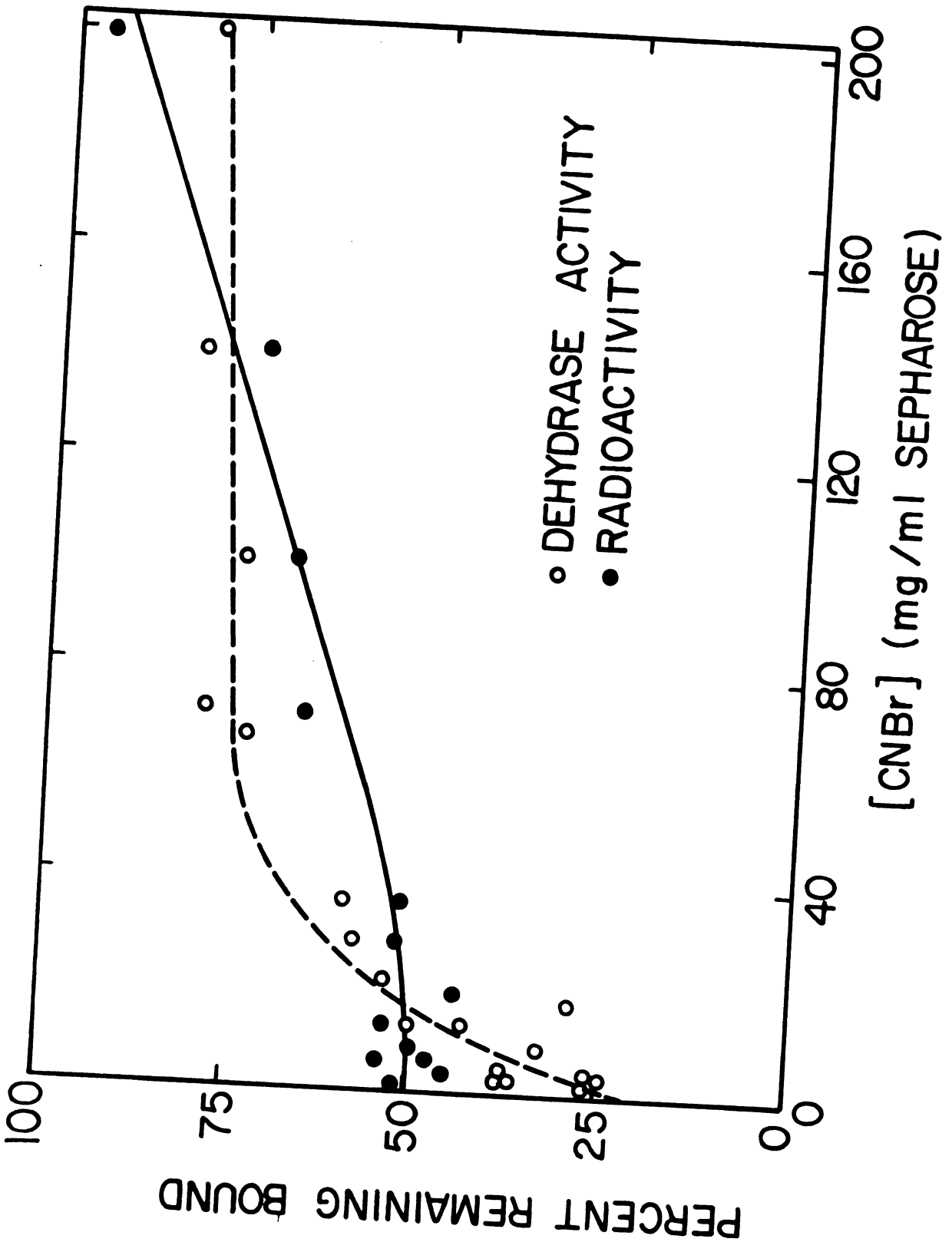
PERCENT REMAINING BOUND
100
75
50
25
0
0
40
80
120
160
200
[CNBr] (mg/ml SEPHAROSE)
° DEHYDRASE ACTIVITY
• RADIOACTIVITY

c. Treatment of Matrix-Bound TDH with Urea and $NaBH_4$

i. Measurement of Radioactivity

To determine whether significant amounts of non-covalently linked subunits remained on the matrix, matrix-bound enzyme was treated with urea and $NaBH_4$ as shown in Table 8.

Urea (9 M) was capable of removing 80% of the radioactivity from matrix-bound TDH labelled with ^{3}H-PLP.[16] This was expected from the ability of urea to resolve the radioactive PLP from soluble dehydrase (Figure 6). When the PLP was covalently attached to the protein by reduction with $NaBH_4$ (see Materials and Methods), only 40-50% of the radioactivity was removed while 52.2% remained bound.[16] As reported above after washing the matrix with AMP-free buffer, 54.1% of the original radioactivity remained bound. Thus, washing matrix-bound TDH under highly denaturing conditions (9 M urea) removed only an additional 2% of the subunits than did washing with AMP-free buffer. This suggests that the majority of subunits remaining attached to the matrix after washing in the absence of AMP are bound covalently.

ii. Measurement of Enzyme Activity

Additional evidence for the conclusion that the TDH bound to Sepharose 4B after washing with AMP-free buffer was bound covalently was obtained by measurement of enzyme activity after urea wash of matrix-bound TDH and subsequent renaturation.

As shown in Figure 22, soluble TDH in 9 M urea at room temperature loses 98% of its activity within 30 minutes. However a large amount of reactivation occurs when the denatured enzyme is diluted 100-fold into a buffer containing 10 mM AMP, 1 mM EDTA, 1 mM DTT, 0.1 mM PLP and 0.5 M

Table 8

Effect of Urea or AMP-Free Buffer Wash on Untreated or $NaBH_4$ Reduced Matrix-Bound Associated ^{3}HPLP-Labelled TDH

Treatment[a]	Fraction	Radioactivity Recovered in Fraction (% Initially bound)	
		$NaBH_4$ Reduced	Untreated
8 M Urea Wash[b]	Soluble	38.6	84.0
	Bound	52.2	0.1
AMP Free[c] Buffer Wash	Bound	--	54.1

[a]2.5 ml bed volume of matrix-bound associated ^{3}H-PLP labelled TDH washed with indicated buffer at room temperature followed by 20 ml wash with 1 mM DTT, 1 mM EDTA, 5 mM AMP, 0.1 M potassium phosphate pH 8.0

[b]25 ml of 8 M Urea, 50 mM Penicillamine, 1 mM DTT, 1 mM EDTA, 0.1 M potassium phosphate, pH 8.0.

[c]25 ml of 1 mM DTT, 1 mM EDTA, 0.1 M potassium phosphate, pH 8.0.

Figure 22. Renaturation of TDH after Treatment with 9 M Urea. TDH (0.25 mg) in 0.05 ml of 1 mM DTT, 1 mM EDTA, 5 mM AMP, 0.1 M potassium phosphate pH 6.8 was brought to 9 M urea by ten-fold dilution into 10 M urea, 1 mM DTT, 1 mM EDTA, 0.1 M potassium phosphate pH 6.8. For assay of urea denaturation aliquots (●) were diluted 100-fold into 1 mM DTT, 5 mM AMP, 0.1 M potassium phosphate, pH 8.0 and 0.01 ml were immediately assayed in the standard catalytic assay. At the arrows, aliquots were diluted 100-fold into 10 mM AMP, 1 mM EDTA, 1 mM DTT, 0.1 mM PLP and 0.5 M potassium phosphate pH 6.8. These dilutions were incubated at room temperature and at various times thereafter 0.01 ml aliquots (○) were withdrawn and assayed in the standard catalytic assay for assay of renaturation. The activity is expressed as a percentage of the original TDH present before exposure to 9 M urea as determined in control assays.

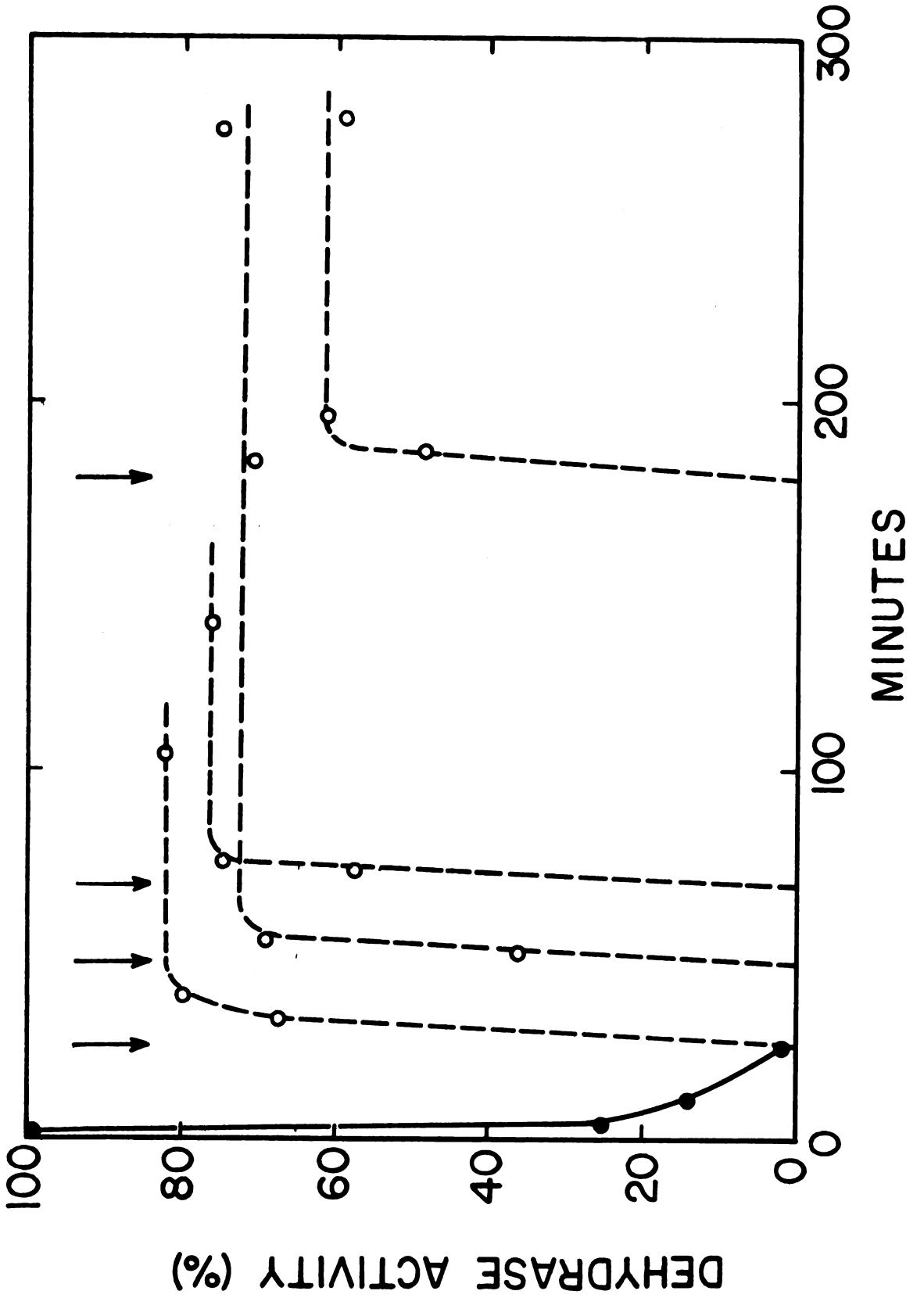
DEHYDRASE ACTIVITY (%)
100
80
60
40
20
0
0
100
200
300
MINUTES

potassium phosphate, pH 6.8.[17] As much as 80% of the original activity was regained immediately after denaturation; also, 62% was still recoverable after 2.5 hours.

When matrix-bound TDH was extensively washed with 9 M urea activity was completely lost. The renaturation procedure recovered 14.4% of the original bound activity. Since the urea treatments in a column required 3 h to perform, recovery of activity would be expected to be about 60% (Figure 22) if recovery of matrix-bound activity parallels that in solution. Recovery of matrix-bound enzyme following urea denaturation may be lower than that in solution, especially if the TDH is present as isolated subunits. Thus the amount of "potential" enzyme activity remaining on the matrix is probably greater than 14%/0.6 = 24%. This value compares well with the 25-35% of activity that remains bound when matrix-bound, associated TDH on such gels is washed with AMP deficient buffer (see Figure 21). This result further suggests that matrix-bound, dissociated TDH is attached covalently to the matrix.

d. Uptake of Soluble TDH Monomers by Matrix-Bound, Dissociated TDH in the Presence of AMP.

De-oligomerization of soluble TDH dimers by either dilution or by removal of AMP can be reversed by re-introduction of AMP (68). The above results show that freshly prepared matrix-bound, associated TDH can be dissociated by removal of AMP. It was of interest to learn whether the matrix-bound, dissociated TDH retained the ability to reassociate with soluble TDH in the presence of AMP.

As shown in Table 9, matrix-bound, dissociated TDH retained only 65% of radioactivity and 22% of the enzyme activit of the original

Table 9

Specific Uptake of Soluble TDH by Matrix-Bound, Dissociated TDH

Form of Matrix Bound TDH	Soluble TDH Added[a]		Final TDH Remaining Bound				I.U./dpm x 10^{-4}
	I.U.	dpm	I.U.	(%)	dpm	(%)	
Associated	none		1.50	(100)	7,546	(100)	2.01
Dissociated	none		0.33	(22)	4,910	(65)	0.67
Blank Sepharose	28.0	112,000	0.01	(1)	235	(3)	0.64
Associated	28.0	112,000	1.64	(108)	7,998	(108)	2.06
Dissociated	28.0	112,000	1.64	(108)	8,634	(114)	1.91
Dissociated	14.0	56,000	1.44	(95)	7,607	(101)	1.88
Dissociated	7.0	28,000	1.49	(99)	7,680	(102)	1.96
Dissociated	3.5	14,000	1.43	(94)	6,380	(85)	2.24

[a]A 0.3 ml bed volume of matrix bound TDH or blank Sepharose in a total volume of 0.6 ml in 1 mM DTT, 1 mM EDTA, 0.1 M potassium phosphate, pH 8.0 was stirred at room temperature. The indicated amounts of soluble TDH (specific activity 2.5 x 10^{-4} I.U./dpm) in 0.01-0.08 ml of the same buffer were added an 0.015 ml of 200 mM AMP pH 8 was added rapidly then the slurry was allowed to incubate at room temperature for 2 h. The matrix was then washed with coupling buffer and KCl as described for preparation of matrix bound, associated TDH in Materials and Methods.

matrix-bound associated TDH. This resulted in a greatly reduced specific activity (0.67×10^{-4} I.U./dpm) compared to that before washing with AMP deficient buffers (2.01×10^{-4} I.U./dpm). When AMP was added to matrix-bound, dissociated TDH in the presence of excess soluble TDH, enzyme activity and radioactivity became attached to the matrix. In contrast very little enzyme or radioactivity was attached either to matrix-bound, associated TDH or to blank Sepharose that had been activated and treated in parallel with the matrix-bound associated TDH, but not exposed to TDH. The increases in bound enzyme and radioactivity varied only slightly with the amount of soluble TDH added during the reassociated process, being greater when the excess of soluble TDH was large. Since this TDH remained bound after extensive washing with buffer containing 1 M KCl and AMP, the reassociation did not appear to be due to a non-specific electrostatic attachment. The product of this re-attachment process is referred to as "matrix-bound, <u>reassociated</u> TDH".

Strong evidence for the specificity and nature of the re-attachment comes from the fact that the matrix reassociated TDH possesses nearly the same catalytic activity and radioactivity as the original matrix-bound, associated enzyme, largely independent of the amount of soluble TDH present during the re-attachment process. Thus the specific activity of the matrix-bound, reassociated TDH ($1.91 - 2.24 \times 10^4$ I.U./dpm) is nearly the same as that of the matrix-bound, associated TDH (2.01×10^4 I.U./dpm).

It is not possible to account for the increase in enzyme activity or specific enzyme activity merely based on the amount of additional soluble TDH (specific activity 2.5×10^{-4} I.U./dpm) which became attached to the matrix.[18] The matrix-bound, reassociated TDH showed an average

increase in radioactivity of 8883 dpm/ml. This could result in a maximum increase in activity of only 2.22 I.U./ml whereas the observed increase was 5.01 - 1.1 = 3.9 I.U./ml. It seems reasonable to suggest that the other 3.9 - 2.22 = 1.68 I.U./ml was due to activation of the matrix-bound, dissociated TDH molecules resulting from attachment to soluble TDH. This represents a net activation (i.e. increase in V_{max}) of (1.68 + 1.11)/1.11 = 2.5 fold.

e. Kinetic Behavior of Immobilized TDH

i. Hysteresis in the AMP Activation of Matrix-Bound, Dissociated TDH.

When AMP is added to active matrix-bound, dissociated TDH, a brief, and barely detectable transient activation is observed. However at comparable levels of enzyme activity this hysteresis is greatly reduced over that observed with soluble TDH. This is illustrated in Figure 23. These reaction time courses show that there is an immediate increase in activity upon addition of AMP to active matrix-bound, dissociated TDH. This rapid increase is followed by a slower increase of 10-20% over a period of 1-2 min. This initial increase in rate is much larger than any immediate increase observed with soluble TDH. However, the final rates achieved by the immobilized enzyme (solid lines) are smaller than those attained by the soluble enzyme (dashed lines). The same behavior was observed when matrix-bound, dissociated TDH was added directly to an AMP-containing reaction mixture.

No hysteresis was ever observed when any form matrix-bound TDH, which had been pretreated with AMP, was added to assay mixtures. Thus hysteresis due to diffusion of substrate or product within the matrix is not present.

Figure 23. Time Course of Activation of Matrix-Bound, Dissociated TDH by AMP. Experimental conditions are those of Figure 6 except that either 0.027 I.U. or 0.23 I.U. were present in the cuvette (designated 0.8 or 6.8 in the figure). The dashed lines represent the data of Figure 7 reproduced here for reference. The numbers near the lines give the relative amounts of dehydrase activity present in the cuvet as determined by separate catalytic assays.

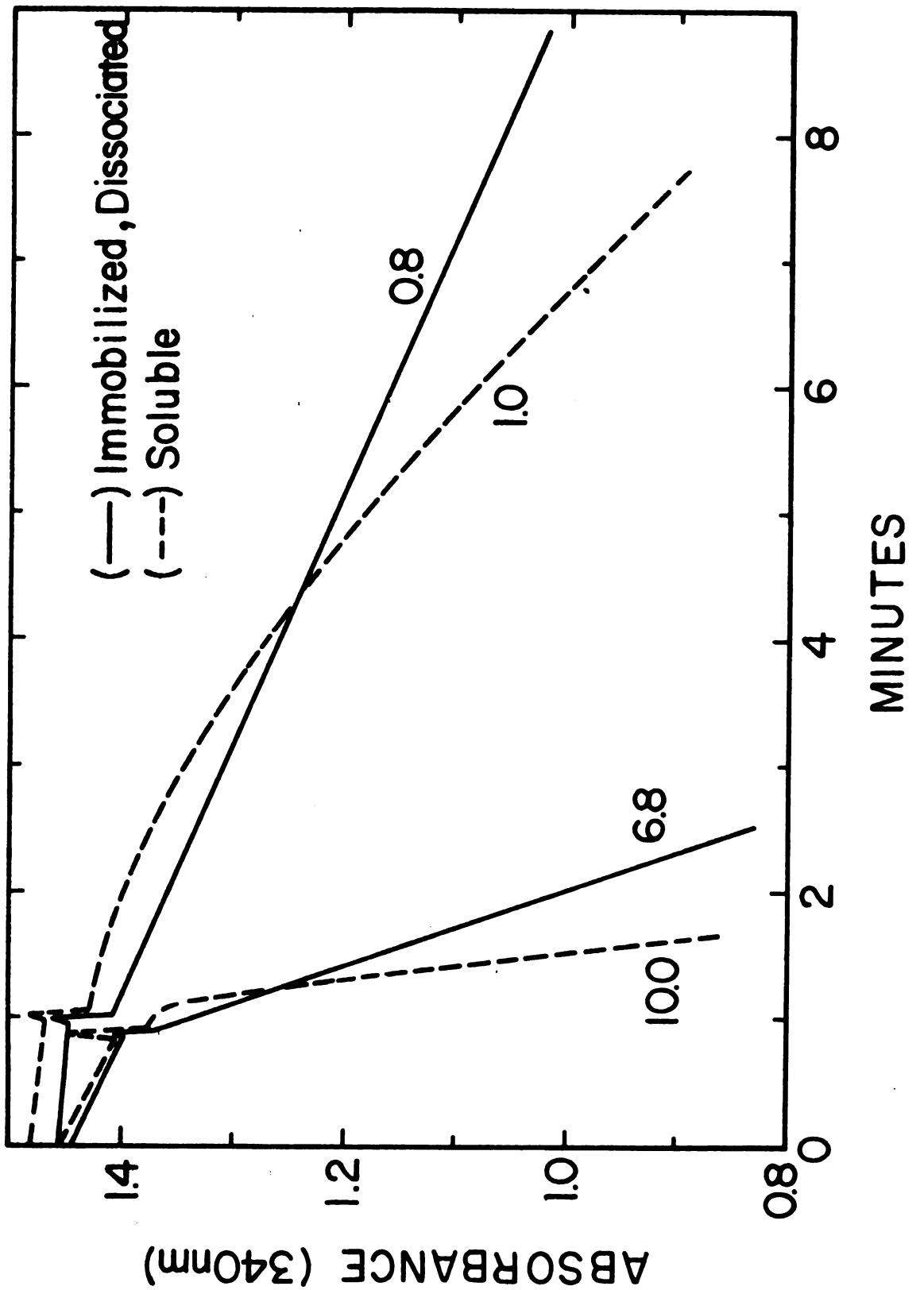
(—) Immobilized, Dissociated
(---) Soluble
0.8
1.0
6.8
10.0
ABSORBANCE (340nm)
MINUTES
0.8
1.0
1.2
1.4
0
2
4
6
8

ii. Effect of L-Threonine Concentration on the Activity of Matrix-Bound TDH.

Substrate "saturation" profiles of either matrix-bound, associated, dissociated or reassociated forms of immobilized TDH in the presence of AMP are shown in Figure 24 (open symbols). Also shown for comparison is the saturation profile of matrix-bound, dissociated TDH in the absence of AMP (closed symbols). These profiles are plotted on a semilog scale in order to accommodate a wide range of L-threonine concentrations. The lines through the data are least squares best fits obtained as described in Materials and Methods.

Both the associated and reassociated forms of the matrix-bound enzyme appear similar in their overall kinetic characteristics, except for a small difference in maximum specific activity. The best fit lines through these two profiles appear to represent the data well except at elevated substrate levels where some inhibition appears in both cases. The specific activity of the matrix dissociated TDH in the absence of AMP appears depressed relative to that of the associated forms.

The maximum specific activity of the associated forms in the presence of AMP is higher and the $S_{0.5}$ values appear much lower than those of the unactivated, dissociated form. These observations are in accord with the data of Table 6 which shows that specific activity is lower and $S_{0.5}$ higher when AMP is absent and the dehydrase (consequently) is deoligomerized.

AMP raises the specific activity of the matrix-bound, dissociated TDH (open squares), however the latter specific activity remains depressed relative to that of the associated forms. The effect of AMP on the half saturation constant of the dissociated form is complex since the data appear to define multiple inflection points.

Figure 24. Substrate Saturation Steady State Kinetics of Various Forms of Matrix Bound TDH. Associated (Δ) and dissociated (□, ▽) forms of matrix bound TDH were prepared as described in Materials and Methods from soluble ^{3}H-PLP labelled TDH (specific radioactivity 3.5 x 10^{-4} I.U./dpm). Matrix-bound, reassociated TDH (○) was prepared using 28 I.U. of TDH as described in Table 9. The initial catalytic rates were measured as described for the standard catalytic assay except that the concentration of L-threonine was varied, and the stirred reaction volume was 2 ml. The content of ^{3}H-PLP in the matrix was measured as described in Materials and Methods. Assay of the dissociated form in the absence of AMP was done exactly as described for assay in the presence of AMP except the matrix was washed free of AMP immediately prior to assay with 1 mM DTT, 0.1 M potassium phosphate pH 6.8

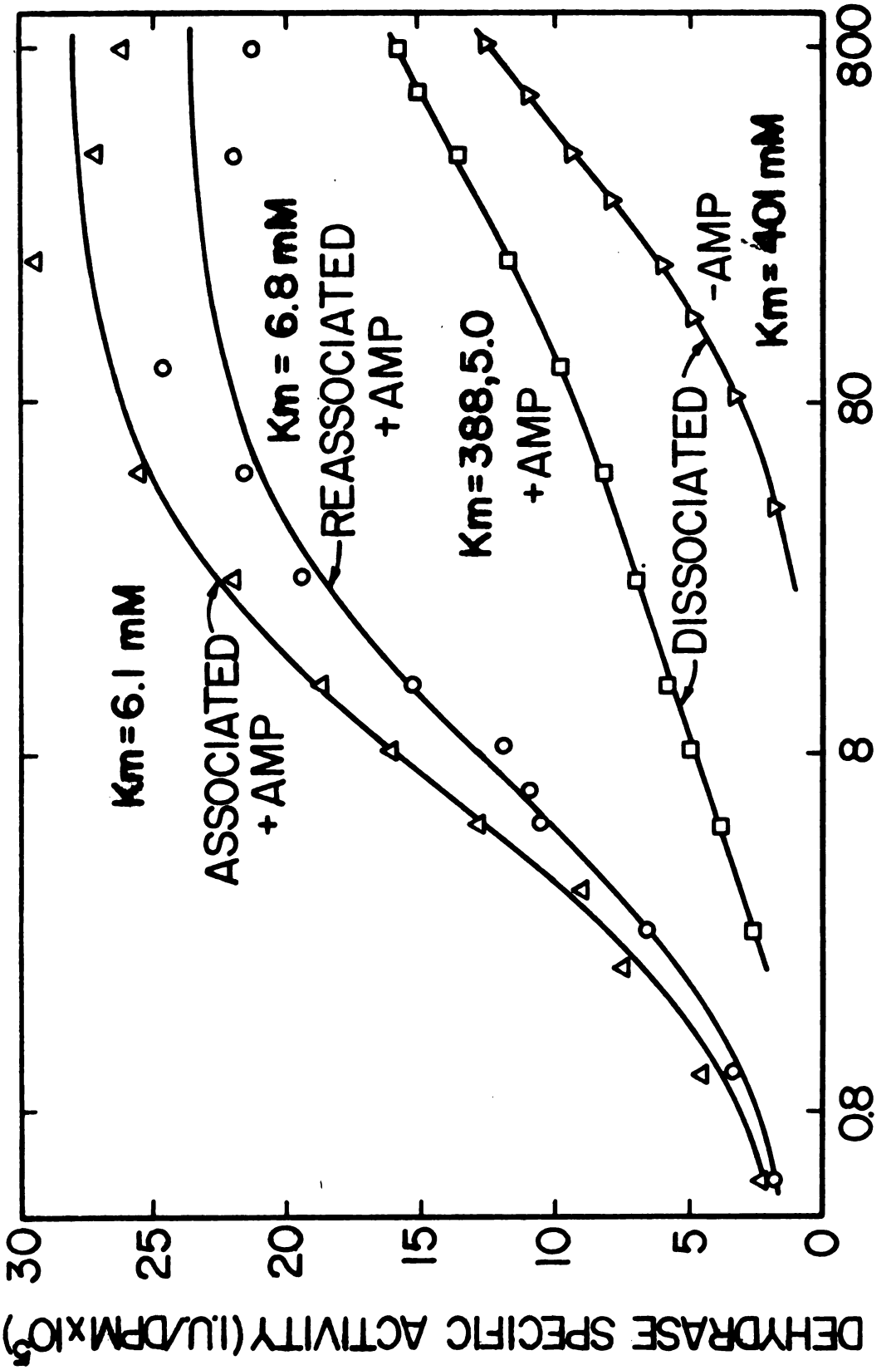
DEHYDRASE SPECIFIC ACTIVITY (I.U./DPM x 10⁵)
30
25
20
15
10
5
0
0.8
8
80
800
[L-THREONINE] mM
Km=6.1 mM
ASSOCIATED
+AMP
Km = 6.8 mM
REASSOCIATED
+AMP
Km=388,5.0
+AMP
DISSOCIATED
-AMP
Km = 401 mM

Table 10 lists the substrate kinetic parameters of the various forms of the immobilized enzyme. These were derived from least-squares fits to the data in Figure 24. In the presence of AMP, the matrix-bound, associated form possesses a V_{max} of 2.81×10^{-4} I.U./dpm and an $S_{0.5}$ of 6.1 mM. The data in Table 6 gives the comparable parameters for the soluble enzyme as 3.51×10^{-4} I.U./dpm and 6.75 mM. Thus immobilization results in a 20% drop in V_{max}, as expected from the data in Figure 19, but no significant change in $S_{0.5}$. These $S_{0.5}$ values are very close to that required to fit the kinetics of the matrix-bound, reassociated enzyme. This latter enzyme form has 85% of the V_{max} of the matrix-bound, associated form. The correlation coefficient for the fit to the data of the matrix-bound, reassociatd TDH is also lower than those for soluble or matrix-bound, associated enzyme forms.

When assayed in the absence of AMP, the matrix dissociated form possesses a V_{max} closely resembling that of soluble enzyme (Compare Tables 6 and 10). The respective $S_{0.5}$ values differ by a factor of 1.5, being lower for the soluble enzyme form. However the significance of data obtained at high substrate concentrations (300-400 mM) must be questioned. The limited solubility of L-threonine makes it impossible to obtain data beyond 2-3 fold the $S_{0.5}$ values of these forms. Other artifacts due to elevated substrate concentrations (non-specific effects on enzyme structure, possible substrate inhibition) raise doubts about the accuracy of these values. An elevation of $S_{0.5}$, upon attachment to an insoluble support, is not unexpected, however (102).

A satisfactory fit to the kinetic data of the dissociated form in the presence of AMP could not be made using the simple Michaelis-Menten

Table 10

Michaelis-Menten Parameters of Various Forms of Matrix-Bound TDH

Form of Matrix Bound TDH	AMP Present During Assay	V_{max} (± s.d.) (I.U./dpm x 10^{-4})	$S_{0.5}$ (± s.d.) (mM)	Correlation Coefficient
Associated	+	2.81 (± 0.06)	6.1 (± 0.4)	0.9933[a]
Reassociated	+	2.39 (± 0.07)	6.8 (± 0.8)	0.9494[a]
Dissociated	-	1.86 (± 0.06)	401.0 (± 29)	0.9953[a]
"	+	1.22 (± 0.03) 0.74 (± 0.02)	338.0 (± 35) 5.0 (± 0.4)	- [b] - [b]

[a]Fit by the linear method of Wilkinson (91).

[b]Fit by non linear computer program KINFIT (92).

Model. The data were fit with the program KINFIT, using a modified Michaelis-Menten model for 2 classes of non-interacting active sites (equation 6). The relative amounts (V_{max} values) and the Michaelis constants ($S_{0.5}$ values) for each site were optimized as parameters of the fit. The $S_{0.5}$ values for these two sites are remarkably similar to the $S_{0.5}$ values for soluble enzyme in the presence or absence of AMP. The higher $S_{0.5}$ (388 mM) is also close to that of the matrix-bound, dissociated TDH assayed in the absence of AMP, while the lower $S_{0.5}$ (5.0 mM) resembles that of the associated enzyme forms assayed in the presence of AMP (see Table 10). It was argued earlier in this Section that the matrix-bound, dissociated form consists largely of isolated subunits incapable of oligomerization. It would appear that, in the absence of oligomerization, less than half of these matrix-bound, dissociated TDH subunits can respond to AMP (Table 10).

From the relative V_{max} values of the low and high affinity forms of the matrix-bound, dissociated enzyme (1.22 and 0.74 I.U./dpm, respectively) it appears that only 38% of the enzyme subunits present are activated by AMP. If AMP activation results in a 1.5-2.0 fold increase in V_{max}, as suggested by Tables 6 and 9, this percentage may actually be only 19%. A percentage of "activatable monomers" of 19-38% agrees with the statistical fraction of subunits capable of reassociating (30-50%; see footnote 14). Since the matrix-reassociated form of the enzyme appears to be adequately characterized by a single low $S_{0.5}$ value, addition of subunits to the matrix-bound, dissociated form renders the remaining 62-81% of the subunits AMP responsive. This is in agreement with the kinetic data presented earlier and strongly suggest the concept that oligomerization is required in the AMP activation of TDH.

D. DISCUSSION

1. Improved Purification Procedure

The published purification procedures for TDH (68,69) are tedious and lengthy which may account for the lack of studies where large quantities of enzyme are required. The simple, two step procedure described in Materials and Methods makes large quantities of high quality TDH readily available.

This procedure was largely developed independently although the use of a nucleotide wash during affinity chromatography was suggested by the work of others (94). Later, it was found that elevated levels of nucleotides in the prewash eliminated the need for a final Sephadex G-200 step (94).

Although the purification procedure did not remove the contaminant containng TDH activity also observed by others (68,69), it appears from gel electophoresis work, that the contaminant represents less than 3% of the total activity. It appears to be a modified or altered form derived from TDH; however, its nature remains obscure.

2. In Vivo Labelling of TDH Using ^{3}H-Pyridoxine

Table 5 shows that the specific radioactivity of the ^{3}H-PLP attached to TDH was nearly equal to that of the ^{3}H-pyridoxine on which the *E. coli* cells were grown. This suggests that under these growth conditions the *E. coli* does not carry out *de novo* synthesis or degradation of PLP. The fact that TDH is produced in high yield on synthetic media lacking pyridoxine (68,60) suggests that the synthetic pathway for pyridoxine synthesis is repressed by pyridoxine in the growth medium.

The availability of ^{3}H-PLP-labelled TDH allowed accurate quantitation of TDH attached to CL-Sepharose. This *in vivo* labelling technique was non-destructive relative to such methods as iodination. The radiolabel obviated the need for quantitation of the amount bound by tedious partial amino acid analysis which would have been affected by the presence of any protein contaminants in TDH preparations.

The dissociation constant for the binding of PLP to TDH has been estimated in cofactor resolution-reactivation studies to be about 8 μM (96), PLP was observed to be tightly bound to TDH as evidenced by the lack of leaching of radioactivity from matrix-bound TDH during washing. Since the lower range of matrix-bound TDH levels encountered was about 1 I.U./ml bed volume (50 nM subunit concentration), this dissociation constant is probably lower than 50 nM. The ability to resolve PLP from TDH in urea and penicillamine (Figure 6) coupled with the potential availability of ^{3}H-PLP derived from ^{3}H-PLP-labelled TDH (^{3}H-PLP is not currently available commercially), should now facilitate determination of the kinetic and equilibrium binding properties of PLP to TDH. The ^{3}H-PLP might also serve as a tag for isolation and identification of possible PLP bound intermediates which can be chemically "fixed" during catalysis (for example, see reference 97).

3. Activation of Soluble TDH by AMP

The kinetic data presented in Figures 10 and 11 and Table 10 suggest that AMP-free TDH diluted in the absence of AMP can be fully reactivated upon re-addition of AMP. This obviates the need to account for anomalous losses of as much as 50% of TDH activity upon dilution of TDH in minus AMP buffers as has been previously proposed (64). The failures to obtain

full reactivation in previous studies (64) is undoubtedly due to the prolonged nature of the second order reactivation process.

If a fraction of the TDH molecules are not inactivated by dilution in AMP-free buffers then the drop in V_{max} observed in the absence of AMP probably represents a real decrease in catalytic efficiency of all the TDH active sites. This is in contrast to the conclusions reached by others who attempted to correct for anomalous losses observed in the absence of AMP. The data presented here suggest that such corrections were inappropriate.

The major conclusion from initial rate of activation studies (Figures 8 and 9) and measurements of AMP activation progress curves (Figures 13 and 15 and Table 7) is that dimerization appears to be rate-limiting, and therefore required in activation of monomeric TDH by AMP. This conclusion is strongly supported by results of TDH immobilization experiments showing that the activity of a large fraction of matrix-bound-dissociated (monomeric) TDH is not significantly affected by AMP (Table 10). Dimerization in solution appears to occur with a second order rate constant of about 8.8×10^5 $M^{-1}sec^{-1}$. This dimerization may be diffusion limited; however, more careful studies of the effects of viscosity, temperature and ionic strength will be required before definite conclusions can be made.

If the data in Figure 8 are interpreted as indicated in the Results section, the data of Figure 8 might be interpreted to indicate an immediate 2-5 fold activation of soluble TDH upon addition of AMP. The extent of this immediate activation seems to be larger at higher TDH levels. Such an effect could be explained by the presence of a small amount of TDH which is already dimerized (due to concentration dependent

oligomerization shown in Figure 12. The activation of these dimers could be much faster than that of monomers if they are not required to first dissociate upon binding of AMP.

While the data of Figure 8 are not precise enough to rule out an initial activation of 1.0 at elevated TDH levels, it is noteworthy that there may also be an immediate activation of a small fraction of matrix bound, dissociated TDH upon AMP addition (Figure 23). This effect may well be accounted for by the presence of a minority of immobilized subunits bound sufficiently close, and with sufficient flexibility to dimerize. Dimerization of such pairs will be faster than if they were distributed randomly in solution.

The experiments presented above do not address the question of whether AMP actually binds more favorably to the monomeric or dimeric form of TDH. Thus it is unknown whether the failure of AMP to activate matrix bound, dissociated (monomeric) TDH results from a poor affinity for the activator. This question could be answered by further kinetic characterization of this species.

However whether the role of dimerization is to facilitate (a) AMP binding or more directly (b) the protein conformational changes that lead to changes in V_{max} and $S_{0.5}$, its importance in the overall activation process seems to be established. The question of whether changes in quaternary structure are required for pyruvate of α-keto butyrate inhibition must await further study.

CHAPTER II

DETERMINATION OF ENZYME KINETIC PARAMETERS BY CONTINUOUS ADDITION OF SUBSTRATE TO A SINGLE REACTION MIXTURE AND ANALYSIS BY A TANGENT-SLOPE PROCEDURE

A. LITERATURE REVIEW

1. The Hill Equation

The Hill equation (see equation 14) continues to be a highly useful approximation of more rigorous and complex models of non-hyperbolic enzyme-substrate[18] interaction. One transformation of this equation (see equation 28) forms the basis of a plot which can yield an estimate of the minimum number of subunits of an oligomeric protein and information regarding ligand interaction energies (103). Departure of the slope of this plot from 1.0 serves as an index of cooperativity and, sometimes can be used to discriminate between different models of allosteric regulation of enzyme activity (104) as well as the oligomeric state of a rapidly associating system (105). A number of techniques have been developed to extract the maximal reaction velocity (V_{max}), the substrate concentration at half maximal rate ($S_{0.5}$), and the Hill slope (n) through an analysis of rate data (106-108).

Typically, enzymatic rate data have been obtained by manually constructing the initial slopes from plots of several reaction progress curves obtained over a range of discrete initial substrate concentrations. These methods can be both subjective and cumbersome; consequently, a variety of modifications have been proposed to remove these limitations. For instance, a more objective method is to fit each reaction progress curve to a polynomial (109), which then allows calculation of the initial rate. However, it is still necessary to analyze a series of

curves over a range of substrate concentrations to obtain the required rate data for further analysis.

2. Kinetic Analysis of Single Reaction Progess Curves

A single progress curve obtained over a range of substrate concentrations which results from substrate consumption during the reaction, has been shown to provide sufficient information for kinetic analysis (110). Two strategies are available for the analysis of such data. Firstly, undifferentiated raw data may be fit directly to an integrated form of the rate equation (111). Since analytical integration of the appropriate rate equation is not always possible, numerical integration must be used. However, this calculation can greatly increase computational time and may not be practical if the integrated equation requires non-linear curve-fitting methods which converge slowly or diverge (see, for example, reference 112). An alternative strategy is to differentiate the raw data across the entire progress curve and fit derived data to the rate equation. Such methods were found useful in analyzing the ligand-induced oligomerization processes of threonine dehydrase (11). Others have similarly reported methods for abstracting and using rate data from enzymatic progress curves (113-115); of particular interest is the secant method of Yun and Suelter (115). These methods are potentially extremely valuable because they permit the highly developed techniques for analyzing rate equations to be applied to progress curves. However, the progress curve approach depends on generation of substrate concentrations in a useful range (i.e., both above and below the K_m or $S_{0.5}$) as a consequence of substrate depletion during the reaction. The concentration range available may be limited by the extinction coefficient of the chromophore

being measured, the sensitivity of the analytical system, and the affinity of the enzyme for its substrate.

3. Independent Control of Substrate Concentration

Another limitation of conventional reaction time course methodology is the constraint placed upon substrate and product concentrations. The sum of these two concentrations is a constant for the majority of enzymatic reactions. Unless product is removed, it may be impossible to prevent build up of an inhibiting concentration during the reaction. When product terms are included in the descriptive equation, excess substrate may be used or product may be added initially to distinguish, for example, ordered from random substrate binding for bi-reactant enzymes (110). In other cases, a more flexible control over these concentrations could be advantageous. This flexibility can be achieved by independent control of substrate concentration by continuous addition.

This chapter examines the reliability of a method for obtaining Hill parameters from a single progress curve produced in a new way; namely, by creating a continuous increase in substrate concentration. This condition is produced by a precisely controlled continuous addition of concentrated substrate throughout the simulated reaction period. The method has been evaluated with a set of computed progress curve data containing varying amounts of random noise in order to evaluate and optimize data generation, collection and processing methods. This approach shows promise of application in work with enzymes.

4. Automation in Enzyme Kinetic Analysis

The previous development of a system for continuous and simultaneous recording of multiple reactions (87) has greaterly increased the accuracy and ease of performing routine optical enzyme assays. Nevertheless, estimation of kinetic parameters is still very laborious, and many investigators are reluctant to undertake systematic studies of parameter behavior in the course of their research. Solutions to this problem have been sought through either: (a) the development of devices which alter substrate concentration; or (b) analysis of reaction progress curves. For instance, enzyme has been mixed with a gradient concentration of substrate in a Technicon analyzer which also performs various laboratory operations and monitors absorbance representing the extent of reaction at some point downstream (115). This approach requires a reproducible gradient device and assumes constant conditions during the run.

Analyses of single reaction progress curves by either differential or integral methods can extract the needed information for estimation of $S_{0.5}$ and V_{max} and reduce the number of kinetic assays (111,115). As substrate is consumed by reaction, kinetic information is obtained over a range of substrate and product concentrations. Of course, such techniques are only applicable when ligand concentrations are altered by reaction. A method for rapidly establishing the pH dependence of enzyme reactions in which either hydrogen or hydroxide ions are consumed or produced (116) is similarly limited. Unfortunately, no system generally applicable to ligand binding, or to physical conditions such as pH and temperature has yet appeared.

Below is presented the theoretical basis for analyzing a reaction progress curve by a tangent-slope method under conditions of a continuous increase in substrate concentration to obtain parameters of the Hill equation. A similar approach has been used to determine activation energies for an enzyme-catalyzed reaction in a single kinetic experiment (117,118).

B. MATHEMATICAL ANALYSIS OF THE METHOD

1. Control of Substrate Concentration by Continuous Addition

Figure 25 describes a hypothetical experiment in which substrate is added at a preset rate into a stirred volume containing enzyme and any other necessary reaction components. At any time, the volume of the reaction is given by equation 8 (for definition of symbols see Symbols and Abbreviations),

$$v_t = v_0 + r \cdot t \qquad [8]$$

As the reaction begins, product will be formed, but the substrate concentration will continue to rise because of continuous addition. These quantities are related by conservation of mass,

$$\text{Total substrate added} = c \cdot r \cdot t = P_t + S_t \cdot v_t \qquad [9]$$

If the reaction can be followed spectrophotometrically, then the absorbance at any time will be the sum of contributions due to: (a) the absorbances of substrate, (b) cosubstrate, (c) product, and (d) any other chromophore present. For a reaction obeying 1:1 stoichiometry where cosubstrate is initially present in the cuvet,

$$A_t = A_0 \frac{v_0}{v_t} - \frac{P_t}{v_t} \times E_C + S_t \cdot E_S + \frac{P_t}{v_t} E_P \qquad [10]$$

2. Analysis of Raw, Undifferentiated Data (Curve-Fit Method)

The raw data set obtained by continuous addition of substrate consists of A_t versus t values. In order to analyze raw data, an equation is needed which relates A_t and t as the sole variables. Two other variables, v_t and P_t, may be eliminated by substitution of equations 8 and 9 into equation 10 to give:

Figure 25. A Hypothetical Substrate Addition Experiment. Arrangement of magnetic stirring disc, light path, and substrate addition tubing is shown.

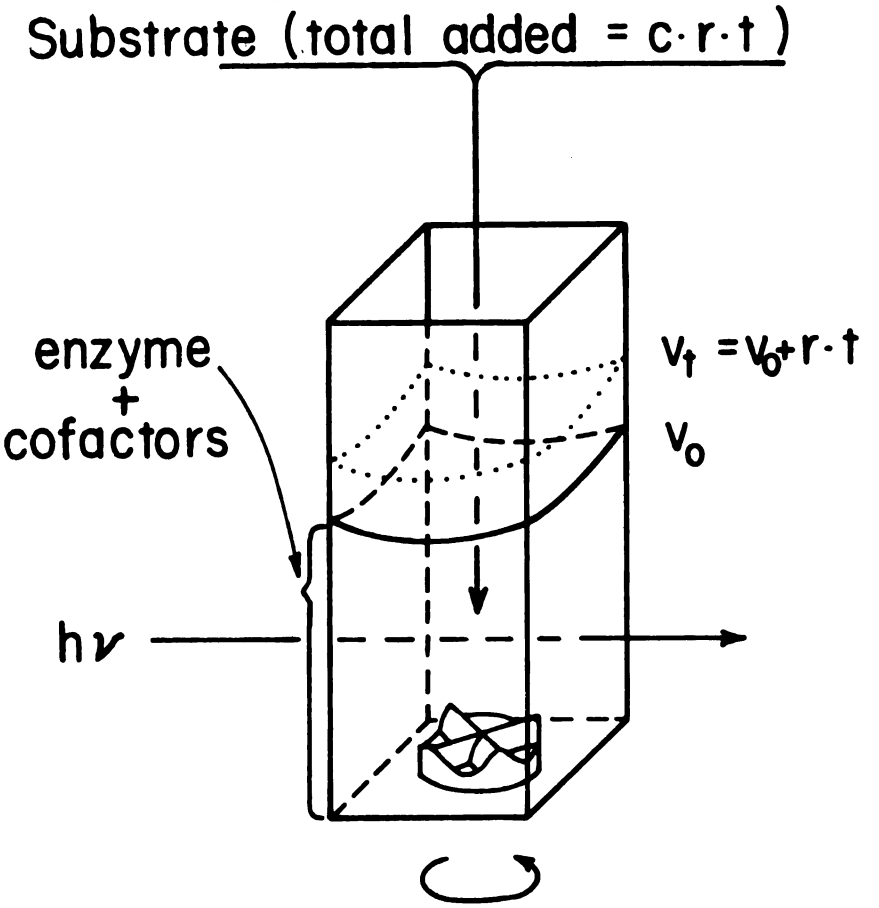
Substrate (total added = c·r·t)
enzyme
+
cofactors
$v_t = v_o + r \cdot t$
v_o
hν

$$A_t = \frac{A_0 \cdot v_0 + c \cdot r \cdot t\,(E_P - E_C)}{v_0 + r \cdot t} + S_t \cdot (E_S - E_P + E_C) \qquad [11]$$

leaving only S_t to be eliminated as a variable. An independent relationship between S_t and t can be obtained by solving equation 10 for S_t and differentiating with respect to time.

$$\frac{dS_t}{dt} = \frac{1}{v_0 + r \cdot t}\left[c \cdot r - S_t \cdot \frac{dv_t}{dt} - \frac{dP_t}{dt}\right] \qquad [12]$$

Now, from equation 8 ,

$$\frac{dv_t}{dt} = r \qquad [13]$$

If the Hill equation is obeyed,

$$Vt = \frac{dP_t}{dt} = \frac{V_{max} \cdot S_t{}^n}{S_t{}^n + S_{0.5}^n} \qquad [14]$$

then equation 12 reduces to:

$$\frac{dS_t}{dt} = \frac{1}{v_0 + r \cdot t}\left[(c - S_t)r - \frac{V \cdot S_t{}^n}{S_t{}^n - S_{0.5}^n}\right] \qquad [15]$$

The integral of equation 15 is:

$$S_t = \int_0^t \frac{1}{v_0 + r \cdot t}\left[(c - S_t)r - \frac{V \cdot S_t{}^n}{S_t{}^n + S_{0.5}^n}\right] dt \qquad [16]$$

Unfortunately, equation 16 may not be integrated analytically. However, numerical integration by the approximation of Runge-Kutta (119) is straightforward. The value of S_t so calculated at any desired time, may be used in equation 11 to solve for A_t. These procedures are used in a computer program designated as MARQ (described below) which analyzes raw substrate addition data by the method of non-linear least squares curvefitting.

3. Analysis of Differentiated Data (Tangent-Slope Method)

The equation relating S_t and V_t (equation 14) is much simpler to use than equations 11 and 16 which relate A_t and t and require numerical solution of S_t. However, use of equation 14 requires numerical differentiation of P_t with respect to t to obtain V_t.

Combining equations 8, 9, and 10 to eliminate S_t and V_t, and then solving for P_t gives:

$$P_t = \frac{v_o \cdot (A_t - A_o) + r \cdot t\,(A_t - c \cdot E_S)}{E_P - E_S - E_C} \qquad [17]$$

Substitution of P_t back into equation 9 allows calculation of S_t.

$$S_t = \frac{c \cdot r \cdot t - P_t}{v_o + r \cdot t} \qquad [18]$$

Thus P_t and S_t may be calculated for each value of A_t and t.

Numerical differentiation is performed by constructing slope-tangents as illustrated in Figure 26. As discussed later, the computed "data" used herein consisted of about 120 points equally spaced in time. A sliding window of w points was used. The velocity, assigned to the

Figure 26. Graphic Illustration of Tangent-Slope Estimation of Reaction Velocity. The subscript, i, is used to emphasize the discrete nature of the data.

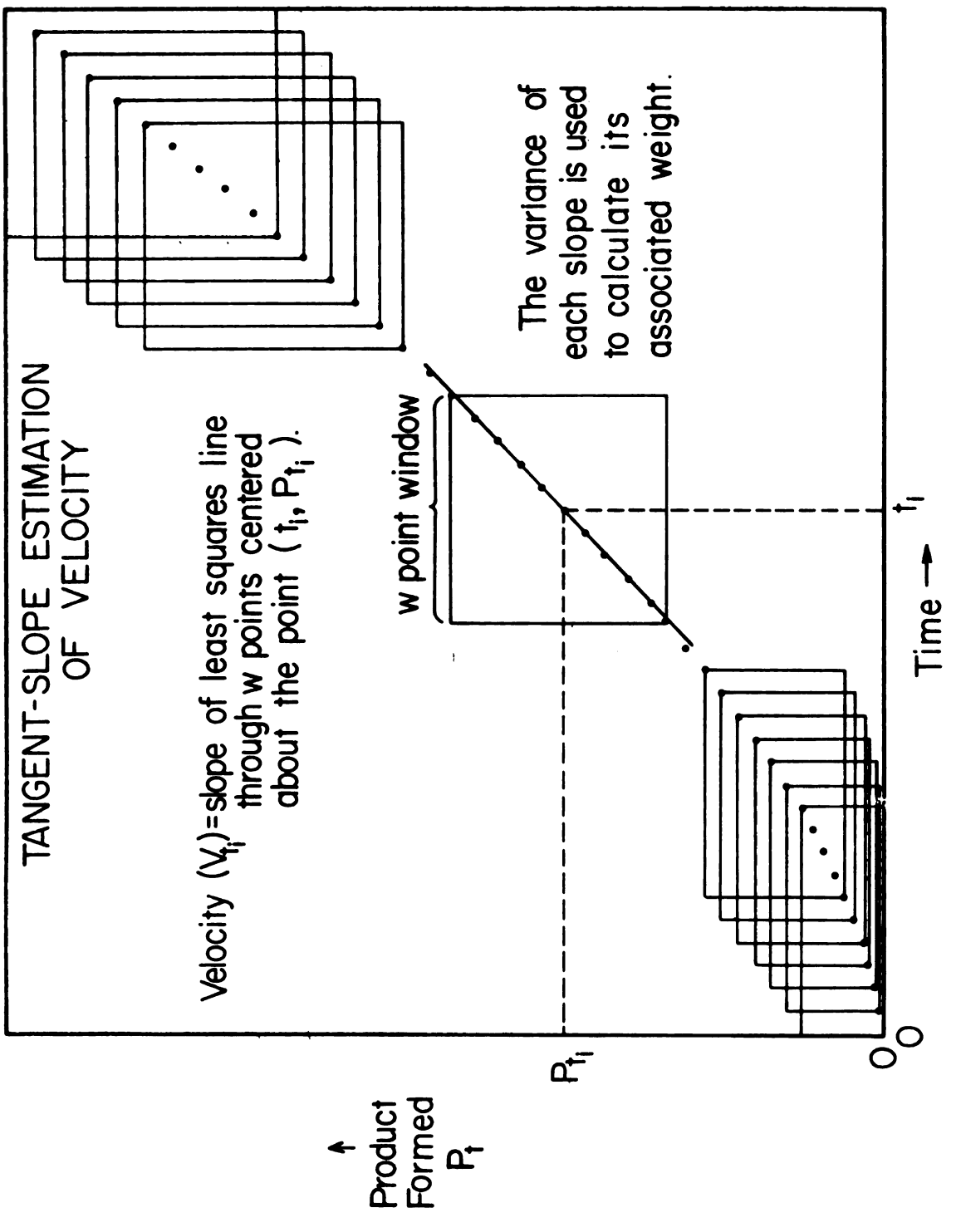
TANGENT-SLOPE ESTIMATION
OF VELOCITY
Velocity (V_{t_i})=slope of least squares line through w points centered about the point (t_i, P_{t_i}).
w point window
The variance of each slope is used to calculate its associated weight.
Product Formed P_t
P_{t_i}
t_i
Time
O
O

center point was approximated as the slope of the linear least squares line through the points in the window; the slope variance is also calculated. Successive windows were constructed by dropping the first and picking up a subsequent datum to maintain constant w. The result is a set of velocity values - one for each time interval excepting the first and last (w-1)/2 points. These calculations and the subsequent analysis of transformed data were carried out by the computer routine, TANKIN, described below.

C. MATERIALS AND METHODS

1. Computer Programs

a. Optimizing Experimental Variables (SSOP)

In order to insure that progress curve data are obtained over a selected range of substrate concentrations and absorbance values within a given period of time, it is helpful to have a method for calculating the pump rate and enzyme concentration which will produce that result.

The pump rate was calculated by rearrangement of equation 17 to give:

$$r = \frac{v_o \cdot [(S_f \cdot (E_p - E_S - E_C) - A_o + A_f]}{t_f \cdot c \cdot (E_p - E_C) - S_f \cdot (E_p - E_S - E_C) - A_f} \quad [19]$$

The total quantity of product formed in such an experiment can be obtained from equations 8 and 9.

$$P_f = (c - S_f)\, t_f\, r - S_f\, v_o \quad [20]$$

Experience with a great deal of substrate addition data, both real and synthetic, suggests that the amount of enzyme needed in units of V_{max} may be approximated closely as:

$$V_{max} \approx \frac{2P_f}{t_f} \quad [21]$$

when $S_f \approx 3 \times S_{0.5}$ and Hill $n \approx 1.0$. When very accurate knowledge of the required V_{max} was needed, equation 21 was used to provide an initial estimate, V_{max}'. The final product concentration, P_f produced by this combination of r and V_{max} was calculated by application of equation 16 and 20. An improved estimate of the required V_{max} was calculated as:

$$V_{max}'' = V_{max}' \cdot \frac{P_f}{P_f'} \qquad [22]$$

This process was repeated until the desired P_f/P_f ratio was within 0.1% of 1.0, which usually required three iterations. The number of integration intervals used in the Runge-Kutta solution of equation 16 was usually 20. Increasing this value to 100 did not significantly alter the final V_{max} value calculated. A computer program (SSOP) was written for a Hewlett Packard Calculator (Model 9815A) to perform these calculations.

b. Generation of Simulated Data (SIMUL)

In evaluating the new method, analysis by continuous substrate addition, the strategy was to prepare and analyze calculated data which simulated a real addition experiment and which contained noise levels expected to be encountered over a range of experimental conditions. In this way it was possible to separate evaluation of the data treatment methods from the evaluation of the instrumental methods. Also, since simulated "data" can be prepared more easily than real data, a larger number of well-defined conditions can be examined and the effect of experimental variables determined. Using this strategy, it was also possible to introduce and study the effects of such anomalies as enzyme inactivation and product inhibition in a controlled way. Artificial data were created by a numerical solution of equation 16 by the method of Runge-Kutta (119) to obtain a series of 120 S_t values at equal time intervals over a period of 4 min. These substrate concentrations were then used in equation 11 to calculate the respective A_t values. Known amounts of

normally distributed random noise were then superimposed on these A_t values to form the final simulated raw "data". In experiments where it was desired to examine the effects of enzyme inactivation or product competitive inhibition during an experiment, equation 14 was modified as follows:

$$\frac{dP_t}{dt} = (e^{-k \cdot t}) \frac{V_{max} \cdot S_t^n}{S_t^n + S_{0.5}^n} \qquad [23]$$

$$\frac{dP_t}{dt} = \frac{V \cdot S_t^n}{S_t^n + S_{0.5}^n \left[1 + \frac{P_t/V_t}{K_i} \right]} \qquad [24]$$

These calculations were made by the interactive FORTRAN computer program SIMUL. The program required the input of the following experimental constants: k, K_i, v_o, r, t_f, c, V_{max}, $S_{0.5}$, n, E_S, E_C, E_P, and A_o. The data were stored and analyzed exactly as were real data.

c. Integral Analysis of Data (MARQ)

A Fortran version (88) of the algorithm of Marquardt was incorporated into a computer program (MARQ) which calculated the best fit of stored absorbance-time data to equation 11. Equation 16 was solved numerically as described for the program SIMUL. Initial estimates of the 3 kinetic parameters, V_{max}, $S_{0.5}$, and n were necessary to begin the iteration; these were provided by the program TANKIN (see below). A minimum

improvement in the sum of the squared residuals of 0.01% was used as the criterion for convergence. In a variety of cases examined, only a single minimum was observed. Convergence was reasonably independent of any combination of initial parameter estimates over a ± 2-fold range as judged by convergence to parameter values which were identical to 4 or 5 decimal places. The quality of the fit was evaluated principally by examining the magnitude of the standard deviation of the data about the fitted line. Approximate marginal standard deviations and partial and multiple correlation coefficients for each parameter were calculated from the normal and inverse error matrices (120).

d. Differential Analysis of Data (TANKIN)

The interactive FORTRAN program TANKIN is illustrated schematically in Figure 27. The routine consists of a main program and a sub-routine to perform weighted least squares regressions. At step 1, experimental constants (v_o, r, c, E_S, Ep, E_C, A_o), number of data points, data collection rate and raw A_{t_i} values are read from disc resident files created by SIMUL. Using the data collction rate, t_i values are calculated and the t_i versus A_{t_i} values are transformed to S_{t_i}, P_{t_i} values with equations 17 and 18 as described earlier (step 2). A window size is entered at step 3 and used in step 4 for slope-tangent estimation of reaction velocities and their variances as shown in Figure 26. The weighting scheme is selected in steps 5 and 6. Either homogeneous (all VV_{t_i} = 1) or individual (calculated VV_{t_i} values) weighting is available. The S_{t_i}, T_{t_i}, VV_{t_i} data are further analyzed by linear regression using the familiar linear transformations of the Hill equation:

Figure 27. General Flowchart for the Computer Program TANKIN, which reduces raw time-absorbance data (t_i, A_i) to substrate-velocity data (S_i, V_i) by the method of tangent-slopes, and determines the optimal Hill parameters (V_{max}, $S_{0.5}$, n) from the strongest linear fit of the data to equations 25, 26, or 27 and 28. Symbols are defined in Symbols and Abbreviations.

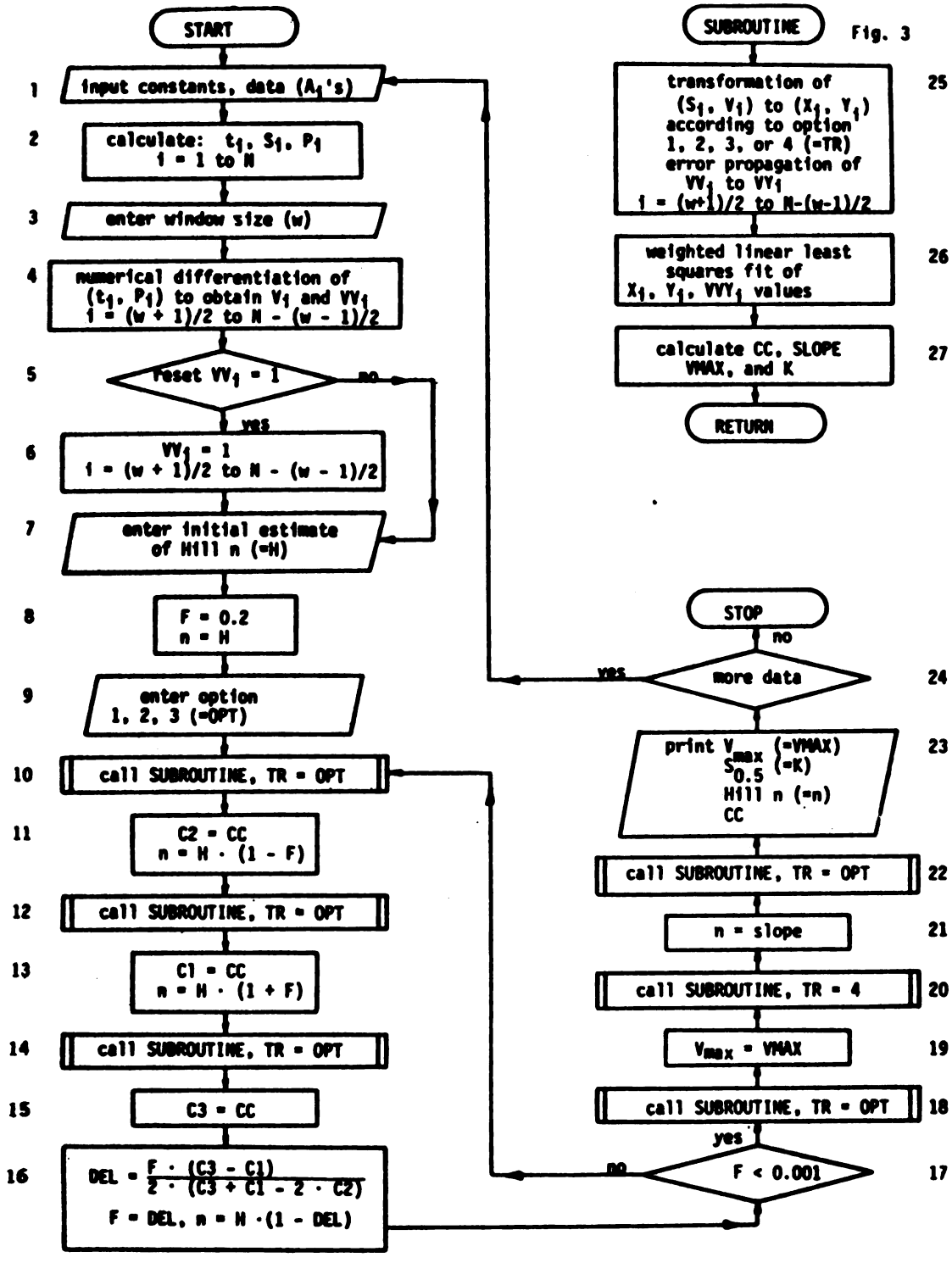
START
1 input constants, data (A_i's)
2 calculate: t_i, S_i, P_i i = 1 to N
3 enter window size (w)
4 numerical differentiation of (t_i, P_i) to obtain V_i and VV_i i = (w + 1)/2 to N - (w - 1)/2
5 reset VV_i = 1
no
yes
6 VV_i = 1 i = (w + 1)/2 to N - (w - 1)/2
7 enter initial estimate of Hill n (=H)
8 F = 0.2 n = H
9 enter option 1, 2, 3 (=OPT)
10 call SUBROUTINE, TR = OPT
11 C2 = CC n = H · (1 - F)
12 call SUBROUTINE, TR = OPT
13 C1 = CC n = H · (1 + F)
14 call SUBROUTINE, TR = OPT
15 C3 = CC
16 DEL = $\frac{F \cdot (C3 - C1)}{2 \cdot (C3 + C1 - 2 \cdot C2)}$ F = DEL, n = H · (1 - DEL)
SUBROUTINE
Fig. 3
25 transformation of (S_i, V_i) to (X_i, Y_i) according to option 1, 2, 3, or 4 (=TR) error propagation of VV_i to VY_i i = (w+1)/2 to N-(w-1)/2
26 weighted linear least squares fit of X_i, Y_i, VVY_i values
27 calculate CC, SLOPE VMAX, and K
RETURN
STOP
no
yes
24 more data
23 print V_{max} (=VMAX) $S_{0.5}$ (=K) Hill n (=n) CC
22 call SUBROUTINE, TR = OPT
21 n = slope
20 call SUBROUTINE, TR = 4
19 V_{max} = VMAX
18 call SUBROUTINE, TR = OPT
yes
no
17 F < 0.001

$$\frac{1}{V_t} = \frac{S_{0.5}^n}{V_{max}} \cdot \frac{1}{S_t^n} + \frac{1}{V_{max}} \qquad \text{option 1 [25]}$$

$$V_t = - S_{0.5}^n \cdot \frac{V_t}{S_t^n} + V_{max} \qquad \text{option 2 [26]}$$

$$\frac{S_t^n}{V_t} = \frac{S_t^n}{V_{max}} + \frac{S_{0.5}^n}{V_{max}} \qquad \text{option 3 [27]}$$

Weights were calculated from the VV_{t_i} values, and the regressions were always weighted according to the method of error propagation (88).

An initial estimate of Hill n is entered at step 9. This estimate is improved by a search which maximizes the strength of the linear fit (maximum linear correlation coefficient) to options 1, 2, or 3. The desired option is chosen in step 9, and improved estimates of Hill n are calculated by a parabolic search (88) as shown in steps 10-16. The search is initiated with F = 0.2 (step 8) and is continued iteratively until F < 0.001 (step 17). From the last fit, a provisional V_{max} value is calculated (step 19). Using this V_{max}, the Hill n is calculated as the slope of the Hill plot (equation 28).

$$\log \frac{V_t}{V - V_t} = n \log S_t - n \log S_{0.5} \qquad \text{option 4 [28]}$$

(Steps 2 and 21). Finally, this Hill n is used to obtain the final

$S_{0.5}$ and V_{max} from the slope and intercept of a fit to options 1, 2, or 3 (step 22). The linear correlation of this final regression is reported as a measure of the goodness of fit.

This fitting procedure has advantages over previously published methods since it avoids time-consuming non-linear techniques and provides for individual weighting of velocities (106-108). Data analysis was fully automated so that a large number of experiments can be analyzed quickly. In addition, the program can produce crude printer plots of A_t vs. t, V_t vs. S_t, or plot of any of the four linear transformations.

e. Weighting in Analysis of Differentiated Data

As shown later, the noise in absorbance measurement is approximately homogeneous. Consequently, in the curve-fit method, raw absorbance values were given equal weight. In the slope-tangent method, two weighting schemes were compared. The first (homogeneous weighting) assumed equal weighting of velocities. In the second (individual weighting), the slope variance was used to calculate a weight for each velocity value.

In the differential method described above, raw absorbance-time data are transformed into substrate-velocity data. To properly weight the transformed data, it is important to consider propagation of errors. It can be shown (89) that the velocity at the ith data point (see Figure 26) can be calculated from equation 29.

$$V_{t_i} = \frac{1}{\Delta T \cdot D} \sum_{j=1}^{W} \left(j - \frac{w+1}{2} \right) P_{t_m} \qquad [29]$$

Where: P_{t_j} = product concentration calculated at the j'th data point; t(min) = data collection interval,

$$m = i - \frac{w + 1}{2} + j,$$

$$D = \sum \left(j - \frac{w + 1}{2} \right)^2$$

If variance in the raw absorbance-time data is due solely to errors in A_t, it can be shown from equations 9 and 11 and error propagation (88) that:

$$\sigma^2 S_t = \frac{\sigma^2 A_t}{E_p - E_S - E_C} \qquad [30]$$

$$\sigma^2 P_t = \frac{v_t \sigma^2 A_t}{E_p - E_S - E_C} \qquad [31]$$

Since noise in absorbance measurement, A_t, is homogeneous (see below) and since variation in v_t will be slight over the span of w points, from equation 29 and 31.

$$VV_t - \frac{\sigma^2 P_t}{\Delta t \cdot D} = \frac{v_t \cdot \sigma^2 A_t}{\Delta t \, (E_p - E_S - E_C) \sqrt{D}} \qquad [32]$$

In the least-squares regressions used in the analysis of transformed data, only V_t is assumed to have error and S_t is treated as an independent, error-free variable. For this to be reasonable,

$$\frac{VV_t}{V_t} > \frac{\sigma^2 S_t}{S_t}$$

or, from equation 30 and 32,

$$\frac{v_t}{\Delta t \cdot V_t \cdot \sqrt{D}} > \frac{1}{S_t} \quad \text{or,}$$

$$\frac{v_t}{\Delta t \cdot \sqrt{D}} > \frac{V_t}{S_t} \qquad [33]$$

If an enzyme obeys equation 14 with n = 1,

$$\frac{V_t}{S_t} < \frac{V}{S_{0.5}} \qquad [34]$$

Combining equations 33 and 34, S_t can be considered errorless if

$$\frac{\Delta t \; v_t \; D}{} > \frac{S^V}{0.5} \qquad [35]$$

For the simulated addition experiments described here: v_t 2 x 10^{-3} L, t = 0.033 min, w - 11 (giving D 10), V_{max} = 10^{-7} mole/min, and $S_{0.5}$ 10^{-4} M. Then from equation 33:

$$6 \times 10^{-3} \; \underline{1}/\text{min} > 10^{-3} \; \underline{1}/\text{min}$$

Therefore, in the studies reported here, S_t may be considered errorless. It can be seen from the work described below, that inequality 35 can readily be maintained during real substrate addition experiments.

Equations 14 and 18 show that both S_t and V_t are functions of P_t, and thus errors in S_t and V_t are correlated. As long as S_t can be considered errorless, these correlations can be ignored. It is

interesting to note, however, that examination of equation 29 shows that V_{t_i} and S_{t_j} are not correlated when i = j.

A more serious consideration is the correlation between neighboring V_{t_i} values (121). The statistically correct way to fit such data would involve the use of the inverted co-variance error matrix to provide appropriate weighting (120). The calculation of the error matrix is not difficult; however, its inversion is extremely costly in computer time.[19] It is shown in the Results section that assuming zero correlation between neighboring V_{t_i} values need not lead to significant errors in the analysis (S_t, V_t) data.

In the program, TANKIN, weights are calculated from the variance (VV_{t_i}) of the least-squares tangent slope (V_{t_i}) as shown below:

$$Vt_i = \frac{w \cdot \sum P_{ti} \cdot t_i - \sum t_i \cdot \sum P_{ti}}{\Delta i}$$

and $$VV_{t_i} = \frac{w\sigma i^2}{\Delta i} \qquad [36]$$

where

$$\Delta i = w \sum t_i^2 - (\sum t_i)^2$$

$$\sigma_i^2 = \frac{1}{w - 2} \left[\Sigma P_{t_i}^2 + wa_i^2 + V_{t_i}^2 \Sigma t_i^2 - 2a_i \Sigma P_{t_i} - 2V_{t_i} \Sigma P_{t_i} \cdot t_i + 2a_i V_{t_i} \Sigma t_i \right]$$

$$a_i = \left[\Sigma t_i^2 \ \Sigma P_{t_i} - \Sigma t_i \ \Sigma t_i \cdot P_{t_i} \right] / \Delta i$$

and Σ represents a sum over all points in the window.

An alternative method of weighting is suggested by equation 32. Since v_t varies less than 10% during a typical addition assay VV_t may be assumed to be constant. This latter method of homogeneous weighting is also used as described in the text.

Because of the correlation between calculated V_t's, the linear correlation coefficient obtained in the TANKIN fit is a biased statistic and cannot be used in estimating probabilities for statistical tests. Nevertheless, as shown below for real and simulated data, it can be a useful indication of the relative fit to the Hill equation.

2. Experimental

a. Biochemicals

Rabbit muscle lactate dehydrogenase, pig heart mitochondrial malate dehydrogenase, *E. coli* β-galactosidase, and their substrates were obtained from Sigma Chemical Co. TDH was isolated as described in Chapter I. Tryptophanase of *E. coli* (122), SOPC, KDPG-aldolase from *Pseudomonas putida*, were gifts of David S. June and Paul Kuipers of the Biochemistry Department at Michigan State University. All other chemicals were reagent grade from Sigma.

b. Immobilization of Lactate Dehydrogenase

Sepharose 4-B and Sephadex G-50 were activated according to the method of Axen *et al.* (86) with 70 mg of cyanogen bromide for each ml of

packed matrix. The coupling solution containing 10 mg of lactate dehydrogenase (in ammonium sulfate suspension) and 5 ml of activated matrix in a total of 7 ml of 0.05 M sodium phosphate, 1 mM dithiothreitol, pH 7.0, was incubated overnight at 4°C. The matrices were washed in columns with 10 ml of buffer containing 1 M sodium chloride, and then with excess buffer. The resulting derivatized support contained 8.8 and 1.92 I.U. of lactate dehydrogenase, respectively, per ml of packed matrix. Soluble activity in both cases was less than 5% of the total.

c. Enzyme Assays

Substrate addition assays were carried out according to the principles outlined above. Each reaction required (a) an enzyme-cosubstrate solution in the stirred cuvet and (b) a concentrated substrate solution in the motor-driven syringe. The cuvet and syringe solutions were chosen to give a composition similar to that for conventional assays given in the literature (see references in Table 11). The concentration of added substrate was adjusted so that the total volume change and mixing noise were minimized. Mixing noise due to continuous addition from the syringe was reduced by using identical buffers in cuvet and syringe solutions. The syringe solution also contained reducing agents where used, but not activators or coupling enzymes. All solutions were prepared fresh daily.

The computer program, SSOP, was used to calculate the rate of substrate addition (pump rate) and the amount of enzyme needed to achieve the specified final absorbance, final substrate concentration, and duration of the experiment. $S_{0.5}$ and Hill n estimates needed in this

Table 11. [a]In addition to substrate, buffer and reducing agent at concentrations shown for cuvet were present;
[b]50 1 packed derivatized Sephadex G-50;
[c]3.5 1 packed derivatized Sepharose 4-B;
[d]Beef heart isoenzyme in I.U. giving 99% of steady state in 1 sec.

Table 11

Protocols for Enzyme Assays - Reaction Mixture in Cuvette

Enzyme	Amount (I.U.)	Initial Volume (ml)	Other Ingredients	Conc.[a] (mM)
Lactate dehydrogenase	0.15	2.5	K^+ phosphate, pH 7.0	100.0
			dithiothreitol	1.0
on Sephadex G-50	0.1[b]	2.0	NADH	0.32-0.40
on Sepharose 4-B	0.03[c]			
Malate dehydrogenase	0.05	2.5	K^+ phosphate, pH 7.5	100.0
			NADH	0.32
β-Galactosidase	0.15	2.5	Na^+ phosphate, pH 7.7	100.0
Tryptophanase	0.075	2.0	K^+ phosphate, pH 8.0	50.0
KDPG Aldolase	0.4	3.0	imidizole HCl, pH 8.0	74.0
			NADH	0.32
			lactic dehydrogenase	9.0[d]
Thronine dehydratase	0.2	2.0	K^+ phosphate, pH 8.0	75.0
			NADH	0.32
			AMP	5.0
			lactic dehydrogenase	550.0[d]

Table 11 (contd.)

Protocols for Enzyme Assays - Solution in Syringe[a]

Components	Conc. (mM)	Rate (µl/ min)	Final [S] (mM)	ΔA	Ref.
Pyruvate	25.0	11.0	0.24	0.75	123
		6.5	0.35	0.70	
		7.8	0.35	0.30	
Oxaloacetate	10.0	8.0	0.075	0.20	124
ONPG	20.0	14.0	0.36	1.0	125
SOPC	2.0	45.0	0.14	0.43	126
KDPG	20.0	11.0	0.28	0.8	127
L-threonine	200.0	22.0	10.6	1.4	128

[a]Addition period, 3-5 min;

calculation were taken from the literature. Protocols were optimized to provide a large absorbance change without excessive product build-up. The final substrate concentration selected was 2.5-3 times the expected $S_{0.5}$, and the duration of each injection was selected to be about 4 min.

All reaction mixtures were maintained at 28°C. Concentrations of substrates were determined from absorbance as follows: NADH, measured by absorbance at 340 nm (E_M = 6220 M^{-1}); orthonitrophenylate, 420 nm 420 nm (E_M = 3100 M^{-1}, pH 7.0, and 4000 M^{-1}, pH 7.7); o-nitrothiophenylate, 370 nm (E_M = 840 M^{-1}, pH 8.0); and SOPC, 370 nm (E_M = 2700 M^{-1}, pH 8.0). Adequate amounts of coupling enzyme to ensure attainment of steady state in 2 sec (99% of steady state for KDPG-aldolase and 90% for threonine dehydrase) were calculated by the method of McClure (73). For comparison, assays were conducted in the spectrophotometric system described below, but without stirring and continuous substrate addition. Individual methods for these assays are similar to those given Table II.

Assay of immobilized enzymes by multicuvet methods was done as described in Chan (74).

d. Instrumental System

The system was constructed by modification of a Gilford model 2000 spectrophotometer to include commercially available components and a data handling system as shown in Fig. 28. Reactions were conducted in a standard 4 ml quartz cuvet containing a small circular teflon stirring pellet. The cuvet, in a cuvet carrier fitted with an alternating field stirring device (Gilford Spectro-stir, model 2445), was positioned in the

Figure 28. A Semi-Automated System for Kinetic Analysis of Enzyme Reactions Used in the Present Studies.

TEMPORARY
SYSTEM FOR KINETIC ANALYSIS OF REACTIONS

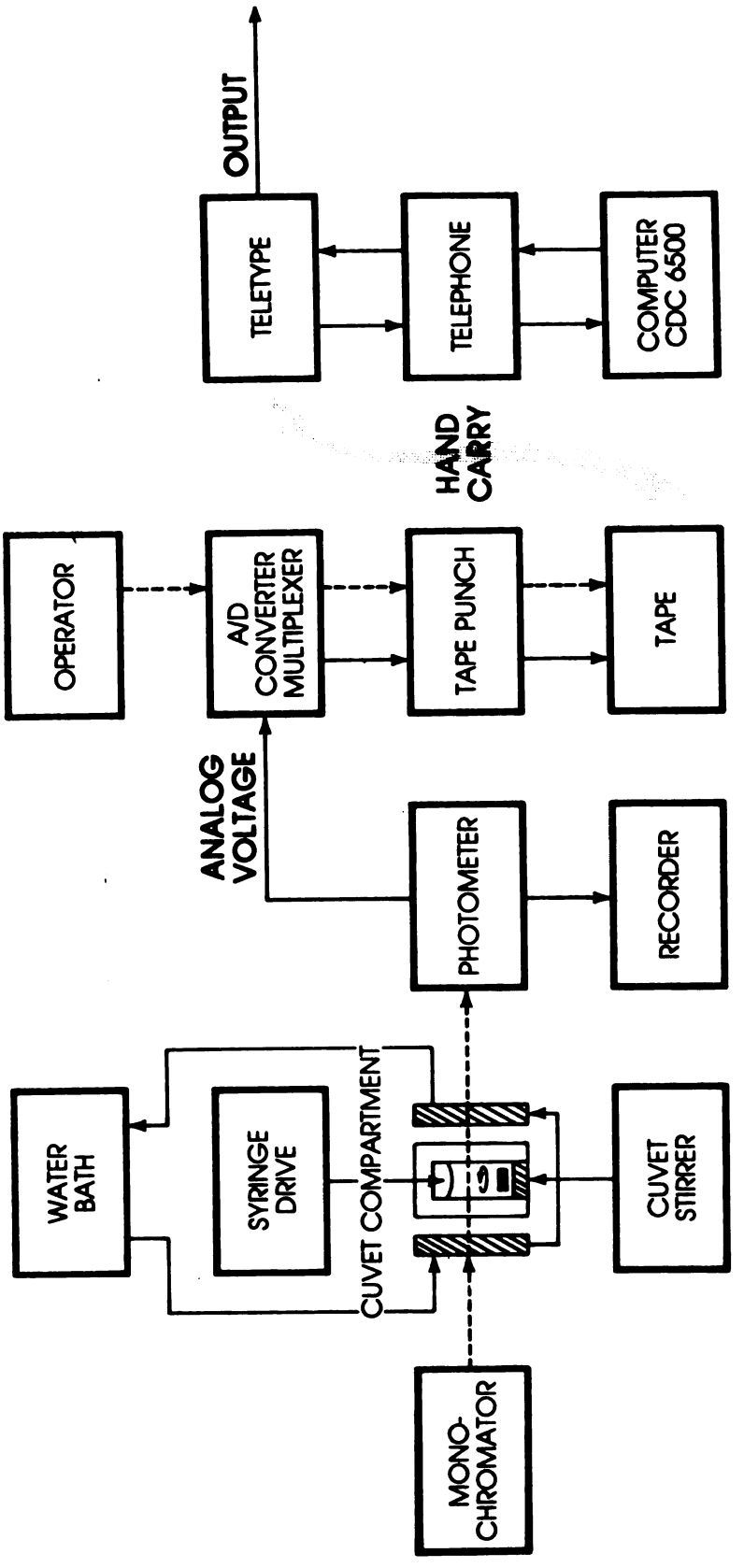

temperature-controlled sample compartment of the spectrophotometer. Concentrated substrate in a Hamilton microliter (25 to 250 ul) glass syringe mounted on a precision syringe drive (Sage, model 255-1) was added continuously to the cuvet solution (see Table 11) via a polyethylene tube (length, 40 cm; i.d., 0.023 in), which passed through a small opening in the top of the sample chamber. The tubing was cut to extend about 1.5 cm below the initial volume meniscus, but to remain above the light path. Noise from stirring or substrate addition was minimized by using the full aperture of the monochromator and offset control on the photometer to make zero adjustment.

The analog photometer output was digitized with absorbance digitizer, (Gilford model 410), which was linked to a digital multiplexer (Gilford model 402) and a paper tape punch (Gilford model 4010). The digitizer converts the voltage analog of absorbance to four binary-coded decimal digits; 0.000 A. The multiplexer converts the binary data into ASCII-coded characters, adds a prefix character to each set to signify an absorbance value, and punches the prefixed set on paper tape.

e. Operation of the System

The cuvet solution (Table 11) was given 5 min equilibration with maximum stirring (1000 rpm). During this period, the syringe was filled with concentrated substrate and advanced to fill the plastic tubing until the liquid meniscus was flush with the end to be immersed in the cuvet. This step minimized any syringe drive backlash and subsequent delay of substrate delivery at the start of the experiment. Noise due to bubble formation during stirring was eliminated by carefully precleaning the stir-pellet and insuring that all solutions were pre-equilibrated at room

temperature. Before substrate addition, the end of the tubing was carefully wiped free of substrate solution. Then 10-15 absorbance values were collected at two second intervals to provide an accurate zero time by simultaneously: (a) lowering the pump tubing into cuvet solution, (b) turning on the syringe drive; and (c) switching to a different channel identification character on the multiplexer to signal the start of substrate addition. Data collection was continued at 2 sec intervals for the specified time in the range of 3.5-5.0 min. Data on paper tape was later read by Teletype paper tape reader, transferred via telephone line modem to a CDC 6500 computer, and processed and stored as disc files (see below).

f. Absorbance Correction and Data Storage

The photometer was largely linear over the range of 0-2.5 A. However, the nature of the diode linearizing network (87) in the instrument caused minor deviations of observed absorbances from the true values.

Plots of O_i (observed absorbance) minus A_i (true absorbance) versus O_i were sinusoidal corresponding to the conducting ranges of linearizing diodes, with a period of 0.5 A and maximal deviatons of ± 0.005 A (Fig. 29A). Although such errors have little effect on individual absorbance measurements, they had a cumulative effect when tangent slopes were calculated for the TANKIN analysis. The curvature of the plots of $O_i - A_i$ vs. O_i (Fig. 29A) obscured any simple relation between A and O. However, plots of $(O_{i+1} - O_i)/(A_{i+1} - A_i)$ vs. O_i were sawtoothed (Fig. 29B) and obeyed the following relation:

Figure 29. Correction of Raw Absorbance Data. (A) Plot of error in observed absorbance (O_i-A_i) as a function of observed absorbance (O_i). (B) Variation in relative instrument response (O_i/A_i) as a function of observed absorbance. Least squares lines through segments of points were calculated to obtain a_j and b_j values (see Appendix). (C) Plot of true absorbance (A_i) vs. observed absorbance (O_j). A_i values were calculated at arbitrary O_i values using equation 2 and the a_j, b_j values obtained from (B). The O_i values are measured as described in the text using a solution of ferricyanide with an absorbance of 0.077 A at 370 nm.

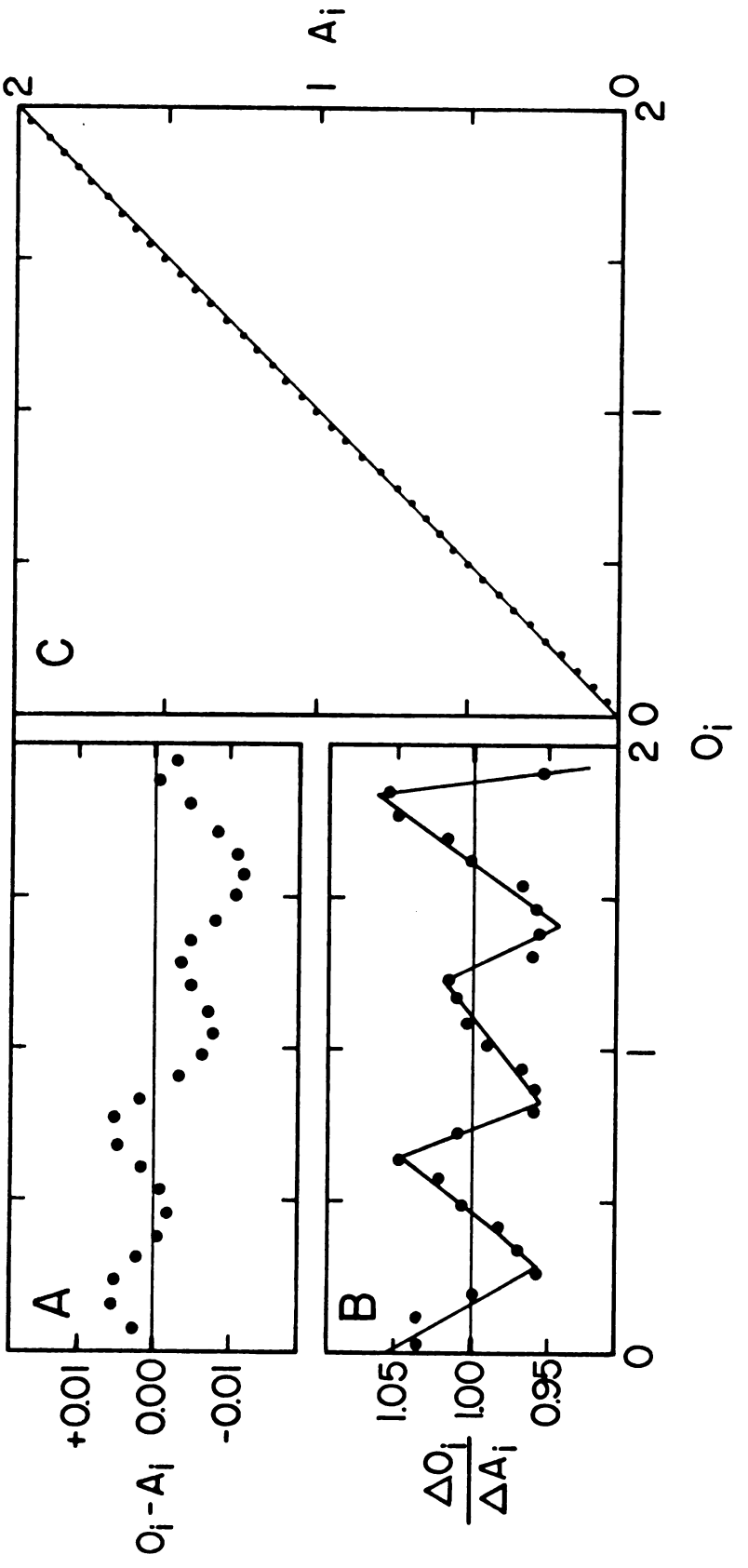

rror in
rved
ument
nce.
e
x).
rbance
lues
m (B).
using a
A at 3%

$$\frac{O_{i+1} - O_i}{A_{i+1} - A_i}\Bigg|_{O_j}^{O_{j+1}} = \frac{\Delta O_i}{\Delta A_i}\Bigg|_{O_j}^{O_{j+1}} \approx \frac{dO}{dA}\Bigg|_{O_j}^{O_{j+1}} = a_i O + b_i \qquad [37]$$

over contiguous intervals, j (= 0, 1, 2, 3,. . . .).

Such plots of measured values for a particular spectrophotometer may be constructed by the method of cumulative addition of small absorbances, ΔA_i (= $A_{i+1} - A_i$). This is accomplished by zeroing the instrument with solvent and measuring O_1 of a solution with a low concentration of some chromophore (true absorbance = ΔA) to give ΔO_1 (= O_1 - 0.0). The slit is then closed so that solvent has the same O_1. Then the absorbing sample is again measured to give O_2 and a second ΔO_2 (= $O_2 - O_1$), and so on, across the absorbance range. Thus, ΔA is constant and dO/dA ($\Delta O/\Delta A$) is evaluated as a function of increasing O_i. In practice, the value of ΔA was between 0.03 - 0.1 A. ΔA was taken as the average of ΔO_i values from O_i = 0.0 A to 2.0 A.

Since slopes (a_i) and intercepts (b_i) could easily be measured from such plots (i.e., Figure 29B), for contiguous intervals from O_0 (O_0 = 0.0 A) to any observed absorbance, (< 2.5 A), it was possible by integration of equation 37 to calculate the correct absorbance, A, corresponding to any observed Ω ($O_{i-1} < \Omega < O_{i+1}$) as follows:

$$A = \sum_{j=0}^{l-1} \int \frac{dO}{a_j \cdot O + b_j} + \int_{O_l}^{\Omega} \frac{dO}{a_l \cdot O + b_l}$$

$$A = \sum_{j=0}^{l-1} \frac{1}{a_j} \ln \frac{a_j \cdot O_{j+1} + b_j}{a_j \cdot O_j + b_j} + \frac{1}{a_l} \ln \frac{a_l \cdot \Omega + b_l}{a_l \cdot O_l + b_l} \qquad [38]$$

Raw observed absorbance values, Ω, were thus corrected by comparison with a table of 50 true and observed absorbance pairs using linear interpolation. The absorbance table for a given instrument was established using a_j, b_j values and equation 38 (Figure 29C), and was found to be valid over a period of at least 1 year. Absorbance correction by FORTRAN program, CATLOG, reduced by half the standard deviation in recorded absorbance during addition of dye, improved the appearance of substrate-velocity plots, and increased by 0.02 the apparent linear correlation coefficient in the TANKIN analysis.

True absorbance vs. time data sets were stored sequentially in disc files along with all the experimental parameters (pump rate, initial volume, extinction coefficients, number of absorbances, data collection rate, initial absorbance, and substrate concentration in the syringe).

D. RESULTS

1. Analysis of Simulated Data

a. Determination of Optimal Window Size for the Tangent-Slope Method

It was to be expected that as the number of points in the window used for data differentiation was increased, estimation of reaction velocities would become more reliable. Yet at large window sizes, the tangent-slope method should introduce bias errors. In order to determine: (a) the extent of such biases, (b) the overall precision of the differential method, and (c) the optimal window size, SIMUL was used to generate noisy "data" which simulated a substrate addition experiment with lactate dehydrogenase. These data were analyzed with TANKIN, employing option 1 (equation 25); the results are shown in Figure 30. The % error in each evaluated constant was calculated and results are expressed as mean ± % standard deviation of six individual determinations. Window sizes from w = 3 to w = 19 were tested and three simulated noise levels are compared.

When three data points are used, the tangent slope method for calculating reaction velocities reduces to that of Balcom and Fitch (113), which has been criticized on statistical grounds (121). The large standard deviations in the evaluated constants at this window size (see Figure 30) suggests that these criticisms may also apply to the analysis of substrate addition data. As window size increases to 9 or 11, however, these standard deviations decrease, and the evaluated constants appear to be unbiased and efficient estimators. Even at the elevated noise levels expected for experiments with immobilized enzymes (2.24 mA RMS error, see below), all three constants can be evaluated with % standard deviations of less than 10%. When larger windows were employed,

Figure 30. Determination of Optimal Window Size for Use in the TANKIN Tangent-Slope Estimation of Velocities by Three Data Noise Levels. Simulated data were prepared by the program SIMUL as described in the text. Input parameters for equation 9 were: $S_{0.5}$ = 0.1 mM, V_{max} = 0.1054 umoles/min, v_o = 2 ml. c_o = 20 mM, r = 9.12 ul/min. Equation 4 was solved for an enzyme reaction where $E_S = E_P = 0$ and E_C = 6220 M^{-1}. A_o was set at 1.5 absorbance units. The simulation protocol was optimized using the program SSOP to give an absorbance change of 0.7 A over a 4 min period, and produce a final substrate concentration of 0.3 mM. The indicated Gaussian noise levels were superimposed upon the calculated absorbance (A_{t_i}) values. The percent errors ± S.D. were determined for the TANKIN estimates of the true $S_{0.5}$ (solid bars), Hill n (hatched bars), or V_{max} (open bars). Each bar trio represents 6 separate simulations.

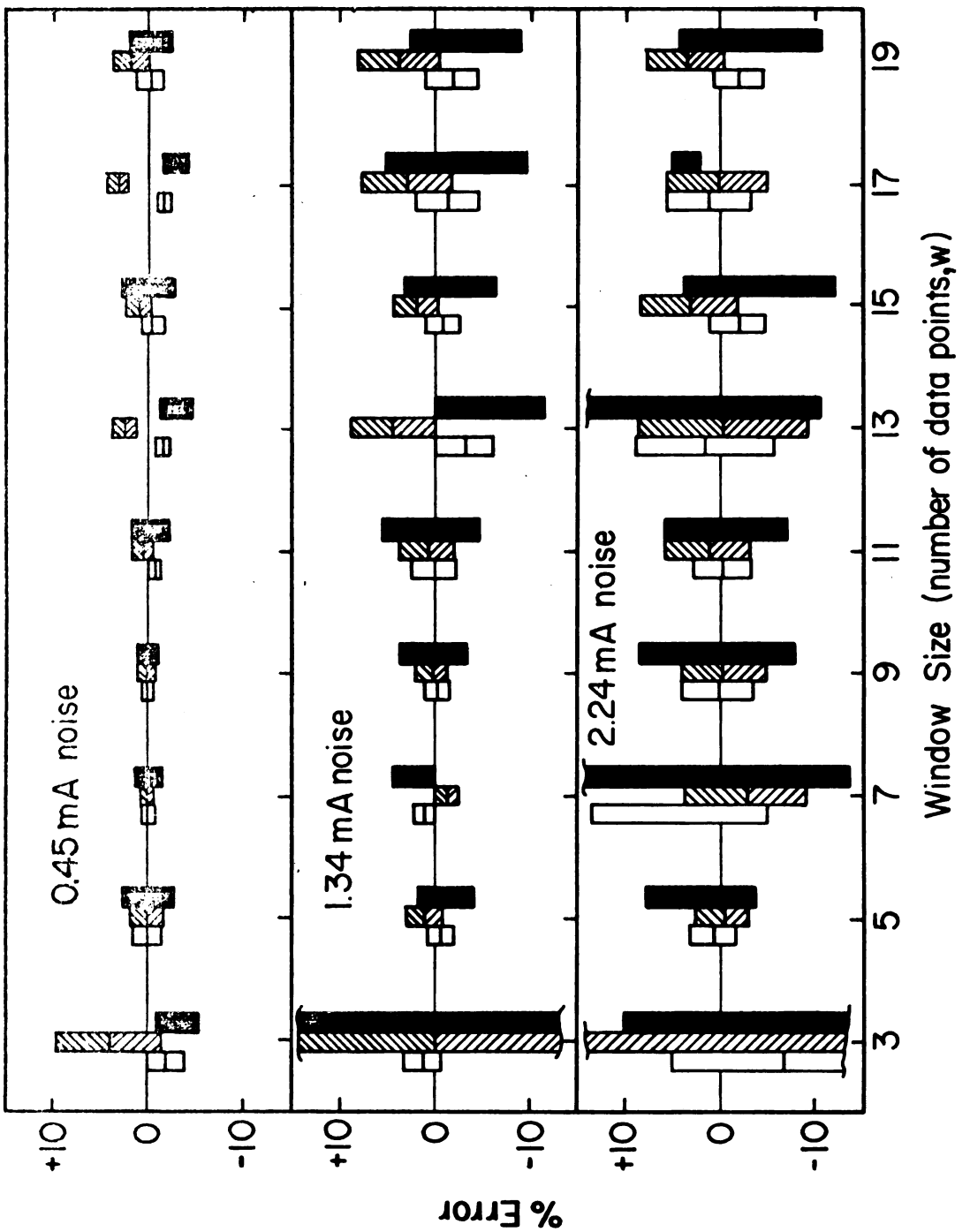
0.45 mA noise
1.34 mA noise
2.24 mA noise
+10
0
-10
% Error
3
5
7
9
11
13
15
17
19
Window Size (number of data points,w)

slight biases were observed. As shown in Figure 30, Hill n appeared high while $S_{0.5}$ and V_{max} values were low. These biases are to be expected because the linear approximation to the product-time curve becomes poorer at larger window sizes (see Figure 30). Even at the largest window sizes, however, biases were never greater than 6%. The data in Figure 30 indicate that valid results can be obtained from tangent-slope analysis of substrate addition data when a window size of 11 was used; hence this window size was used in all subsequent analyses.

Optimal window sizes for options 2 and 3 (equations 26 and 27) were also found to be 9 or 11 points. However, analyses by these options frequently failed to converge to an optimal Hill n at noise levels as high as those to be expected in a real substrate addition experiment. When convergence was obtained, standard deviations in kinetic parameters were about twice those observed with option 1 (data not shown). For these reasons, option 1 (equation 25) was used throughout this study.

b. Determination of Optimal Substrate Concentration Range

It was of interest to know the optimal range of substrate concentrations over which to collect data. Artificial data with RMS error of 0.45 mA were created as in Figure 30, except that pump rate and enzyme concentration, expressed as V_{max}, were varied to produce a range of final substrate concentrations. All other parameters were held constant including net absorbance change. The required r and V_{max} were found using the program SSOP. These data were analyzed by TANKIN and the percent standard deviation in the determination of the Hill parameters was calculated (Figure 31). Each bar in the figure represents the mean and standard deviation of six simulated experiments. Smooth curves drawn

the means illustrate that serious errors and biases are observed especially with V_{max} and $S_{0.5}$ below a final substrate concentration of 1.5 x $S_{0.5}$. At high S_f values only Hill n shows significant bias, and standard deviations for the other two parameters are greatly reduced. The bias in Hill n at elevated final substrate concentration may reflect a sensitivity of this parameter to curvature of the product time course. When $S_f = S_{0.5}$, most of the curvature occurs over a narrow time span. However, these biases are only 4%, and greater accuracy in the determination of Hill n is rarely needed. Between final substrate concentrations of 1.5 - 10 x $S_{0.5}$, biases in the parameters was never more than 5% and percent standard deviations were less than ± 4%. If an evaluated $S_{0.5}$ showed that S_f was out of this range, the experiment could easily be re-optimized using computer program SSOP to produce a more favorable final substrate concentration. The results in Figure 31 suggest that an optimal target value for S_f is about 3 x $S_{0.5}$.

c. Comparison of the Tangent-Slope and Curve-Fit Methods

The data in Figures 30 and 31 show that valid results can be obtained from tangent-slope analysis of simulated substrate addition experiments despite the correlation that occurs between neighboring V_{t_i} values (121). If this correlation seriously interfered with the least squares analysis, then a direct non-linear curve-fit method should result in greatly reduced standard deviation estimates for $S_{0.5}$, V_{max}, and Hill n. That this is not the case is shown in Figure 32. Simulated data for this experiment were generated as described for Figure 30 and analyzed by both TANKIN and MARQ.

Figure 31. Determination of the Optimal Substrate Concentration Range for TANKIN Tangent-Slope Estimation of Hill parameters. Simulated data were calculated as described in Figure 30 except that pump rate, and initial enzyme concentration, were re-optimalized to obtain a series of final substrate concentrations using program SSOP. The simulated noise level was 0.45 mA. These data were analyzed using the program TANKIN (individual weighting, 11 pt. window). Each bar represents 6 separate simulations.

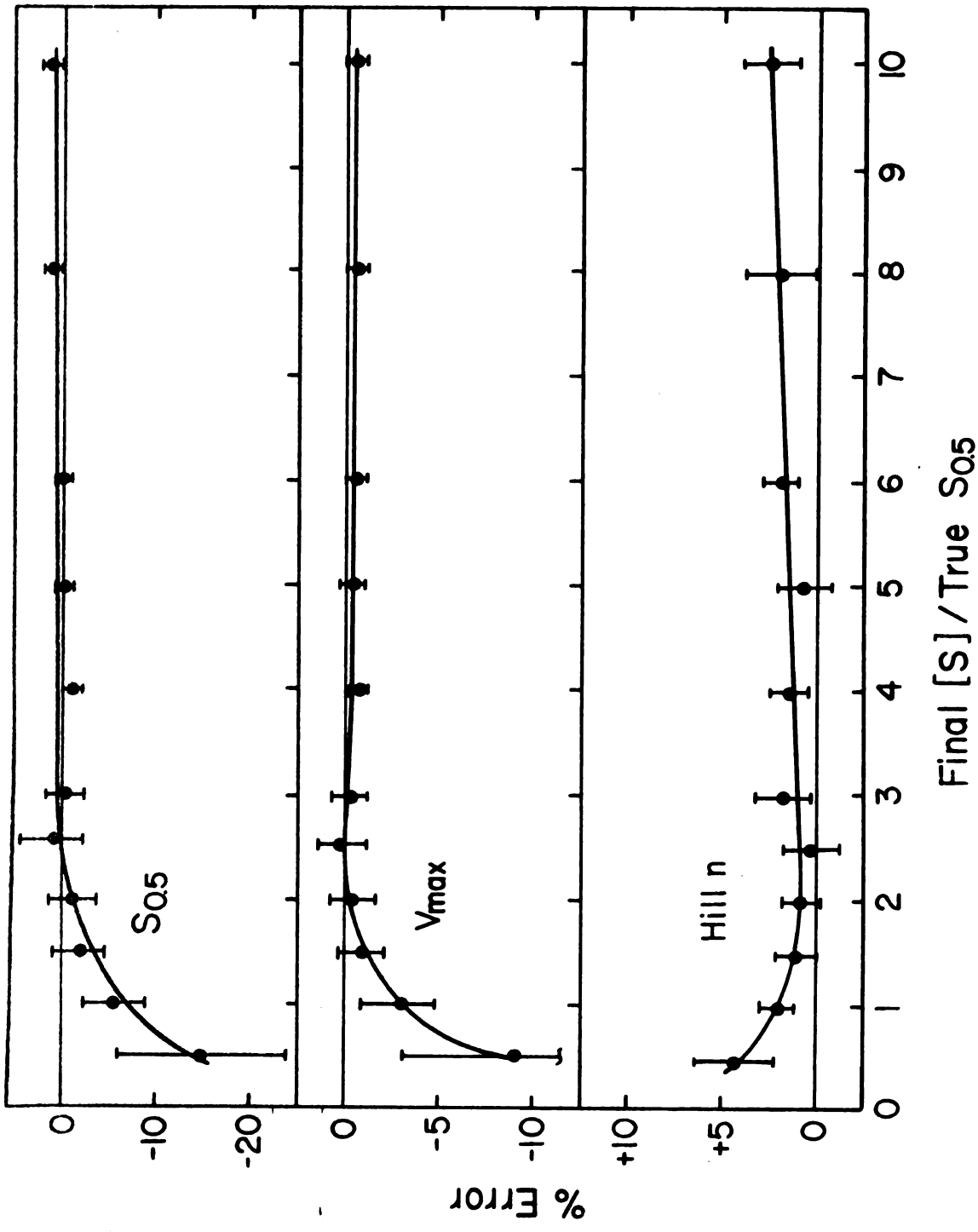
S0.5
Vmax
Hill n
% Error
0
-10
-20
-5
+10
+5
1
2
3
4
5
6
7
8
9
10
Final [S] / True S0.5

Figure 32. Comparison of the Accuracy and Precision of the MARQ (clear bars) and the TANKIN Methods (individual weighting: solid bars, homogeneous weighting: hatch bars). Simulated data were created as described in the legend of Figure 30. Each bar trio represents 6 separate simulations. Eleven points were used in the TANKIN window.

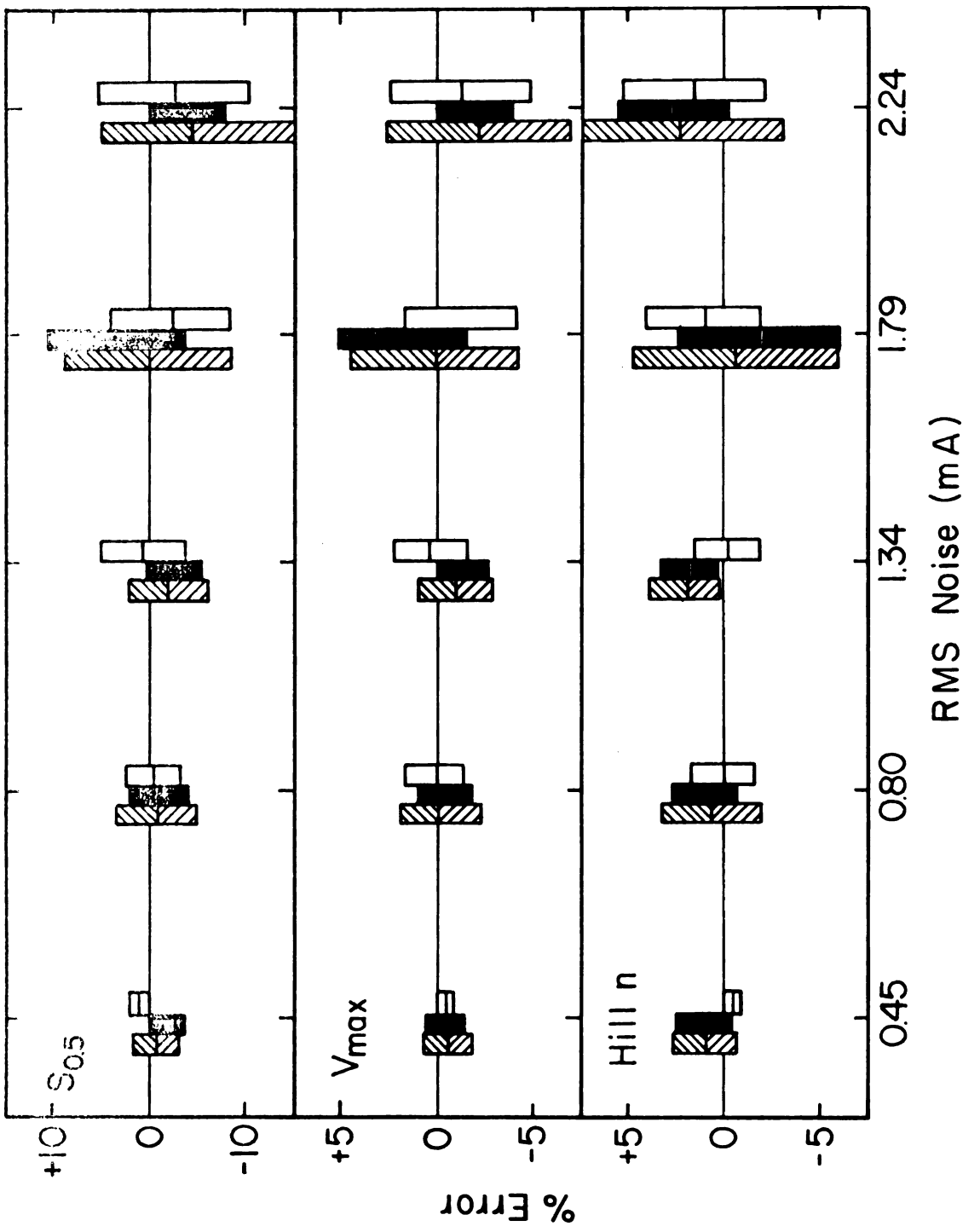
$S_{0.5}$
V_{max}
Hill n
+10
0
-10
+5
0
-5
+5
0
-5
% Error
0.45
0.80
1.34
1.79
2.24
RMS Noise (mA)

Figure 32 also compares homogeneous and individual weighting when TANKIN was used. The method of homogeneous velocity variance (hatched bars) appears less precise at all noise levels than the individual weighting method where velocity variances were approximated as the linear least squares variance of the slope (see Figure 26). The VV_t is expected to be greater in regions of high curvature where velocity is changing fastest and the tangent-slope approximation is poorest. Thus this VV_t provides more appropriate weighting than homogeneous velocity variance and this was used throughout the study. As expected, at all noise levels the curve-fit method (MARQ) is more accurate than the tangent-slope method (TANKIN). However, the increased accuracy was never great ($\leq$ 3% improvement) and was probably due to presence of small biases introduced by the linear approximation of the product-time curve (Figure 26). The precision of the curve-fit method was higher than the tangent slope method at the lower noise levels, but the reverse was true at the highest noise level. Also, the curve-fit method provided more statistical information regarding data quality; however, the most useful information, the mean and standard deviation of parameters from multiple experiments, was available with equal ease from both types of analysis. The tangent-slope method required a tenth or less computing time than did curve fitting when tangent slope-derived parameters were used to obtain initial estimates for curve fitting. When less accurate initial estimates were used, execution time for curve fitting became excessive.

d. Time- or Product-Dependent Effects

If the true rate equation (which describes the kinetic behavior of the enzyme during a substrate addition assay) were known, it could be

substituted for equation 14. Then, using the relationship between product, substrate concentration, and time (equations 9, 10 and 12), parameter values should be obtainable by differential or integral data analysis. The true rate equation would have to describe reaction rate dependencies on time and concentrations of enzyme, reactants, and products as they change throughout the run. Such variations related to changes in enzyme concentration (e.g., due to protomer dissociation - association) would be slight since the net volume change during assay can ordinarily be limited to 5-10%. Also, when cosubstrate concentration can be assumed saturating, its depletion can generally be ignored. However, dependencies on time (due to hysteresis or enzyme inactivation), or on increasing product concentration (due to inhibition or back reaction) could cause major deviations from the Hill approximation. To determine (a) the magnitude of such effects on the Hill parameters and (b) whether time and product effects are distinguishable, artificial data were constructed using equations 23 or 24.

The analysis (Figure 33) showed that as the first order decay constant of enzyme activity (equation 23) rose, the apparent Hill n determined by TANKIN also increased from its true value, while the apparent $S_{0.5}$ and V_{max}, as well as the correlation coefficient, decreased. When k equaled 0.01 min^{-1} (4% loss in enzyme activity during the run), the relative biases in the determination of $S_{0.5}$, V_{max}, and Hill n were -20%, -10%, and +7%, respectively. When K equaled 0.06 min^{-1} (22% loss in enzyme activity) these values were -50%, -35%, and +60%, respectively. Correlation coefficients for inactivation rate constant values of 0, 0.01, and 0.06 min^{-1}, respectively, were 0.995, 0.993, and 0.982 when the data RMS noise level was 0.45 mA. The decrease

Figure 33. Effect of End Point Deletion on the Final Correlation Coefficient (A) and Apparent Hill n (B) at Various Levels of Simulated First Order Enzyme Inactivation During a Substrate Addition Experiment. Simulated data were created as described in the legend of Figure 30 except that equation 23 was used in place of equation 14 in the program SIMUL. A noise level of 0.45 mA was superimposed on the data. The data were analyzed by TANKIN using individual weighting and an 11-point window (k = first order decay constant).

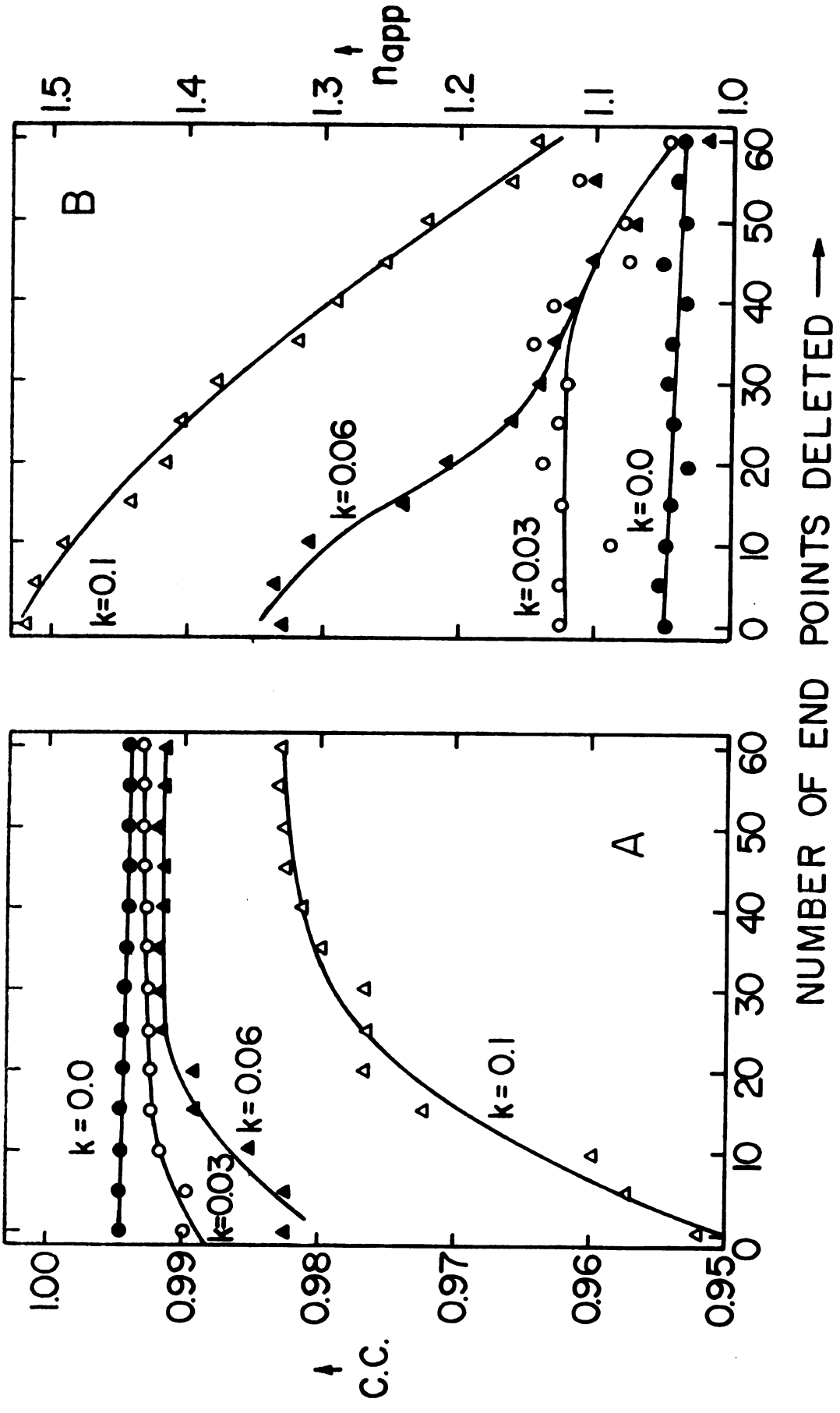
A
B
k=0.0
k=0.03
k=0.06
k=0.1
C.C.
n_{app}
NUMBER OF END POINTS DELETED

in correlation coefficient suggests that differentiated data, transformed according to equation 25, deviated from linearity when enzyme inactivation was present. These deviations were regular and could be revealed in most cases where the inactivation constant is independent of S by TANKIN analysis in which raw data points were progressively deleted from the end of the data set, i.e., from the highest S or longest time. As the data set was shortened, the correlation rose (Figure 33A). The rate of increase was greater with an increased inactivation constant. Under the same conditions, Hill n decreased correspondingly until the Hill n_{app} approached the true value of 1.0.

When product competitive inhibition was simulated using equation 24, very similar biases were introduced into the Hill parameters and the correlation coefficient decreased as K_i (in these tests $P_f = S_{0.5} =$ 0.1 mM). A product inhibition constant of 0.3 mM (three times the final product concentration produced errors in $S_{0.5}$, V_{max}, and Hill n of -20%, -10%, 9%, respectively. When K_i equaled 0.1 mM, the errors rose to -50%, -35%, and +20%. Correlation coefficients for no product inhibition, and for the cases when K_i equals 0.3 mM and 0.1 mM were 0.995, 0.992, and 0.980, respectively, for data with RMS noise levels of 0.45 mA. Unlike enzyme inactivation, end point deletion did not significantly improve the Hill parameters, or the correlation coefficients when there was product inhibition (data not shown). This observation relates to the fact that competitive inhibition does not alter the form of the rate equation (129), making it impossible to detect this type of inhibition in a single run.

To determine whether product competitive inhibition could be distinguished from enzyme inactivation in a series of runs in which

experimental variables were systematically altered, the TANKIN-determined V_{max} ($V_{max_{app}}$), was compared with the V_{max} used in constructing the data set (theoretical V_{max}) (Figure 34). Eleven experimental conditions were defined using the SSOP program in which either the duration (Figures 34A and C), or the final product level (Figures 34B and D) were varied. For each of these 11 conditions, various levels of either enzyme inactivation (Figures 34A and B) or product competitive inhibition (Figues 34C and D) were simulated. All other experimental variables including total number of data points and final substrate concentration were held constant.

As expected from Figure 33, as the overall duration (t_f) increased, so also did the effect of enzyme inactivation on $V_{max_{app}}$ (Figure 34A). The effects of product inhibition on $V_{max_{app}}$, however, were not significantly changed by increasing t_f (Figure 34C). Similarly, increasing P_f, which accumulated during the assay, increased the effects on $V_{max_{app}}$ due to product inhibition (Figure 34A), but not due to enzyme inactivation (Figure 34B). It should be noted that back extrapolation of the fitted least-squares lines to zero t_f (Figure 34A) or zero time P_f (Figure 34D) results in a much better approximation to the true V_{max}. Very similar results were found with $S_{0.5}$ and Hill n (data not shown).

The results from Figures 33 and 34 suggest that serious deviations from the Hill approximation can be expected when there is greater than 4% loss in enzyme activity or when the final product concentration is higher than 30% the K_i for product. Changes in correlation coefficient or Hill n caused by point deletion serve as indicators of excessive (22% loss during assay) enzyme inactivation (Figure 33). It is possible to

Figure 34. Effect of Varying t_f (A and C) or P_f (B and D) During a Simulated Substrate Addition Experiment on the Ratio of $V_{max_{app}}$ to Its Theoretical Value (V_{max}). Simulated data were computed as described in the legend of Figure 30 except that either equation 16 or 17 were substituted for equation 7 in the program SIMUL. The simulated noise level was 0.45 mA. The data were analyzed by TANKIN using individual weighting and an 11-point window. Lines represent least squares regressions through the data.

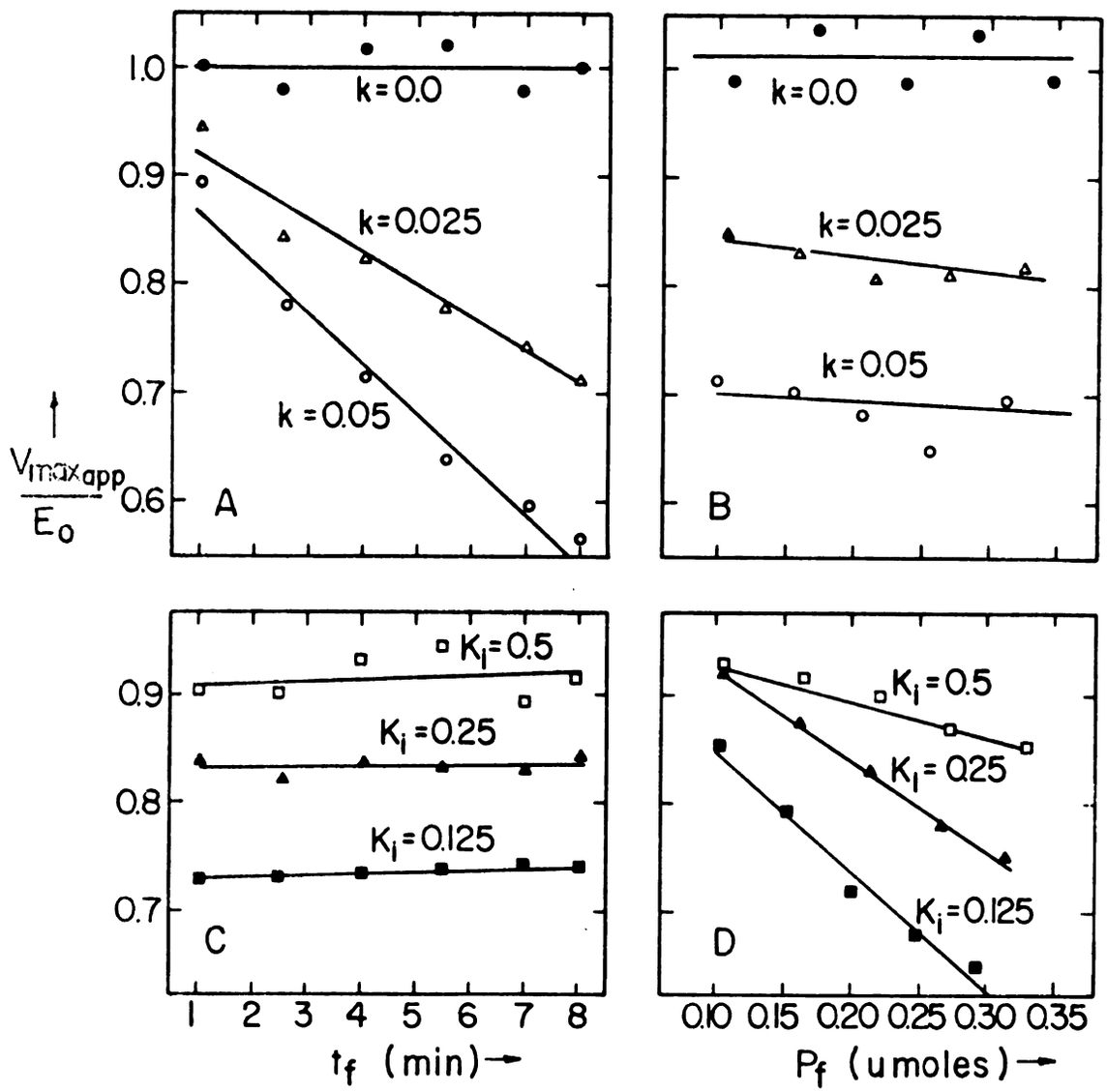
1.0
0.9
0.8
0.7
0.6
k=0.0
k=0.025
k=0.05
A
B
$\frac{V_{max_{app}}}{E_o}$
K_i=0.5
K_i=0.25
K_i=0.125
C
D
1 2 3 4 5 6 7 8
t_f (min)→
0.10 0.15 0.20 0.25 0.30 0.35
P_f (umoles)→

detect lower levels of enzyme inactivation (<10%) and also product inhibition (K_i > 5-fold final product concentration) by systematically varying either the duration of the experiment or the final product concentration.

2. System Performance and Analysis of Real Data

a. Preliminary Evaluation of the System

Initial tests of the instrument system were made to determine the nature and extent of errors in absorbance measurement in a substrate addition experiment. In addition to spectrophotometer noise, drift, and nonlinearity, errors in absorbance measurement could result from inhomogenieties of stirring, mixing, or addition rate. Therefore, the contributions of these factors to overall absorbance error wee closely examined. As shown in Table 12, RMS error in the absence of stirring, mixing, or substrate addition (static cuvet) were about ± 0.6 mA and largely independent of nominal absorbance. A significant portion of this noise was due to truncation error in recording absorbance, since the readout is to the nearest mA. Another component of this noise was spectrophotometer drift which amounted to 0.43 mA over a 3-min period. The increase in noise due to stirring was about ± 0.24 mA. As expected, this noise was also nearly homogeneous in distribution with respect to nominal absorbance. No special precautions were taken to remove small suspended particles which are probably the major contributors to the noise increase during stirring. Since some of the experiments discussed later involve assay of immobilized lactate dehydrogenase, background absorbance and noise levels were also measured with graded amounts (0 to 60 µl) of packed Sephadex G-50 beads in the stirred cuvet. Under these conditions,

Table 12

Noise of Spectrophotometric System and Cuvet Contents

Condition	Volume of Packed Beads (ul)	Nominal Absorbance[a]	RMSb Noise (mA)
Static	None	0.0	0.50
		1.0	0.50
		2.0	0.66
Stirred	None	0.0	0.75
		1.0	0.84
		2.0	0.78
Stirred	3	0.049	1.15
	6	0.084	1.63
	15	0.175	2.14
	30	0.280	3.03
	60	0.480	3.32

[a]At 340 nm. Cuvets without Sephadex beads contained graded amounts of NADH to give nominal absorbance. Solution with Sephadex were blanked against H_2O.

[b]S.D. of all absorbance values. Data were collected at 2 sec intervals for 3 min.

increases in background absorbance (due to light scattering in the bead suspension) in response to added Sephadex G-50 was nearly linear. Even under such extreme conditions, RMS error never rose above ± 3.32 mA; nearly identical results were obtained with Sepharose 4-B (results not shown).

Further evaluation of the effects of mixing and substrate addition was made in two ways: (a) concentrated bromphenol blue, 2 mg/ml, was added dropwise above the meniscus to cause step changes in absorbance; i.e., from 0 to 1.5 A. Strip chart recordings and analysis of data on tape showed that complete mixing occurred in 1.5 sec. (b) NADH (10 mg/ml) bromophenol blue (0.05 to 2 mg/ml), or ferricyanide (24 mg/ml) were added from the syringe pump and the increase in absorbance recorded. Relative increases in absorbance with time (corrected for dilution) were compared with those predicted by Beer's Law. These data revealed no lag in the onset of linear absorbance increase. Calculation of pump rate at various times during chromophore addition from the slope of absorbance vs. time line revealed a relative error of ± 4.1% within individual experiments. When correction for absorbance nonlinearity (see Materials and Methods) was applied, this value dropped to 2.2%. For this reason, the absorbance correction procedure was used in all experiments. When chromophore addition data were fit to theoretical equations (assuming Beer's Law and correcting for dilution), the RMS error depended upon chromophore concentration. For instance, with dye concentrations of 0.5-4.0 mg/ml, this value was 0.55 mA; but it increased to 1.1 mA at higher concentrations, presumably due to a swirling of the dense solution directly into the light path before mixing. Residuals signs tests and residuals distribution plots

(120) showed that error distribution was approximately Gaussian, although some systematic deviations remained.

The above results suggested that the RMS error for substrate injection experiments should be ± 0.5-1.0 mA. However, larger errors may be expected if dense substrate solutions or immobilized enzymes are used. The major component of this noise is probably spectrophotometer instability and nonlinearity, and truncation error. Stirring, mixing, and pumping appear to contribute far less error than had been expected.

b. Kinetic Constants Estimated for Soluble Enzymes

An analysis of simulated data suggested that both nonlinear curvefitting and the tangent-slope methods can be used reliably to analyze reaction progress data with a noise content in excess of that expected from the above evaluation of system performance. While the curvefitting method can provide more meaningful statistical information, the computation time for the tangent-slope analysis is 10-fold shorter and does not require highly accurate initial guesses of the Hill n.

Real data differs from artificial data in that additional biases may come from errors in: (a) the measuring system (instrumental bias); (b) experimental parameters, pump rate, initial volume, etc. (experimental bias) and (c) the experimental model (model bias). To assess the effects of these factors on the reliability of both methods of analysis, substrate addition experiments were performed on a number of soluble enzymes.

Initial observations indicated the need for absorbance correction prior to tangent-slope analysis whenever the total absorbance change was greater than 0.4 A, or when absorbance measurements spanned more than one

absorbance correction interval. Use of absorbance correction improved the appearance of TANKIN-generated substrate-velocity plots and increased the apparent correlation coefficient of the final fit by about 0.02 (e.g., 0.96 to 0.98) in analysis of typical experiments with a number of enzymes. For these reasons absorbance correction was always used for both tangent-slope and curve-fit analyses.

The profile of a typical corrected absorbance-time curve for a pyruvate addition with lactate dehydrogenase is shown in Figure 35A. Absorbance at 340 nm decreases as NADH is consumed by the reaction. The solid line through the data points represents the MARQ-generated curvefit to the data. The RMS error for this curvefit (± 1.08 mA) is slightly higher than expected (0.5-1.0 mA). The extra error may be accounted for by the additional biases introduced in the real experiment as discussed above. However, this error level is well within that required for valid analysis (see Figure 32). From the computer program MARQ, the multiple correlation coefficients given for this fit revealed that all three parameters are highly coupled ($\rho S_{0.5}$ = 0.9998, ρV_{max} = 0.9998, ρn = 0.9855). Partial correlation coefficients (120) showed that this was due mainly to a high correlation between $S_{0.5}$ and V_{max} ($\rho_{S_{0.5},\ V_{max}}$ = +0.9944). Despite this high correlation, percent marginal standard deviations were low ($S_{0.5}$, +2.7%; V_{max}, 1.3%; Hill n, ± 1.0%). This indicates that the optimal parameters are very well defined by the data; this is also indicated by the fact that convergence from a number of combinations of initial guesses, with ± 30% or more deviations from the optimal value, produced the same parameters within 5 significant digits.

Figure 35. Typical Results of Single Cuvet Assays of Hill Parameters for LDH (A and B) and β-Galactosidase (C and D). Corrected absorbance data were analyzed by either the MARQ direct curve-fitting procedure (A and C) or by the TANKIN tangent-slope procedure (B and D). Conditions for the assays are given in Table 11. Lines through the data are theoretical and are derived from the optimal kinetic parameters obtained from the MARQ (A and C) or the TANKIN (B and D) analyses, respectively.

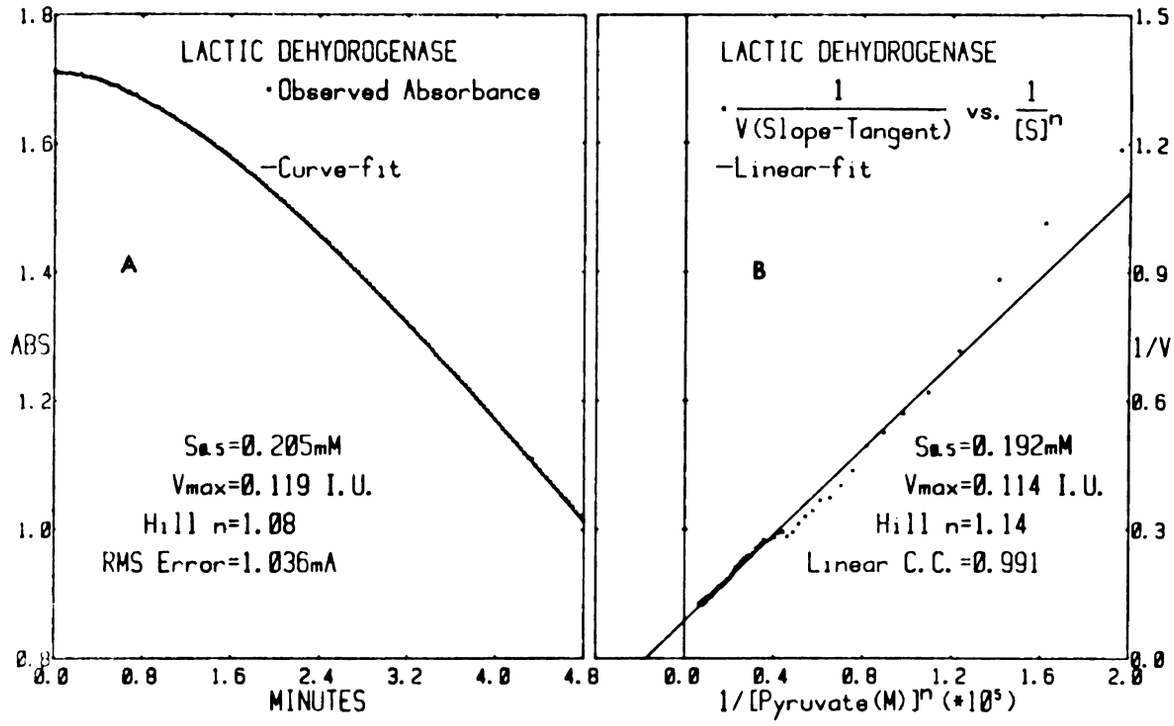
LACTIC DEHYDROGENASE
·Observed Absorbance
—Curve-fit
A
Sas=0.205mM
Vmax=0.119 I.U.
Hill n=1.08
RMS Error=1.036mA
ABS
MINUTES
LACTIC DEHYDROGENASE
· 1/V(Slope-Tangent) vs. 1/[S]^n
—Linear-fit
B
Sas=0.192mM
Vmax=0.114 I.U.
Hill n=1.14
Linear C.C.=0.991
1/V
1/[Pyruvate(M)]^n (*10^5)

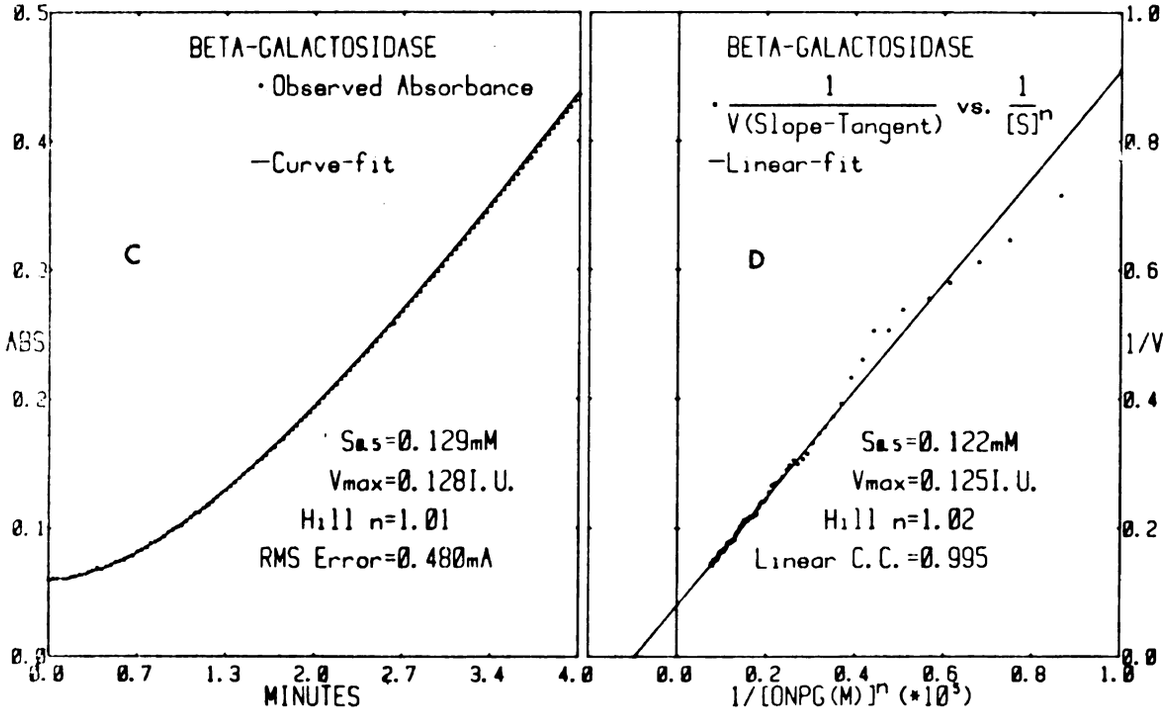
BETA-GALACTOSIDASE
·Observed Absorbance
—Curve-fit
C
Sas=0.129mM
Vmax=0.128I.U.
Hill n=1.01
RMS Error=0.480mA
ABS
MINUTES
BETA-GALACTOSIDASE
· 1/V(Slope-Tangent) vs. 1/[S]^n
—Linear-fit
D
Sas=0.122mM
Vmax=0.125I.U.
Hill n=1.02
Linear C.C.=0.995
1/V
1/[ONPG(M)]^n (*10^5)

Fitting these data by the method of tangent slopes, resulted in comparable kinetic parameters (Figure 35B). Deviations from linearity in the modified Lineweaver-Burk plot were traced to truncation errors[21] (deviations were also present after analysis of artificial data similarly truncated) and to absorbance nonlinearities that were not fully corrected. This effect is largest at lower velocities where the effects of truncation are most important. In order to quantitate the effects of experimental bias in TANKIN analysis, experimental input variables were changed and the resulting Hill parameters compared to those in Figure 35B. An error or +4% in initial volume resulted in the following errors: $S_{0.5}$, -5%; V_{max}, +4%; and Hill n, 0%. Error of +1% in pump rate gave errors of +2%, 0.04%, and 0.1%; +16% error in substrate concentration produced deviations of +15%, 0.1%, and -2.7%, respectively. Thus the results from the tangent-slope method do not appear to be unduly susceptible to experimental bias.

Model bias could result from the effects of cosubstrate depletion, product inhibition, or reaction reversibility. Calculations show that the NADH concentration is always 15-fold above the $S_{0.5}$ for NADH [ca. 10^{-5} M (123)]. Assuming the kinetics with respect to NADH to be hyperbolic, the reduction in effective V_{max} due to NADH depletion could be no more than 2.3%. Since changes in effective V_{max} of less than 4% during a substrate addition experiment may be neglected, NADH can be assumed to be saturating throughout the addition period. When the final absorbance change was held constant at 0.6 A, but the initial NADH concentration was halved to 0.16 mM, a 30% reduction occurred in $S_{0.5}$ and V_{max}, indicating the effects of cosubstrate depletion.

The analysis of artificial data demonstrated that product inhibition can be detected by varying the final product concentration in an addition experiment. This approach was tested with lactate dehydrogenase, which is known to be subject to product inhibition (123). When the final absorbance change was varied from 0.12 to 0.8 A (equivalent to production of 0.02 to 0.13 mM lactate and NAD^+), variations in the slope tangent-derived Hill parameters were less than 10%. Equations describing the kinetics of lactate dehydrogenase (123) can be used to show that reduction in reaction rate due to lactate or NAD^+ inhibition would never be greater than 1% for the experiment in Figures 35A and 35B. Similarly, it can be shown that the back reaction would always be less than 0.35% of the forward. Thus, small amounts of product inhibition or reaction reversibility do not significantly interfere with these assays.

Figures 35C and D show the results of a representative addition experiment with β-galactosidase. In this case, absorbance at 420 nm increases as nitrophenylate is produced. The RMS error for the curvefit (Figure 35C) is low. This may be due to the fact that the entire absorbance range lies within 1 absorbance correction interval, and deviations due to inadequacies of the absorbance correction procedure are reduced. The Hill parameters obtained by integral analysis (Figure 35C) are in good agreement with those obtained by differential analysis (Figure 35D) of the same data. The apparent linear correlation coefficient is higher for this experiment than for that of Figure 35B and is close to that obtained using artificial data with a similar Gaussian noise level and absorbance range (see Figure 32). The calculated $S_{0.5}$ is in good agreement with literature values (124). Some addition experiments were performed using K^+ in place of Na^+ as the monovalent cation activator

(see Table 11). Under these conditions, the $S_{0.5}$ rose to 0.8 mM ± 24% (n = 3) with no significant change in Hill n. This effect was expected from the known cation specificities of this enzyme (130). It appears unlikely that product inhibition or back reaction participate since the inhibition constant of galactose is high (9.4 mM) and the reaction is essentially irreversible (130).

Table 13 compares kinetic constant evaluated for 6 enzymes, including lactate dehydrogenase and β-galactosidase. The data were derived by the substrate addition method and were analyzed by both the differential slope-tangent method (TANKIN) and the integral curve-fit method (MARQ). These results are also compared with kinetic parameters obtained from convential multicuvet assays or with published values. The percentage standard deviations were calculated from replicate experiments. Agreement of Hill parameters both between the two methods of analysis and between substrate addition and multicuvet methods is generally good, underscoring the lack of significant bias in the substrate addition technique.

Preliminary experiments with yeast pyruvate kinase revealed the expected effects of fructose-1, 6-bisphosphate on $S_{0.5}$ (0.056 mM to 0.927 mM) and Hill n (0.85 to 1.99).

It should be noted that these determinations were made on enzymes whose $S_{0.5}$ values vary over a wide range (0.02-5.0 mM) and whose Hill n value varied between 1 and 2.

TANKIN is written so that determinations can be made when cosubstrate, product, or both substrate and product have absorbance. A comparison of product inhibition, Michaelis and equilibrium constants with the low maximum product concentrations obtained with malate dehydrogenase

Table 13

Kinetic Constants for Soluble Enzymes

Enzyme (Determinations)	Constant	Slope-Tangent[a]	Curve-fit[a]	Manual or Literature[a]
Lactate dehydrogenase (4)[b]	$S_{0.5}$[c]	0.12 ± 8%	0.11 ± 9%	0.097 ± 20%
	V_{max}[d]	0.18 ± 11%	0.18 ± 6%	0.15 ± 6%
	Hill n	1.06 ± 4%	1.06 ± 2%	1.31 ± 7%
	cc	0.991	---	
	RMS noise[e]	---	1.02	
Malate dehydrogenase (4)	$S_{0.5}$	0.030 ± 17%	0.028 ± 18%	0.033
	V_{max}	0.032 ± 30%	0.030 ± 27%	0.03
	Hill n	1.06 ± 8%	1.15 ± 8%	---
	cc	0.970	---	
	RMS noise	---	0.60	
β-Galactosidase (3)	$S_{0.5}$	0.10 ± 20%	0.10 ± 20%	0.11
	V_{max}	0.23 ± 9%	0.23 ± 9%	0.2
	Hill n	1.10 ± 8%	1.08 ± 7%	---
	cc	0.997	---	
	RMS noise	---	0.69	

[a]Mean ± % S.D. of separate determinations. See Table I for experimental protocols.
[b]Numbers in parenthesis refer to the number of runs averaged.
[c]$S_{0.5}$ in mM.
[d]V_{max} in International Units.
[e]RMS error in milliabsorbance.

Table 13 (contd.)

Kinetic Constants for Soluble Enzymes

Enzyme (Determinations)	Constant	Slope-Tangent[a]	Curve-fit[a]	Manual or Literature[a]
KDPG aldolase (6)	$S_{0.5}$[c]	0.019 ± 10%	0.019 ± 10%	0.02 ± 9%
	V_{max}[d]	0.13 ± 15%	0.13 ± 15%	---
	Hill n	1.6 ± 6%	1.6 ± 6%	1.5 ± 8%
	cc	0.971	---	
	RMS noise[e]	---	0.99	
Tryptophanase (1)	$S_{0.5}$	0.15	0.09	0.06
	V_{max}	0.09	0.07	0.075
	Hill n	1.11	1.13	1.0
	cc	0.981	---	
	RMS noise	---	0.79	
Threonine dehydratase (6)	$S_{0.5}$	4.9 ± 8%	5.0 ± 16%	4.6 ± 6%
	V_{max}	0.23 ± 4%	0.23 ± 9%	0.15 ± 2%
	Hill n	1.2 ± 8%	1.2 ± 17%	0.97 ± 3%
	cc	0.992	---	
	RMS noise	---	2.05	

[a]Mean ± % S.D. of separate determinations. See Table I for experimental protocols.
[b]Numbers in parenthesis refer to the number of runs averaged.
[c]$S_{0.5}$ in mM.
[d]V_{max} in International Units.
[e]RMS error in milliabsorbance.

(131), and KDPG-aldolase (134) suggest that product inhibition or back reaction could not be significant under the conditions given in Table 11. The values for KDPG-aldolase do not agree with those published previously (135); however, conventional determinations made in this study and the substrate addition methodology gave the same results.

Standard deviations of the Hill parameters obtained by the tangent-slope method are also comparable to those obtained by curvefitting. The standard deviations for V_{max} are 2- to 4-fold greater than those observed for simulated data (see Figure 32). Part of this increase may be attributed to errors in addition of enzyme in different runs. However, errors in $S_{0.5}$ and Hill n are also about 2-fold greater than expected from simulated data (see Figure 32), and this may result from experimental biases and the elevated instrumental noise levels. The average RMS error observed about the MARQ-fitted curve are also listed. The value for malate dehydrogenase is about that expected from dye addition experiments; however, for other enzymes this value is slightly larger than expected. Comparison of Tables 11 and 13 shows that the largest RMS errors are associated with threonine dehydrase and lacatate dehydrogenase which also have large absorbance changes during the assay. Since this is probably not due to product inhibition or back reaction during substrate addition, it is assumed that residual errors in absorbance resulting from incomplete absorbance correction are contributing to errors. The unusually large RMS noise associated with the threonine dehydrase experiments may also be due to the high concentrations of the substrate in the syringe solution (24 mg/ml) and of coupling enzyme in the cuvet solutions (1 mg/ml), which may have produced optical discontinuities in the light path.

The average apparent linear correlation coefficients reported for the tangent-slope method in Table 13 do not correlate directly with the RMS errors of the curvefit method. This is because the correlation coefficient is a relative measure of data error and varies with the range of velocity values spanned during an experiment. Since this value will vary between enzymes, correlation coefficients for different enzymes are not directly comparable; and they are presented here only to give their approximate magnitudes. These correlation coefficients were comparable between experiments with equivalent quantities of the same enzyme, however, and could be used to identify unreliable assays.

c. Kinetic Constants for Immobilized Lactate Dehydrogenase

Tests with artificial data suggested that reliable Hill constants could be obtained even at the higher noise levels encountered in the presence of insoluble supports. To examine this possibility, substrate addition progress curves were obtained for lactate dehydrogenase in the presence and absence of Sephadex G-50 (which excludes lactate dehydrogenase). The results in Table 14 show that Hill parameters obtained by substrate addition assays were not significantly altered by the presence of Sephadex during the assays. From the data given in Table 12, it was determined that the level of Sephadex added (50 µl packed volume) should produce an RMS noise level of about 2.5 mA. The error obtained from the curvefit of the data obtained in the presence of Sephadex is in close agreement with this value. Similar results (not shown) were obtained with elevated levels of Sepharose 4-B. These findings suggest that the elevated noise level in the presence of the matrices does not interfere with the determination of the kinetic parameters.

The average apparent linear correlation coefficients reported for the tangent-slope method in Table 13 do not correlate directly with the RMS errors of the curvefit method. This is because the correlation coefficient is a relative measure of data scattering variables with the range of velocity values spanned during an experiment. Since this value will vary between enzymes, correlation coefficients for different systems are not directly comparable, and they are presented only to give their approximate magnitudes. These correlation coefficients were comparable between experiments with equivalent enzyme concentrations, however, and could be used to identify anomalies in data.

c. Kinetic Constants for Inhibition of Sucrase Activity

Tests with artificial data showed that data with constant could be obtained even at the point where small concentrations of presence of insoluble sucrase. At maximum velocity, substrate addition progress curves were useful in the inhibition of presence and absence of Sephadex G-50 (which retards lactase activity) were used. The results in Table 14 show that Hill parameters obtained by sucrase addition assays were not significantly altered by the presence of Sephadex during the assays. From the data given in Table 12, it was determined that the level of Sephadex added (50 µl packed volume) should produce an RMS noise level of about 2.5 mA. The error obtained from the curvefit of the data obtained in the presence of Sephadex is in close agreement with this value. Similar results (not shown) were obtained with elevated levels of Sephadex 1-8. These findings suggest that the elevated noise level in the presence of the matrices does not interfere with the determination of the kinetic parameters.

Table 14. [a]Mean ± % S.D. of separate determinations. See Table I for experimental protocols.
[b]Numbers in parenthesis refer to the number of runs averaged.
[c]$S_{0.5}$ in mM.
[d]V_{max} in International Units.
[e]RMS error in milliabsorbance.

Table 14

Kinetic Constants for Soluble and Immobilized LDH[a]

Enzyme (Determinations)	Constant	Slope-Tangent	Curve-fit	Manual
Soluble (5)	$S_{0.5}$[b]	0.12 ± 25%	0.12 ± 17%	0.097
	V_{max}[c]	0.065 ± 8%	0.067 ± 4%	0.08
	Hill n	1.23 ± 6%	1.17 ± 4%	1.31
	cc	0.991	---	
	RMS error[d]	---	1.02	
+Sephadex G-50 (4)	$S_{0.5}$	0.18 ± 28%	0.16 ± 13%	---
	V_{max}	0.09 ± 11%	0.08 ± 12%	0.08
	Hill n	1.0 ± 20%	1.1 ± 9%	---
	cc	0.955	---	
	RMS error	---	2.29	
Immobilized -Sephadex G-50 (4)	$S_{0.5}$	0.10 ± 9%	0.11 ± 9%	0.15
	V_{max}	0.065 ± 5%	0.066 ± 5%	0.07
	Hill n	1.19 ± 5%	1.2 ± 8%	1.26
	cc	0.907	---	
	RMS error	---	2.78	
Immobilized -Sepharose 4-B (5)	$S_{0.5}$	0.20 ± 24%	0.23 ± 17%	0.122
	V_{max}	0.06 ± 13%	0.06 ± 11%	0.052
	Hill n	1.30 ± 7%	1.21 ± 5%	1.15
	cc	0.987	---	
	RMS error	---	0.975	

Lactate dehydrogenase bound to Sephadex G-50 (surface coupling) exhibited similar kinetic constants when assayed either by substrate addition or conventional initial velocity methods as shown in Table 14. The $S_{0.5}$ determined by substrate addition is somewhat lower; however, only one determination was made by the conventional multicuvet method. The 3 kinetic parameters appear very similar for soluble and Sephadex G-50-immobilized lactate dehydrogenase. This lack of immobilization effect has also been observed for lactate dehydrogenases attached in a variety of ways (135-138), although large effects have also been reported (139) for others. The effects of immobilization apparently depend upon the species of lactate dehydrogenase, the mode of coupling, and the nature of the insoluble support.

When lactate dehydrogenase bound to Sepharose 4B (internal coupling) was assayed by the same procotol, a large Hill n value of 1.7 was obtained (data not shown). Although substrates must diffuse into the bead and products must diffuse to the exterior, the high Hill n value was not due to a prolonged approach to the steady-state reaction rate dictated by the substrate concentration, because initial rate measurement showed that a constant rate was reached in less than 2 sec after substrate addition to lactate dehydrogenase immobilized on either Sephadex G-50 or Sepharose 4-B. Instead, qualitative tests indicated that the $S_{0.5}$ for NADH was much higher for enzyme bound to Sepharose 4B than for either soluble or Sephadex-bound enzyme. Substrate addition experiments were then performed with elevated levels of NADH, and pump rate and enzyme concentration were adjusted so that net change in NADH concentration was much less (see Table 11). The results in Table 14 show that the Hill n value was significantly reduced from 1.7 to a level comparable to the initial rate

assays. The discrepancies between $S_{0.5}$ values determined for lactic dehydrogenase immobilized on Sepharose 4-B by either substrate addition or conventional initial rate assays appears slightly larger than those observed for soluble enzymes. This probably represents the imprecision of initial rate estimation from tracings containing elevated noise and not any bias inherent in the addition assay. Because the $S_{0.5}$ for NADH was not determined, it is not known whether NADH was saturating during these assays.

E. DISCUSSION

1. Analysis of Simulated Data

These results indicate that a tangent-slope method can be reliably applied to the analysis of a reaction progress curve of A vs. t generated by substrate addition. The accuracy and precision of the Hill parameters obtained by this method are comparable to those obtained by direct non-linear curve fitting. The tangent-slope method requires an estimate of one variable, Hill n, rather than all three as in curve-fit method. Valid results may be obtained over a wide range of final substrate concentrations (1.5-10 x $S_{0.5}$), and a low degree of enzyme inactivation (> 4% during assay) or product competitive inhibition (K_i > 3x final product concentration) do not seriously bias the analysis. These findings indicate that differential methods may have wider application than has been suggested (121).

The use of differential methods has been discouraged on the basis of statistical arguments (121). It was thus important to examine more closely the present application of such potentially useful techniques. Using simulated data, we have demonstrated that a differential method, using a tangent-slope approximation to the reaction rate, can confidently be applied to the analysis of substrate addition data using the Hill equation. Others have demonstrated that differential methods for the analysis of reaction time courses compare well with conventional initial rate assays, but are more convenient. Balcom and Fitch (113) utilized a simple difference method to study effects of temperature, pH, ionic strength, and modifiers on kinetic constants. Bizozero *et al.* (114) fit progress curve segments to polynomials from which they calculated velocities and substrate concentrations. Yun and Suelter (115) expanded on the

approximation of Lee and Wilson (140) to obtain substrate-velocity data across the entire progress curve. These authors demonstrated the reliability of their technique using both real and simulated data and provided a sound theoretical basis for its use. Their approach which also considers effects of reaction reversibility and product inhibition, provides a flexible analysis of progress curves in which substrate concentration passively declines by depletion.

The addition method has some advantages over conventional progress curve methods. With the substrate depletion method excessive product is present at low, but not high, substrate concentrations; whereas the inverse is true for substrate addition. For this reason, the effects of competitive product inhibition should be reduced when the substrate addition method is used. Greater control is possible over the substrate and product concentrations encountered in the addition method. The experiments can be planned such that product build-up is minimized (perhaps to no more than would occur during an initial rate assay) without changing the range of substrate concentration spanned. The extent to which product concentration can be attenuated is limited only by the sensitivity of the assay. For instance, using the program OPT the total activity and pump rate parameters can be raised resulting in greater product buildup without changing the final substrate concentration (Figures 34C and D). However, in the present analysis of the Hill equation, it is assumed that product effects are unimportant.

Further, a second advantage of the addition method is that it is not limited to the study of substrate kinetics, but can also be applied to analysis of effectors, coenzymes, and cofactors which are not altered by reaction. In addition the tangent slope approach can be used to obtain

from single reaction mixtures velocities during a continuous change of pH or temperature to give pH dependency curve or an Arrhenius plot.

The speed of the TANKIN analysis and the wide variety of potential applications of addition methodology suggest that these techniques may provide a flexible system for enzyme studies. To be most useful, this system should include a direct, computer-spectrophotometer interface for rapid, on-line processing of raw data. The availability of simplified least-squares procedures for data differentiation (89) makes large, expensive computers unecessary for this purpose. It has proved feasible to program TANKIN analysis into a Hewlett-Packard 9815A calculator which has interface capabilities.[22] Incorporation of programs for differential analysis of conventional progress curves (115) should greatly expand the utility of this system.

2. Analysis of Real Data

The accuracy of kinetic constants obtained by the single cuvet, substrate addition method could be diminshed by significant amounts of product inhibition, enzyme inactivation, reaction reversal, cosubstrate depletion, or of hysteresis. Unfortunately for most enzymes a comprehensive rate equation and kinetic constants are not available to aid in eliminating many of the above possibilities as was done herein for lactic dehydrogenase. Also, there are no easily observable signs of these effects in the reaction progress curve as may be observed when conventional steady state assays and related plots depart from linearity. To obtain the increased accuracy potentially available with the substrate addition method, it is necessary to determine whether any of the above effects are involved. Diagnostic procedures and an approximation of

errors to be expected for enzyme activation and product inhibition have been described. For other interfering effects, separate tests should be run in the usual ways as would be done in ordinary kinetic studies. Thus, one of the major uses of the substrate addition method in the thorough characterization of a reasonably well understood enzyme.

The data presented show that kinetic parameters for enzymes can be estimated by the described addition-slope-tangent analysis system with a reliability comparable to that of curvefitting to a reaction progress curve, and much above that normally experienced by conventional methods. In view of the degree of control that can be exerted over substrate and product concentrations, as well as the rapidity and convenience of making determinations, it appears that the system described can do much to release the burdensome work normally required in detailed studies of these parameters.

Analysis of sources of error has shown that a major segment derives from two instrument-related characteristics. One source stems from the acquisition of absorbance data to only four significant digits (0.000 A) leading to errors in calculations due to the truncation of the 4^{th} significant digit. Since there is now at least one spectrophotometer available in which special precautions have been taken to decrease base-line noise and drift, and which reads to 5 significant digits (0.000 A), there is reason to believe that substitution of such a unit for the ordinary 15-year-old unit used in these studies would significantly decrease noise and attendant error. In this connection the noise can be reduced further by signal averaging; that is, by recording absorbances at very short intervals and averaging n values to give each 2 sec absorbance measurement. Such an approach would reduce random noise by a factor of

errors to be expected for enzyme activation and product inhibition have been described. For other interfering effects, separate tests should be run in the usual ways as would be done in ordinary kinetic studies. Thus, one of the major uses of the substrate addition method in the thorough characterization of a reasonably well understood enzyme.

The data presented show that kinetic parameters for enzymes can be estimated by the described addition-slope-based analysis system with reliability comparable to that of curve-fitting of a reaction progress curve, and much above that normally experienced by conventional methods. In view of the degree of control that can be exercised over substrate and product concentrations, as well as the speed and convenience of making determinations, it appears that the system described can do much to release the burdensome work normally required in detailed studies of these parameters.

Analysis of sources of error has shown that a major segment derives from two instrument-related characteristics. One source stems from the acquisition of absorbance data to only four significant digits (0.000 A) leading to errors in calculated due to the truncation of the 4th significant digit. Since there is now at least one spectrophotometer available in which special precautions have been taken to decrease baseline noise and drift, and which reads to 5 significant digits (0.0000 A), there is reason to believe that substitution of such a unit for the ordinary 15-year-old unit used in these studies would significantly decrease noise and attendant error. In this connection the noise can be reduced further by signal averaging; that is, by recording absorbances at very short intervals and averaging n values to give each 2 sec absorbance measurement. Such an approach would reduce random noise by a factor of

$\sqrt{n}$. For the absorbance digitizer (Gilford 410) and similar digital voltmeters in one of the newer spectrophotometers, data acquisition is at the rate of 7.7 points per sec. Thus for a 2.078 sec interval made up of 16 data points, the random noise of the averaged interval would be reduced by a factor of 4.

A second source of error is the imperfect nature of the absorbance correction. By approximating the sawtoothed error line (see Figure 29). This error behavior derives from use of a set of diodes to correct the systematic departure from the absorbance line (87) which performs well for the usual purposes; however, these small errors have a cumulative effect in tangent-slope calculations. The systematic absorbance error without the diode network, while much greater, can be better corrected by fitting a polynomial to the observed absorbance line and using that expression to make the corrections (see Chapter I).

Another source of error results from temperature drift in the cuvet in the water-jacketed compartment. A higher degree of temperature control can be accomplished by electronically controlled Peltier-effect plates which are directly in contact with the cuvet (141). Such an arrangement would allow determination of kinetic constants over a wide temperature range above and below ambient temperature with greater precision. An experimental combination Peltier effect temperature control and alternating field stirring cuvet holder was used in Chapter I.

Validation of the tangent-slope method makes possible the study of a wide range of variables which in addition to substrates have effects on enzyme activity. For other ligands, whose concentrations are not altered by the reaction, a simple option in the program TANKIN allows calculation of ligand concentration at any time. For other variables such as

temperature, pH, and ionic strength, a second data channel utilizing either digital thermometer, pH meter, or conductivity meter together with A-D converter and interface are needed. In addition, a method is required to vary smoothly the temperature, pH, or ionic strength from one limit to another. This can be accomplished by the temperature controller sweep control or by the addition of buffers or salts via the syringe drive.

Figure 36 gives an improved version of the original system incorporating a spectrophotometer reading to 0.1 mA and a Peltier-effect stirring cuvet. Absorbance can be recorded at high rates and averaged in the Hewlett Packard 9815 desk top programmable calculator. This unit can accomodate two data channels, one of which would alternate with the Hewlett Pakcard X-Y plotter. The HP 9815 also has the capability to initiate the physical tasks needed to initiate a run; i.e., start the syringe pump and immerse substrate input tube in the cuvet, as well as to signify the start of substrate addition. These would be activated by a command from the operator.

Although this system and associated programs are only partially developed and tested, it is clear that the velocity measurements, calculations, and plots of absorbance vs. time and $1/v$ vs $1/S^n$ for a determination of the three kinetic parameter can be made in 20 min.

Figure 36. Proposed, Fully Automated System for Kinetic Analysis of Enzyme Reactions. Provisions have been made for calculator control of syringe drive and auxilliary data collection from thermometer, pH meter, or conductivity meter.

PROPOSED
SYSTEM FOR KINETIC ANALYSIS OF REACTIONS

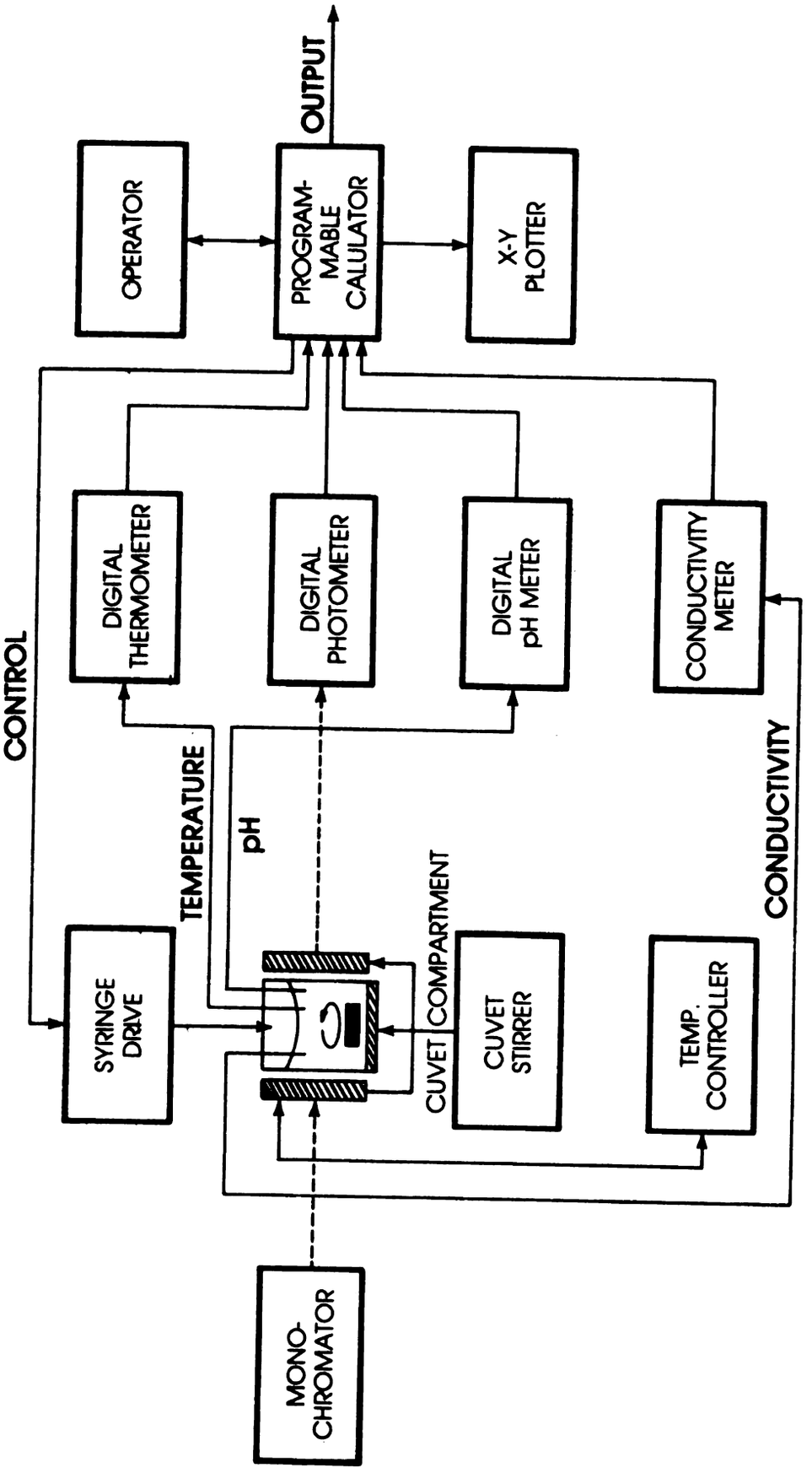

SYNOPSIS AND CONCLUSIONS

The research described herein has depended heavily on development of new techniques and approaches. Improved TDH purification, *in vivo* radio-labeling techniques, the ability to renature the dehydrase from urea and resolve it with urea-penicillamine, optimization of TDH immobilization methodology, and the soft and hardware development of the analytical instrumentation have been the *sine qua non* in these studies.

The single basic hypothesis tested in Chapter I of this thesis concerned the requirement for subunit dimerization in the AMP activation of TDH. This hypothesis was tested using both kinetic and immobilization methodologies. These methodologies have been extensively used by others to answer similar questions about the importance of subunit structure in other enzymatic systems. The behavior of both soluble and matrix-bound TDH is consistent with dimerization being a required, integral part in the activation process.

The substrate addition methodology described in Chapter II of this work, largely removed from studies TDH, represents a significant departure from conventional steady state kinetics, and as such required a more extensive analysis than the other procedures utilized. Although its efficacy seems proven, quality control must always be considered when evaluating the results obtained with this technique.

APPENDIX

APPENDIX

STEREOSPECIFICITY OF DEUTERIUM INCORPORATION INTO THE PRODUCT OF THE TDH REACTION

Previous work has shown that one deuterium is incorporated from D_2O into the product of the TDH reaction during tautomeric rearrangement and hydrolysis of α-aminocrotonate (97). The chirality of the product, 1-D-α-ketobutyrate, has implications for the catalytic mechanism of TDH since any asymetry in the deuterium incorporation requires that the rearrangement occur on the enzyme surface rather than spontaneously in solution.

The method presently available for determination of the chirality of 1-D-α-ketobutyrate involves the large scale formation of 1-D-α-ketobutyrate, oxidative decarboxylation to propionate with H_2O_2, isolation and crystallization of sodium propionate and determination of its specific rotation. This procedure has been used to investigate the mechanisms of KDPG-aldolase (142), pyruvate kinase (143) and cystathionase (144). However this procedure is insensitive, inconvenient and not amenable to a large number of experiments.

An intensive effort employing this technique to confirm the partial chirality of 1-D-α-ketobutyrate produced when the TDH reaction is carried out in D_2O proved unsuccessful. It was suspected that chirality of 1-D-α-ketobutyrate may only be partial and was somehow lost during the oxidation process. A more direct and sensitive assay for the chirality of 1-D-α-ketobutyrate was therefore desired.

The molecule α-ketobutyrate possesses an absorbance maximum at 320 nm due to the α-keto group. It would not be unexpected for an asymetric carbon neighboring the keto group (e.g., in 1-D-α-ketobutyrate) to induce a chirality into the absorption band at 320 nm. If this occurred, a CD signal would be expected at this wavelength (145). Such a CD signal might allow a direct assay of chiral 1-D-α-ketobutyrate.

To investigate this possibility 1-D-α-ketobutyrate was produced by a KDPG-Aldolase which is known to catalyze a stereospecific exchange of position 1 hydrogen with deuterium in D_2O (142).

Figure 37 shows that a transient positive CD is produced when KDPG-Aldolase and α-ketobutyrate were incubated in D_2O but not in H_2O. As the enzyme concentration is increased both the rate of appearance and disappearance of the signal appears to be increased. Such behavior might be expected if KDPG-Aldolase catalyzed incorporation of deuterium into the 1-proR and 1-proS positions of α-ketobutyrate at 2 different rates.

To corroborate the possibility that chiral 1-D-α-ketobutyrate is present at the peak of the CD signal, a reaction mixture was prepared identical to the one in Figure 37 containing 0.1 mg/ml of KDPG-Aldolase but in a 25 ml volume. After 1.5 h incubation, propionate was formed, isolated, crystallized and quantitated exactly as recommended (144). Relative intensities of the position 3 and 2 hydrogens determined by proton NMR in D_2O suggested that the propionate was 40% deuterated in the 2 position. ORD measurements indicated a 14% excess of S-3-^{2}H,H propionate (α_{230} = 2.8 degrees, see reference 144). The chirality is lower than expected (142), but indicates that a positive CD signal may be associated with 1-S-D-α-ketobutyrate.

The molecule α-ketoglutarate possesses an absorbance maximum at 320 nm due to the α-keto group. It would not be unexpected for an asymmetric carbon neighboring the keto group (eg. an L-α-ketoglutarate) to induce a chirality into the absorption band at 320 nm. If this occurred, a CD signal would be expected at that wavelength (142). Such a CD signal might afford a direct assay of chiral L-α-keto

To investigate this possibility L-α-ketoglutarate was produced by a KDPG-Aldolase which is known to catalyze a stereospecific cleavage of position 1 hydrogen with deuterium in D$_2$O (143).

Figure 37 shows that a racemic mixture (D,L-α-ketoglutarate) and Aldolase and α-ketoglutarate were incubated in D$_2$O buffer at the same concentration it is observed both CD(λ) signals of a disappearance of the signal assay. In an enzyme with specific proton be expected if KDPG-Aldolase catalyzes stereospecific deuteration the L-pro R and L-pro S positions at α-ketoglutarate is

To corroborate the possibility that the α-ketoglutarate is present at the peak of the CD signal, a reaction mixture was prepared identical to the one in Figure 37 containing 0.1 mg/ml of KDPG-Aldolase but in a 25 ml volume. After 1.5 h incubation, pyruvate was formed, isolated, crystallized and quantitated exactly as recommended (144). Relative intensities of the position 2 and 3 hydrogens determined by proton NMR in D$_2$O suggested that the pyruvate was 40% deuterated in the 3 position. DRO measurements indicated a 14% excess of S-3-^{2}H pyruvate ($\alpha_{230} = 2.8$ degrees, see reference 145). The chirality is lower than expected (142), but indicates that a positive CD signal may be associated with L-2-D-α-ketoglutarate.

Figure 37. CD Observed During the Exchange of Deuterium into α-Ketobutyrate from D_2O Catalized by KDPG-Aldolase. The reaction was started by addition of KDPG Aldolase at the indicated concentrations (mg/ml) to a 1 ml solution containing 0.1 M Na α-ketobutyrate and 0.1 M potassium phosphate in 98% D_2O solution (solid lines) or H_2O solution (dashed line). Final pH was 7.7 uncorrected for the presence of D_2O. The solution was immediately mixed and transferred to a water jacketed cylindrical fused silica cuvet. The CD measurements were made at 28°C and 320 nm with a Durrum-Jasco ORD/UV-5 spectropolarimeter with a CD attachment.

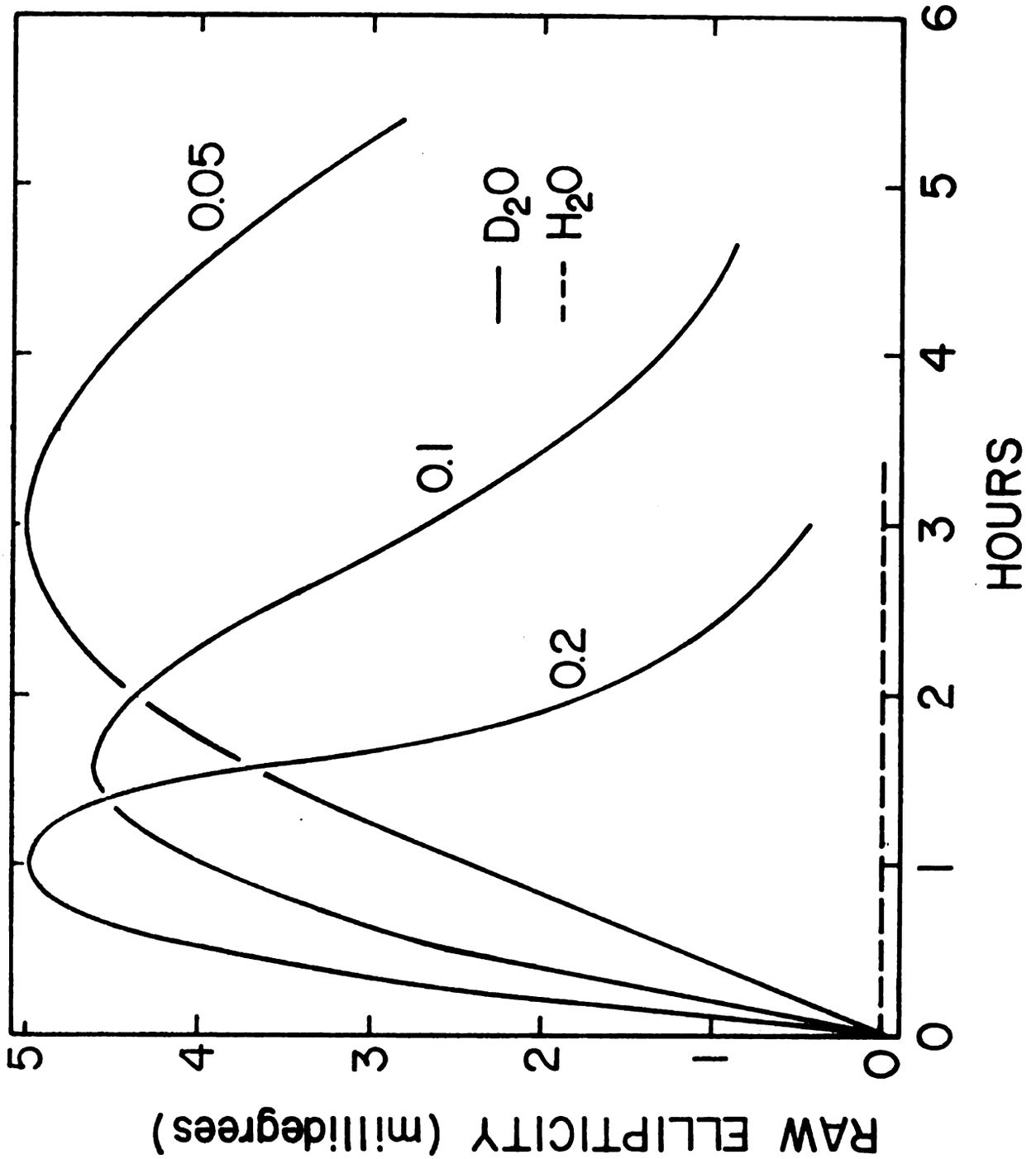
RAW ELLIPTICITY (millidegrees)
HOURS
0.05
0.1
0.2
D_2O
H_2O
0
1
2
3
4
5
6

A positive CD signal was also produced at 320 nm when the TDH reaction was carried out in D_2O but not in H_2O (Figure 38A). The well documented CD change between 400 and 450 nm due to the PLP cofactor is also shown in this figure. Figure 38B also indicates that the chirality produced depends upon the buffer conditions and the presence or absence of AMP in the TDH reaction mixture. Chirality increased slightly in the absence of AMP, and even further when pH is elevated and potassium ion removed in addition.

Because no attempt was made to isolate and positively identify the chiral species produced by KDPG-Aldolase and TDH in the experiments of Figures 37 and 38, it would be inappropriate to draw strong conclusions. However the CD signals observed in Figure 38 raise the possibility that the terminal stages in the mechanism of TDH occur on the enzyme surface, and may be regulated by AMP.

Figure 38. CD Observed During the TDH Reaction in D_2O as a Function of Buffer Conditions and the Presence or Absence of AMP. Reactions were started by addition of 0.01 mg of TDH (specific acitivty 401 I.U./mg) to 1 ml solutions containing either 200 mM (Figure A) or 100 mM (Figure B) L-threonine, 1 mM DTT, and either (Figure A), 5 mM AMP and 0.1 M potassium phosphate pH 7.7 (uncorrected), or (Figure B) the indicated buffer and AMP conditions (5 mM where indicated). Measurements were made as indicated in Figure 37.

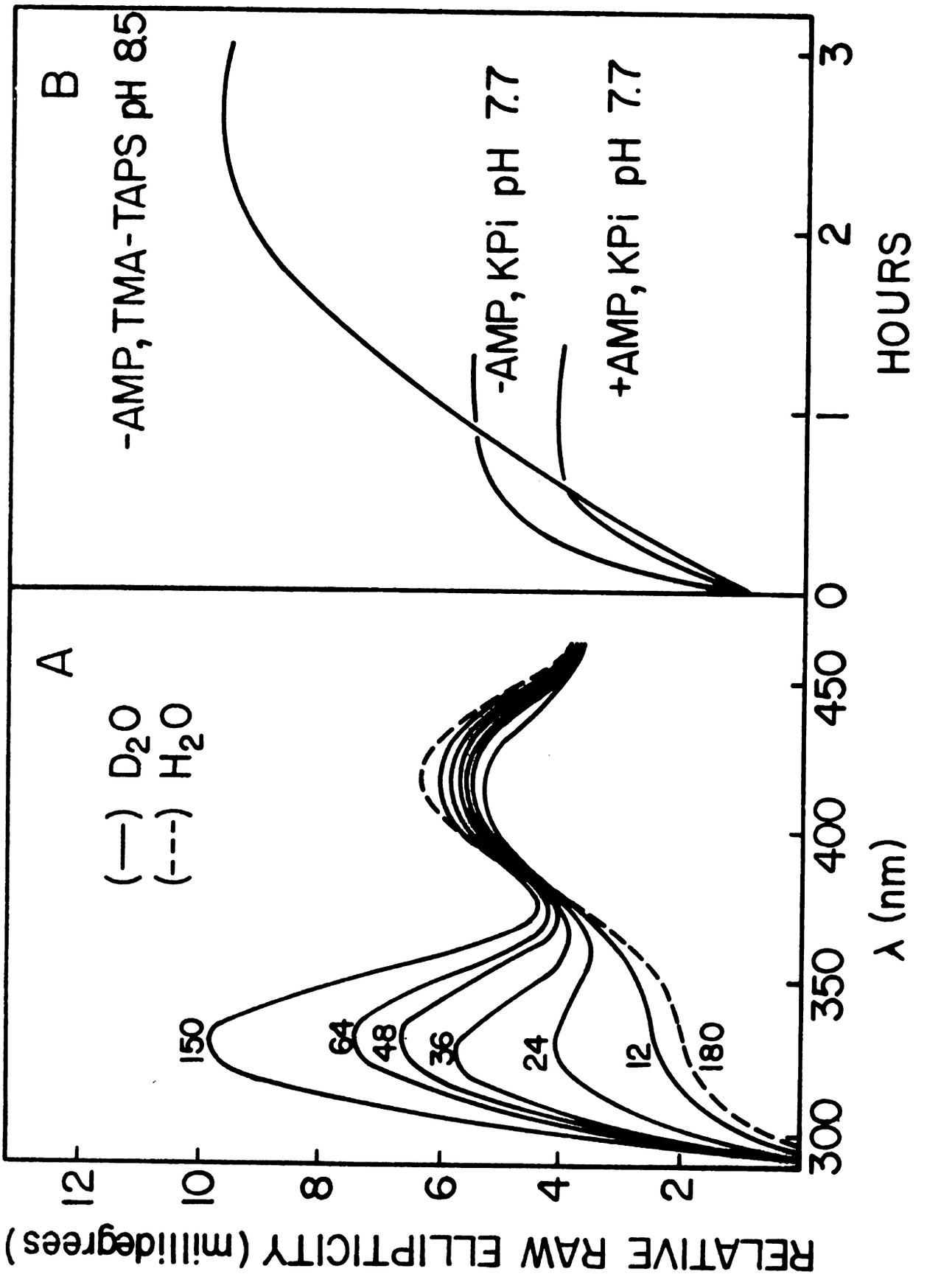
A
(—) D_2O
(---) H_2O
150
64
48
36
24
12
180
RELATIVE RAW ELLIPTICITY (millidegrees)
12
10
8
6
4
2
300
350
400
450
λ (nm)
B
-AMP, TMA-TAPS pH 8.5
-AMP, KPi pH 7.7
+AMP, KPi pH 7.7
0
1
2
3
HOURS

LIST OF FOOTNOTES

1. In this dissertation, the terms hysteresis and hysteretic effects (12) are used to refer to changes in kinetic or molecular properties of TDH upon the addition or removal of AMP, which occur slowly relative to the rate of the catalytic reaction.

2. In this dissertation the terms "oligomerization" and "deoligomerization" refer to changes in quaternary structure of soluble enzymes. These terms are to be distinguished from "associated", "dissociated", and "reassociated" which describe the states of matrix-bound enzyme forms.

3. TDH will henceforth refer to the biodegradative TDH of E. coli.

4. For reassociation to be significant during catalysis,

   Rate of association ≈ Rate of catalysis

   $$\text{or } k_2M^2 \approx k_cM$$

   $$\text{or } k_2 \approx k_c/M$$

   Where k_2 is the second order rate constant for association, k_c is the catalytic turnovr rate and M represents the concentration of TDH monomers of molecular weight 40,000. Under typical assay conditions, where k_c = 480 I.U./mg and M = 5 nanomolar, k_2 may be shown equal to 10^{11} $M^{-1}sec^{-1}$.

5. PMSF is best added to the buffer from a 25 mg/ml 1-butanol solution. All solutions containing this chemical must be handled with gloves since PMSF is a deadly poison.

6. The enzyme concentration (I.U./ml) used in previous studies (11) may be calculated by dividing the observed ΔA/min by the extinction coefficient of NADH (6,220 $M^{-1}cm^{-1}$).

7. At a given extent of activation by AMP, the catalytic rate should be proportional to enzyme concentration. However, if dimerization is the rate limiting step in activation, then the rate of activation will be proportional to the square of enzyme concentration. Thus a greater extent of activation should occur at elevated dehydrase levels, for a given extent of catalytic reaction.

8. Substituting the Hill parameters given in Table 6 into the Hill equation (equation 14) yields a value for the ratio of the AMP activated to the unactivated catalytic rate of 19.8.

9. In this somewhat subjective procedure low weight was given to apparent outliers and account was taken of the fact that rates at very short times (3-5 seconds) may be low due to coupling lag in the assay.

10. Assuming an 9th order dependence on TDH concentration,

$$\text{activation rate} = k \cdot [\text{TDH}]^9$$

$$\log(\text{activation rate}) = 9 \log k + a \cdot \log [\text{TDH}]$$

where k is the 8th order constant for activation.

11. If V is the rate of the dehydrase reaction (I.U./ml), L the TDH protomer molar concentration at zero time, and r_L and r_H the specific reaction rates (I.U. $\cdot$ $nmol^{-1}$) of the protomer in the monomer and activated dimer forms respectively, then:

$$V = L (r_L - r_H) + L_o r_H$$

$$\frac{dV}{dt} = \frac{dL}{dt} (r_L - r_H)$$

but since $\frac{dL}{dt} = k_2 L^2$ for a second order process, where k_2 is the second order rate constant for protomer association ($M^{-1}s^{-1}$)

$$\frac{dV}{dt} = k_2 L^2 (r_H - r_L)$$

$$\log \frac{dV}{dt} = 2 \log L + \log k_2 (r_H - r_L)$$

since it is shown in the text that

$$\frac{r_H}{r_L} = 20, \quad r_H >> r_L$$

$$\text{intercept} \quad \log k_2 r_H$$

$$k_2 = \frac{10^{\text{intercept}}}{r_H} = \frac{10^{14.49} \text{ I.U. ml}^{-1} \text{ min}^{-1}}{(480 \text{ I.U./mg}) (40{,}000 \text{ mg/mmol}) (60 \text{ s/min})}$$

$$= 2.7 \times 10^5 \text{ M}^{-1} \text{ s}^{-1}$$

12. The reaction must be terminated because NADH becomes limiting. To overcome this problem, and to increase slightly the extent of activation within the assay period, the increased and the reaction observed at a wavelength of reduced sensitivity. This was done in the experiment of Figure 13 (see Figure Legend for details), however completion was still not obtained.

13. It can be shown that a dimerizing species will be 50% dimerized when present at the level of the dissociation constant. In the above experiment, little dimerization has occurred at 8.4 I.U./ml so the dissociation constant must be above this value. Conversely also, the value must be less than 107 I.U./ml.

14. In conventional units, the dissociation constant was 2.34×10^{-6} M (68). To convert to activity units, 2.34×10^{-6} M) $(4 \times 10^{4}$ g/mol) (480 I.U./mg) $(10^{3}$ mg/g) $(10^{-3}$ l/ml) = 44.9 I.U./ml.

15. Upon addition of AMP, "neighboring" bound monomers could conceivable reassociate. Such closely spaced subunits could arise by "pair coupling" of a dimer species to the matrix leaving both subunits covalently attached. Although each subunit might acquire a new soluble partner during the coupling period, they could reassociate after the AMP-free buffer wash when AMP is re-introduced during assay.

    For such pair couplings to occur, cyanogen bromide activated groups must be within a TDH molecular diameter, d, of each other. For the TDH dimer of molecular weight 80,000 (66) and partial specific volume 0.738 (66), d=55 Å, The probability (ϕ) of such occurrences is (44):

$$\phi = 1 - \text{EXP} \frac{-d \cdot C^{1/3}}{7.4}$$

    where C is the molar concentration of CNBr activated sites. At 2.5 mg CNBr/ml,

$$C = 1.1 \times 10^{-3} \text{ M (44) and } \phi = 0.54$$

    The actual number of twin couplings will be lower than 54% for the following reasons: (1) A fraction of these closely spaced linkage points (about 17% from the above equation) will be within a subunit radius and thus too close to bind to the adjacent subunit; (2) not every potential linkage point pair will have the appropriate orientation to link both subunits.

    The above equation may also be used to estimate the probability of <u>independently</u> attached subunits still being close enough to recombine due to matrix flexibility. With uncrossedlinked Sepharose 4B, monomers may be able to move though distances of 200 A (44). The concentration of such monomers at 2.5 mg/ml CNBr would be about 1.3×10^{-7} M. For this situation, d = 200 Å and ϕ = 0.17. This precentage would be greatly reduced with the crosslinked Sepharose 4B used in the present studies (44).

    These arguments suggest that 30-50% of the subunits may be able to reassociate.

16. Solutions counted in the presence of urea were not fully corrected for quenching. Thus solutions of released radioactivity contained fewer detectable counts than actually present.

17. Dependence of rate or extent of reactivation on the components of the renaturation buffer was not extensively investigated. However, the rate of renaturation was much slower when PLP was omitted from the mixture.

18. Assuming that attachment to the matrix does not raise the specific activity of the dehydrase or in some ways preferentially bind only more highly active TDH molecules.

19. Analysis of rate data using the Hill equation presupposes that reaction velocity is proportional to ligand or substrate binding.

20. D. LeBlond and W.A. Wood, 1978 unpubished data.

21. The mean chi-square for these curve fits was 0.997 ± 0.05 (s.d.) suggesting that parameters evaluated by this method were indeed optimal for the data (88).

22. Errors in reaching absorbance at the 4th digit (0.0000) due to the use of an analog-to digital converted with only four significant digits (0.000).

23. H. Pawlowski, D. LeBlond, S.A. Douglass, W.A. Wood, 1977 unpublished data.

LIST OF REFERENCES

LIST OF REFERENCES

1. Perutz, M.F.; Rossman, M.G.; Cullis, A.F.; Muirhead, H.; Will, G. and North, A.C.T. (1960) Nature 185, 416-422.

2. Phillips, A.T.; Egan, R.M. and Lewis, B. (1978) J. Bacteriol. 135, 828-840.

3. Phillips, A.T. and Wood, W.A. (1964) Bioch. Bioph. Res. Commun. 15, 530-535.

4. Shizuta, Y.; Kurosawa, A.; Ioue, K.; Tanabe, T. and Hayaishi, O. (1973) J. Biol. Chem. 248, 512-520.

5. Feldman, D.A. and Datta, P. (1975) Biochemistry 14, 1760-1767.

6. Wood, W.A. and Gunsalus, I.C. (1949) J. Biol. Chem. 181, 171-182.

7. Whanger, P.D.; Phillips, A.T.; Rabinowitz, K.W.; Piperno, J.R.; Shanda, J.D. and Wood, W.A. (1969) J. Biol. Chem. 243, 167-173.

8. Dunne, C.P. and Wood, W.A. (1975) Cur. Top. in Cell. Regul. 9, 65-101.

9. Phillips, A.T. (1974) Crit. Rev. in Biochem. 2, 343-378.

10. Shizuta, Y. adn Hayaishi, O. (1976) Cur. Top. in Cell. Regul. 11, 99-146.

11. Gerlt, J.A.; Rabinowitz, K.W.; Dunne, C.P. and Wood, W.A. (1973) J. Biol. Chem. 248, 8200-8206.

12. Frieden, C. (1971) Ann. Rev. Biochem. 40, 653-698.

13. Baldwin, J. and Chothia, C. (1979) J. Mol. Biol. 129, 175-220.

14. Chan, W.W.-C. (1975) J. Biol. Chem. 250, 668-674.

15. Monod, J.; Wyman, J. and Changeaux (1965) J. Mol. Biol. 12, 88-118.

16. Koshland, D.E.; Nemethy, G. and Filmer, D. (1966) Biochemistry 5, 364-385.

17. Levitzki, A. and Koshland, D.E. (1969) Proc. Nat. Acad. Sci. U.S.A. 62, 1121-1128.

18. Wyman, J. (1972) Cur. Top. In Cell. Regul. 7, 209-226.

19. Weber, G. (1972) Biochemstry 11, 864-878.

20. Weber, G. (1975) Adv. Protein Chem. 29, 1-83.

21. Noble, R.W. (1969) J. Mol. Biol. 39, 479-491.

22. Levitzki, A. and Koshland, D.E. (1972) Biochemistry 11, 247-252.

23. Nichol, L.W., Jackson, W.J.H. and Winzor, D.J. (1967) Biochemistry 6, 2449-2456.

24. Klotz, I.M. (1974) Accounts Chem. Res. 7, 162-168.

25. Kurganov, B.I., Dorozhko, A.I., Kagan, Z.S. and Yakovlev, V.A. (1976) J. Theoret. Biol. 60, 247-269.

26. Cohen, R.J., Jedziniak, J.A. and Benedek, G.B. (1976) J. Mol. Biol. 108, 179-199.

27. Colman, R.F. and Frieden, C. (1966) J. Biol. Chem. 241, 3661-3671.

28. Rudolph, R., Gerschitz, J. and Jaenicke, R. (1978) Eur. J. Biochem. 87, 601-606.

29. Carvajal, N., Martinez, J., de Oca, F.M., Rodriguez, J. and Fernandez, M. (1978) Biochem. Biophys. Acta 527, 1-7.

30. Chan, W.W.-C., Mort, J.S., Cong, D.K.K. and Macdonald, P.D.M. (1973) J. Biol. Chem. 248, 2778-2781.

31. Chan, W.W.-C and Mawer, H.M. (1972) Arch. Biochem. Biophys. 149, 136-145.

32. Chan, W.W.-C., Kaiser, I., Salvo, J. and Lawford, G.R. (1974) J. Mol. Biol. 87, 847-852.

33. Chan, W.W.-C., Schutt, H. and Brand, K. (1973) Eur. J. Biochem. 40, 533-541.

34. Feldmann, K., Zeisel, H. and Helmreich (1972) Proc. Nat. Acad. Sci. U.S.A. 69, 2278-2282.

35. McVittie, J.D., Esnouf, M.P. and Peacocke, A.R. (1977) Eur. J. Biochem. 81, 307-315.

36. McKarcken, S. and Meighen, E. (1980) J. Biol. Chem. 255, 2396-2404.

37. Bartholmes, P. and Jaenicke, R. (1978) Eur. J. Biochem. 87, 563-567.

38. Nagradova, N.K., Golovina, T.O. and Mevkh, A.T. (1974) FEBS Letters 49, 242-245.

39. Pollard, H.B. and Steers, E. (1973) Arch. Biochem. Biophys. 158, 650-661.

40. Jaenicke, R., Rudolph, R. and Heider, I. (1979) Biochemistry 18, 1217-1223.

41. Jaenicke, R. (1974) Eur. J. Biochem. 46, 149-155.

42. Chan, W.W.-C. and Mosbach, K. (1976) Biochemistry 15, 4215-4222.

43. Green, N.M. and Toms, E.J. (1972) Biochem. J. 130, 707-711.

44. Green, N.M. and Toms, E.J. (1973) Biochem. J. 133, 687-700.

45. Bickerstaff, G.F. and Price, N.C. (1976) FEBS Letters 64, 319-322.

46. Chan, W.W.-C. (1975) J. Biol. Chem. 250, 661-667.

47. Chan, W.W.-C. (1974) FEBS Letters 44, 178-181.

48. Fontan, E. and Bachi, P.T. (1978) J. Biol. Chem. 253, 2754-2757.

49. Frieden, C., Gilbert, H. and Bock, P.E. (1976) J. Biol. Chem. 251, 5644-5647.

50. Wohl, R.C. and Markus, G. (1972) J. Biol. Chem. 247, 5785-5792.

51. Carlier, M.-F. and Pantaloni, D. (1978) Eur. J. Biochem. 89, 511-516.

52. LeJohn, J.B., McCrea, B.E., Suzuki, I. and Jackson, S. (1969) J. Biol. Chem. 244, 2484-2493.

53. Harmony, J.A.K. and Himes, R.H. (1975) J. Biol. Chem. 250, 8049-8054.

54. deRiel, J.K. and Paulus, H. (1978) Biochemistry 17, 5134-5140.

55. Gawronski, T.H. and Westhead, E.W. (1969) Biochemistry 8, 4261-4270.

56. Bickerstaff, G.F. and Price, N.C. (1978) Biochem. J. 173, 85-93.

57. Tuominen, F.W. and Bernlohr, R.W. (1971) J. Biol. Chem. 173, 85-93.

58. Chan, W.W.-C. (1976) Can. J. Biochem. 54, 521-528.

59. Wood, W.A. (1969) Curr. Top. in Cell. Regul. 5, 151-181.

60. Egan, R.M. and Phillips, A.T. (1977) J. Bacteriol. 132, 370-376.

61. Yui, Y., Watanabe, Y., Ito, S., Shizuta, Y. and Hayaishi, O. (1977) J. Bacteriol. 132, 363-369.

62. Tokushige, M. (1972) Proteins: Structure and Function, pp. 141-201.

63. Beitz, D., Whangar, P. and Wood, W.A. (1971) unpublished experiments.

64. Dunne, C.P. Gerlt, J.A., Rabinowitz, K.W. and Wood, W.A. (1973) J. Biol. Chem. 248, 8189-8199.

65. Rabinowitz, K.W., Niederman, R.A. and Wood, W.A. (1973) J. Biol. Chem. 248, 8207-8215.

66. Sacki, Y., Ito, S., Shizuta, Y., Hayaishi, O., Kagamiyama, H. and Wada, H. (1977) J. Biol. Chem. 252, 2206-2208.

67. Wyman, J. (1964) Advanc. Protein Chem. 19, 223-286.

68. Menson, R.C. (1976) Ph.D. Thesis, Department of Biochemistry, Michigan State University, East Lansing, Michigan.

69. Shizuta, Y., Nakazawa, A., Tokushige, M. and Hayaishi, O. (1969) J. Biol. Chem. 244, 1883-1889.

70. Dunne, C.P., Menson, R.C., Gerlt, J.A. and Wood, W.A. (1973) in Metabolic Interconversion of Enzymes. Third International Symposium held in Seattle, Washington, June 5-8, 1973, ed. Fischer, E.H., Krebs, E.G., Neurath, H. and Stadtman, E.R. Springer-Verlag, New York.

71. Shizuta, Y., Kurosawa, A., Tanaba, T., Inone, K. and Hayaishi, O. (1973) J. Biol. Chem. 248, 4213-4219.

72. Gutfreund, H. (1972) Enzymes: Physical Principals, p. 159, John Wiley and Sons Ltd., New York.

73. McClure, W.R. (1969) Biochemistry 8, 2782-2786.

74. Mort, J.S., Chong, D.K.K. and Chan, W.W.-C. (1973) Anal. Biochem. 52, 162-168.

75. Lowry, O.H., Rosenbrough, N.J., Farr, A.L. and Randall, R.J. (1951) J. Biol. Chem. 193, 265-275.

76. Bohlen, P., Stein, S., Dairman, W., Udeufriend, S. (1973) Arch. Biochem. Biophys. 155, 213-220.

77. Spector, T. (1978) Anal. Biochem. 86, 142-146.

78. Spaceman, D.H., Stein, W.H. and Moore, S. (1958) Anal. Chem. 30, 1190-1200.

79. Ornstein, L. (1964) Ann. N.Y. Acad. Sci. 121, 321-341.

80. Davis, B.J. (1964) Ann. N.Y. Acad. Sci. 121, 404-427.

81. Malik, N. and Berrie, A. (1972) Anal. Biochem. 49, 173-177.

82. Feldman, D. (1973) Ph.D. Thesis, Department of Biochemistry, University of Michigan, Ann Arbor, Michigan.

83. Steck, L. (1977) Anal. Biochem. 78, 459-465.

84. Weber, K. and Osborn, J. (1969) J. Biol. Chem. 244, 4406-4412.

85. Riebow, J. (1978) M.S. Thesis, Department of Biochemistry, Michigan State University, East Lansing, Michigan.

86. Axen, R., Porath, J. and Ernback, S. (1967) Nature 214, 1302-1304.

87. Wood, W.A. and Gilford, S.R. (1961) Anal. Biochem. 2, 589-609.

88. Bevington, P.R. (1969) Data Reduction and Error Analysis for the Physical Sciences, McGraw-Hill, New York.

89. Savitzky, A. and Golay, M.J.E. (1964) Anal. Chem. 36, 1627-1639.

90. Frost, A.A. and Pearson, R.G. (1961) Kinetics and Mechanism. John Wiley and Sons, inc.

91. Wilkinson, G.N. (1961) Biochem. J. 80, 324-332.

92. Dye, J.L. and Nicely, V.A. (1971) J. Chem. Educ. 48, 443-448.

93. Svedberg, T. and Pedersen, K.O. (1940) The Ultracentrifuge pp. 277-283.

94. Bhadra, R. and Datta, P. (1978) Biochemistry 14, 1691-1699.

95. Datta, P. and Bhadra, R. (1973) Eur. J. Biochem. 91, 527-532.

96. Tokushige, M. (1967) J. Vitaminology 13, 165-172.

97. Phillips, A.T. and Wood, W.A. (1965) J. Biol. Chem. 240, 4703-4709.

98. Rabinowitz, K.W. (1970) Ph.D. Thesis, Department of Biochemistry, Michigan State University, East Lansing, Michigan.

99. Holleman, A.B. (1966) Ph.D. Thesis, Department of Biochemistry, Michigan State University, East Lansing, Michigan.

100. Handbook of Chemistry and Physics (1974) p. D-231, Chemical Rubber Co. Press, Cleveland, Ohio.

102. Goldstein, L. (1979) Methods in Enzymology 42, 397-443.

103. Wyman, J. (1964) Advan. Protein Chem. 19, 223-286.

104. Cornish-Bowden, A. and Koshland, D.E., Jr. (1975) J. Mol. Biol. 95, 201-212.

105. Dunne, C.P. and Wood, W.A. (1975) Curr. Top. in Cell. Regul. 9, 65-101.

106. Wieker, H.-J., Johannes, K.-J., and Hess, B. (1970) FEBS Letters 8, 178-185.

107. Atkins, G.L. (1973) Eur. J. Biochem. 33, 175-180.

108. Nimmo, I.A., and Bauenmeister, A. (1977) Anal. Biochem. 82, 468-472.

109. Philo, R.D. and Selwyn, M.J. (1973) Biochem. J. 135, 525-530.

110. Bates, D.J. and Frieden, C. (1973) J. Biol. Chem. 248, 7878-7884.

111. Duggleby, R.G. and Morrison, J.F. (1977) Biochim. Biophys. Acta 481, 297-312.

112. Atkins, G.L. and Nimmo, I.A. (1973) Biochem. J. 135, 779-784.

113. Balcom, J.K. and Fitch, W.M. (1970) J. Biol. Chem. 245, 1637-1647.

114. Bizzozero, S.A., Kaiser, A.W. and Dutler, H. (1973) Eur. J. Biochem. 33, 292-300.

115. Yun, S.-Y. and Suelter, C.H. (1977) Biochim. Biophys. Acta 480, 1-13.

116. Jordan, F., Kuo, D.J. and Monse, E.U. (1978) Anal. Biochem. 86, 298-302.

117. Blasier, R.B., Wilson, J.E. and Holland, J.F. (1974) Anal. Biochem. 57, 336-342.

118. Lucas, D. (1978) Anal. Biochem. 91, 394-402.

119. Carnahan, B. and Wilkes, J.O. (1973) Digital Computing and Numerical Methods, pp. 389-391, John Wiley, N.Y.

120. Hamilton, W.C. (1964) Statistics in Physical Science, p. 124-185. Ronald Press, New York.

121. Cornish-Bowden, A.J. (1972) Biochem. J. 130, 637-639.

122. Suelter, C.H., Wang, J. and Snell, E. (1976) Anal. Biochem. 76, 221-232.

123. Zewe, V. and Fromm, H.J. (1962) J. Biol. Chem. 237, 1668-1675.

124. Wallenfels, K. and Weil, R. (1972) in The Enzymes (editors . . .) Vol. 7, pp. 617-663, Academic Press, New York.

125. Bergemayer, H.U., Gawean, K. and Grassl, M. (1974) in Methods of Enzymatic Analysis, (H.U. Bergemayer, editor) Vol. I, p. 425-522, Academic Press, New York.

126. Suelter, C.H., Wang, J. and Snell, E. (1976) FEBS Letters 66, 230-232.

127. Meloche, H.P., Ingram, J.M. and Wood, W.A. (1966) Methods Enzymol. 9, 520-524.

128. Dunne, C.P., Gerlt, J.A., Rabinowitz, K.W. and Wood, W.A. (1973) J. Biol. Chem. 248, 8189-8199.

129. Cornish-Bowden, A. (1976) Principles of Enzyme Kinetics, p. 144. Butterworths, Boston.

130. Kuby, S.A. and Lardy, H.A. (1953) J. Amer. Chem. Soc. 75, 890-896.

131. Raval, D.N. and Wolfe, R.G. (1962) Biochemistry 1, 1112-1117.

132. Watanabe, T. and Snell, E.E. (1972) Proc. Nat. Acad. Sci. U.S.A. 69, 1086-1090.

133. Rabinowitz, K.W., Niederman, R.A. and Wood, W.A. (1973) J. Biol. Chem. 248, 8207-8215.

134. Meloche, H.P. and Wood, W.A. (1964) J. Biol. Chem. 239, 3511-3514.

135. Kovachevich, R. and Wood, W.A. (1964) J. Biol. Chem. 197, 745-756.

136. Wilson, R.J.H., Kay, G. and Lilly, M.D. (1968) Biochem. J. 108, 845-853.

137. Stolzenbach, F.E. and Kaplan, N.O. (1976) in Methods Enzymol. 44, 929-936.

138. Daka, N.J. and Laidler, K.J. (1978) Can. J. Biochem. 56, 774-779.

139. Levi, A.S. (1975) Arch. Biochem. Biophys. 168, 115-121.

140. Lee, H.-J. and Wilson, I.B. (1971) Biochim. Biophys. Acta 242, 519-522.

141. Douglass, S.A. (1978) Amer. Lab. 10, 123-127.

142. Ingram, J.M. and Wood, W.A. (1966) J. Biol. Chem. 241, 3256-3261.

143. Bondinell, W.E. and Sprinson, D.B. (1970) Bioch. Biophys. Res. Commun. 40, 1464-1467.

144. Krongelb, M., Smith, T.A. and Abeles, R.H. (1968) Biochim. Biophys. Acta 167, 473-475.

145. Duffield, J.J. and Shumays, A. (1966) Anal. Chem. 38, 29A-58A.